QUANTIFICATION OF GROUNDWATER RECHARGE RATES IN NEW MEXICO USING BOMB 36CL, BOMB-3H, AND CHLORIDE AS SOIL-WATER TRACERS

by

Julie L. Mattick and Thomas A. Duval
Graduate Research Assistants
Department of Geoscience

and

Fred M. Phillips
Principal Investigator
Department of Geoscience

TECHNICAL COMPLETION REPORT

Project Nos. 1423638 and 1423654

March 1987

New Mexico Water Resources Research Institute

in cooperation with

Geoscience Department and Geophysical Research Center
New Mexico Institute of Mining and Technology

The research on which this report is based was financed in part by the United States Department of the Interior, Geological Survey, through the New Mexico Water Resources Research Institute. Additional funding was provided by the U.S. Department of Energy program for Master's thesis research on nuclear waste management.

Project Numbers: 1423638, 1423654.

DISCLAIMER

The purpose of Water Resources Research Institute technical reports is to provide a timely outlet for research results obtained on projects supported in whole or in part by the institute. Through these reports, we are promoting the free exchange of information and ideas and hope to stimulate thoughtful discussion and action that may lead to resolution of water problems. The WRRI, through peer review of draft reports, attempts to substantiate the accuracy of information contained in its reports, but the views expressed are those of the authors and do not necessarily reflect those of the WRRI or its reviewers.

Contents of this publication do not necessarily reflect the views and policies of the United States Department of the Interior, nor does mention of trade names or commercial products constitute their endorsement by the United States Government.

ABSTRACT

Significant amounts of chlorine-36 (36Cl) and tritium (3H) were released into the environment as a result of nuclear weapons testing in the 1950s and 1960s. These anthropogenic radionuclides were used to estimate natural ground-water recharge rates and to determine soil dispersive properties in arid climates near Socorro and Las Cruces, New Mexico.

Ground water recharge estimates based on a mass balance of the chloride ion indicate that only about one percent of the average annual precipitation becomes recharge. These results are considerably lower than those estimated by a soil-physics study at the same location near Socorro. Discrepancies may be attributed to lateral components of flow and differences in liquid and solute transport.

Relative positions of the 3H and 36Cl profiles indicate that moisture movement by vapor transport is significant. Tritiated water moves in both the liquid and vapor phases while chloride moves only as a dissolved constituent in the liquid phase. A combined liquid and vapor flux may drive 3H deeper into the soil than chloride.

One-dimensional finite-element models were used to simulate transport of 3H and 36Cl through unsaturated soils near Socorro. Dispersivities equal to 5 cm and 8 cm provided the best fit of the computed curve to the observed 3H and 36Cl profiles, respectively.

Key words: groundwater recharge, natural; chlorine radiosotopes; tritium; dispersion.

TABLE OF CONTENTS

List of Tables

List of Figures

INTRODUCTION

Replenishment of groundwater is called recharge. Since New Mexico is dependent on groundwater, the rate of groundwater recharge limits New Mexico's water use and thus its economic development. This fact establishes a need to know the amount of water available in aquifers and the rate at which this water is recharged.

Quality degradation of groundwater resources is another reason to study groundwater recharge. Many sources of groundwater pollution, such as domestic wastes, fertilizers and sanitary landfills, are located at or near the ground surface. In order for contaminants to enter the groundwater, they must first pass through the unsaturated zone between the surface and the water table. In areas where recharge through the unsaturated zone is significant, the danger of groundwater contamination from surface waste is much greater than in areas where recharge is negligible.

This same principle applies to utilization of the deeper unsaturated zone as a repository for nuclear waste. In areas where recharge is significant, seepage from hazardous wastes could contaminate underlying aquifers.

In addition to recharge rates, mechanical mixing of fluid parcels and molecular diffusion of solutes affect contaminant migration in the unsaturated zone. This kind of mixing, called hydrodynamic dispersion, causes spreading and dilution of the solute.

Thus, knowledge of groundwater recharge rates and of the dispersive processes occurring during partially saturated flow are essential prior to identifying sites for waste disposal.

The major objectives of this study are to:

1. quantify groundwater recharge rates through the unsaturated zone by using chloride in soil water and by measuring 36Cl and 3H released in the environment by atmospheric nuclear weapons testing,
2. compare groundwater recharge rates obtained using 36Cl and 3H with those obtained using physical techniques at the same location,
3. study vapor transport by comparing the relative movement of 36Cl and 3H, and
4. use the data obtained from the isotope tracing to determine soil-dispersive properties.

BACKGROUND

Chlorine-36 Production and Fallout

Chlorine-36 is an unstable isotope of chlorine with a half-life of 3.01 x 10^5 years. It is continuously produced in the terrestrial environment in small amounts. Chlorine-36 of natural atmospheric origin is derived from cosmic-ray spallation of 40Ar by the reaction 40Ar(x,x'α)36Cl and neutron activation of 36Ar through the reaction 36Ar(n,p)36Cl (Bentley, Phillips, and Davis 1986).Production of 36Cl at the earth's surface is predominantly from spallation of K and Ca, and neutron activation of 35Cl. Neutrons are produced at the earth's surface by cosmic-ray spallation and from decay of elements in the uranium and thorium decay series (Bentley et al. 1986). Chlorine-36 is also produced in the deep subsurface by neutron activation of 35Cl. The major source of neutrons in the deep subsurface is decay of uranium and thorium series elements (Bentley et al. 1986).

Chlorine-36 was also produced in large amounts by neutron activation of marine 35Cl and released into the environment during atmospheric nuclear weapons testing in the 1950's and 1960's. This anthropogenic 36Cl is referred to as "bomb-36Cl".

Two-thirds of the total atmospheric production of 36Cl is in the stratosphere (Bentley et al. 1986). Nuclides are transferred from the stratosphere to the troposphere during periods of vertical mixing that occur during the winter and early spring (Feely and Seitz 1970; Peterson 1970). Because transfer is associated with seasonal mixing, 36Cl fallout is expected to vary with latitude (figure 1). Bomb-36Cl should also show this variation if the

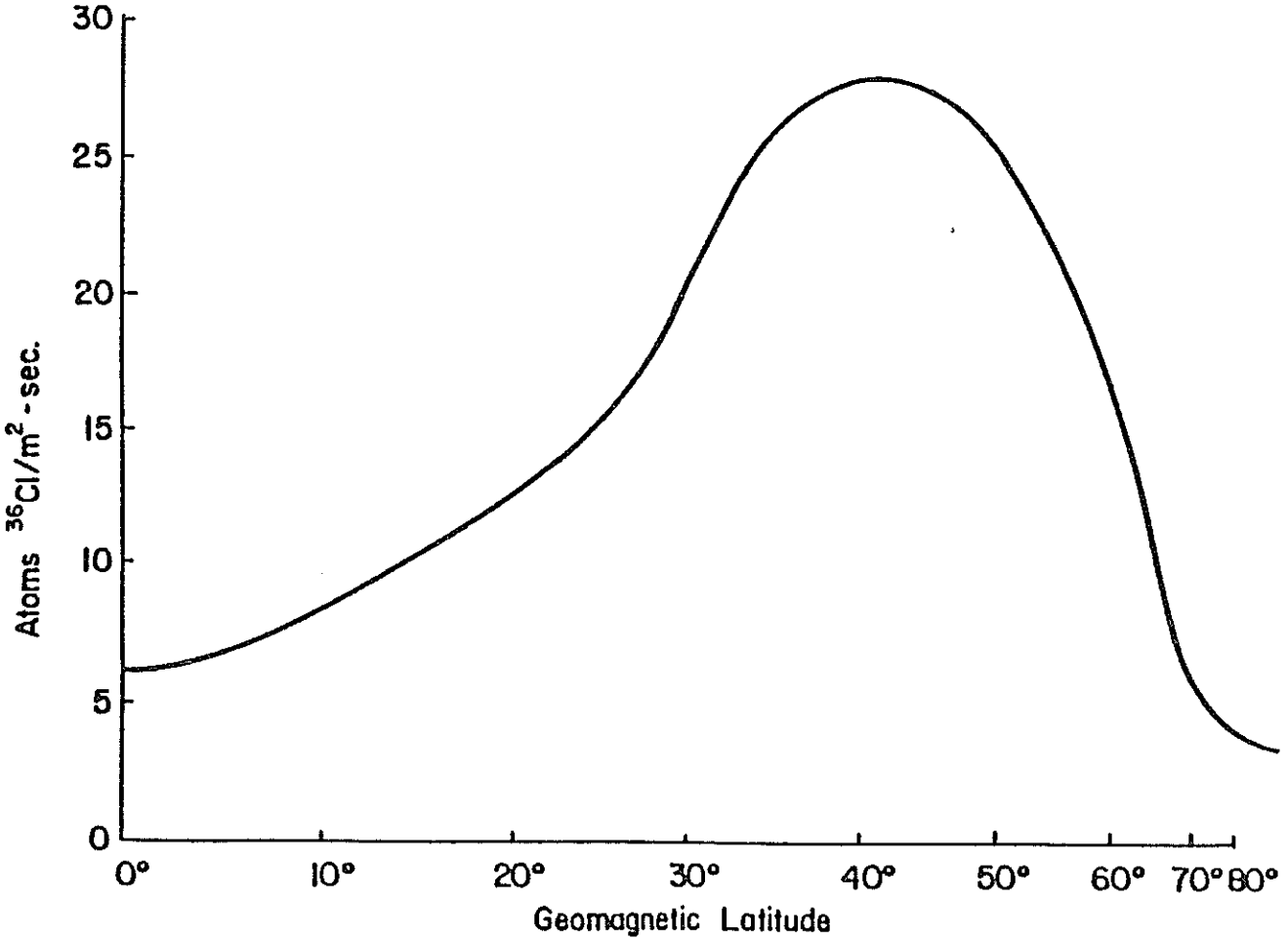

Fig. 1. Meteoric 36Cl fallout as a function of latitude. From Bentley et al. (1986).

test explosion clouds penetrated the stratosphere. The variation of bomb-36Cl fallout has been calculated from the data of Peterson (1970) and from bomb-36Cl injection data (Bentley et al. 1982), and is illustrated in figure 2. Once 36Cl reaches the troposphere, it mixes with stable chloride derived from sea spray and is then removed from the troposphere by rainfall and dry deposition. The mean residence time is about one week (Bentley and Davis 1982).

By superimposing the latitudinal variation of pre-bomb 36Cl on the continental variation of stable chloride, Bentley and Davis (1982) calculated 36Cl/Cl fallout ratios for the United States (figure 3).

Bomb-36Cl fallout (figure 4) was calculated on the basis of an atmospheric box model. Only explosions which occurred near large amounts of chloride and whose radioactive clouds penetrated the stratosphere were used as input for the model (Bentley et al. 1986).

Because of its long half-life, 36Cl is suitable for many geologic applications. Until recently, however, the natural abundance of 36Cl has often been below the sensitivity limits of standard decay-counting techniques, thus limiting its use. With the application of tandem accelerator mass spectrometry (TAMS) to 36Cl analysis, all natural samples, excluding marine salts, are now within the range of detection (Bentley et al. 1986).

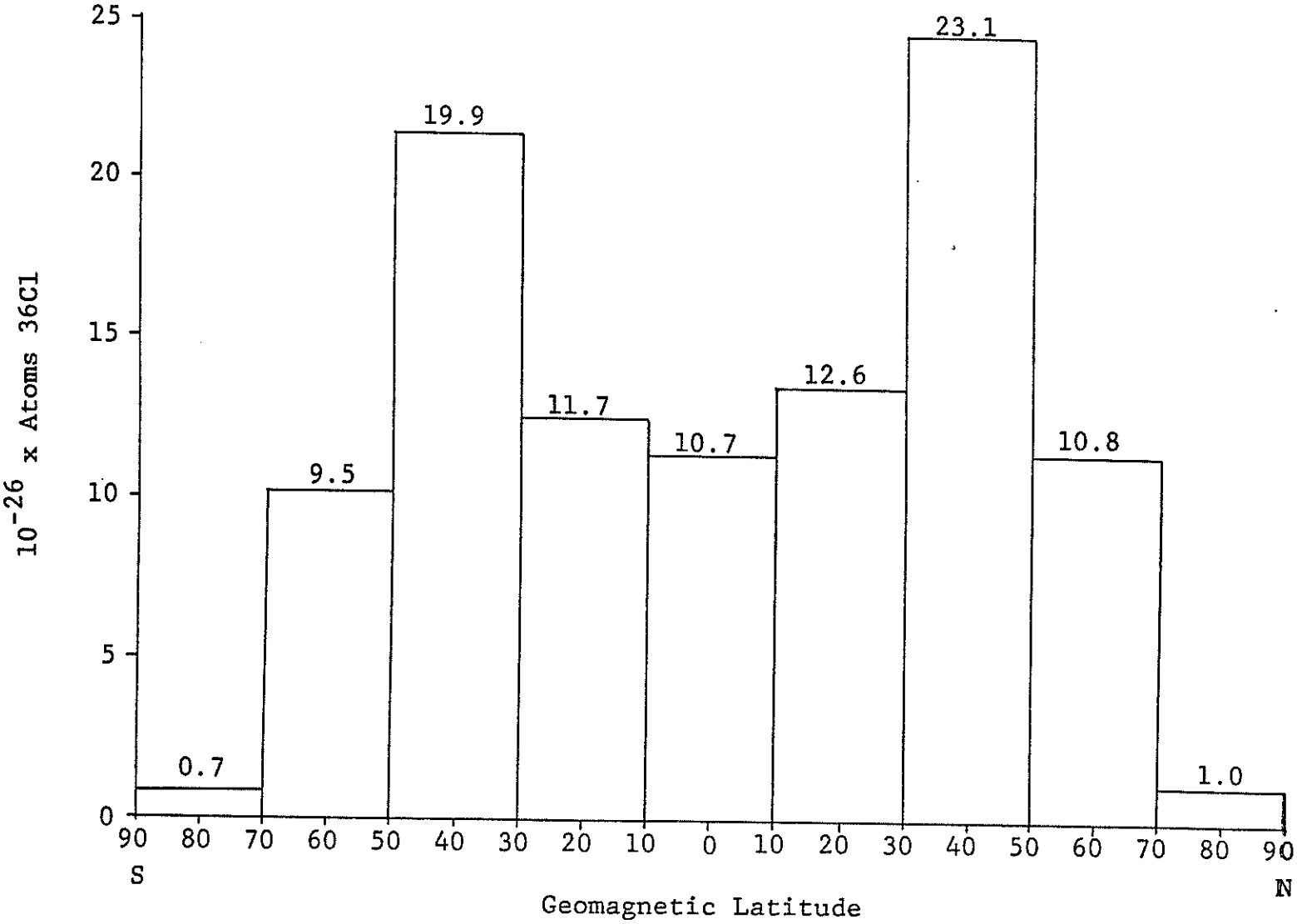

Fig. 2. Bomb-36Cl fallout with latitude. Numbers represent percentage of total global fallout.

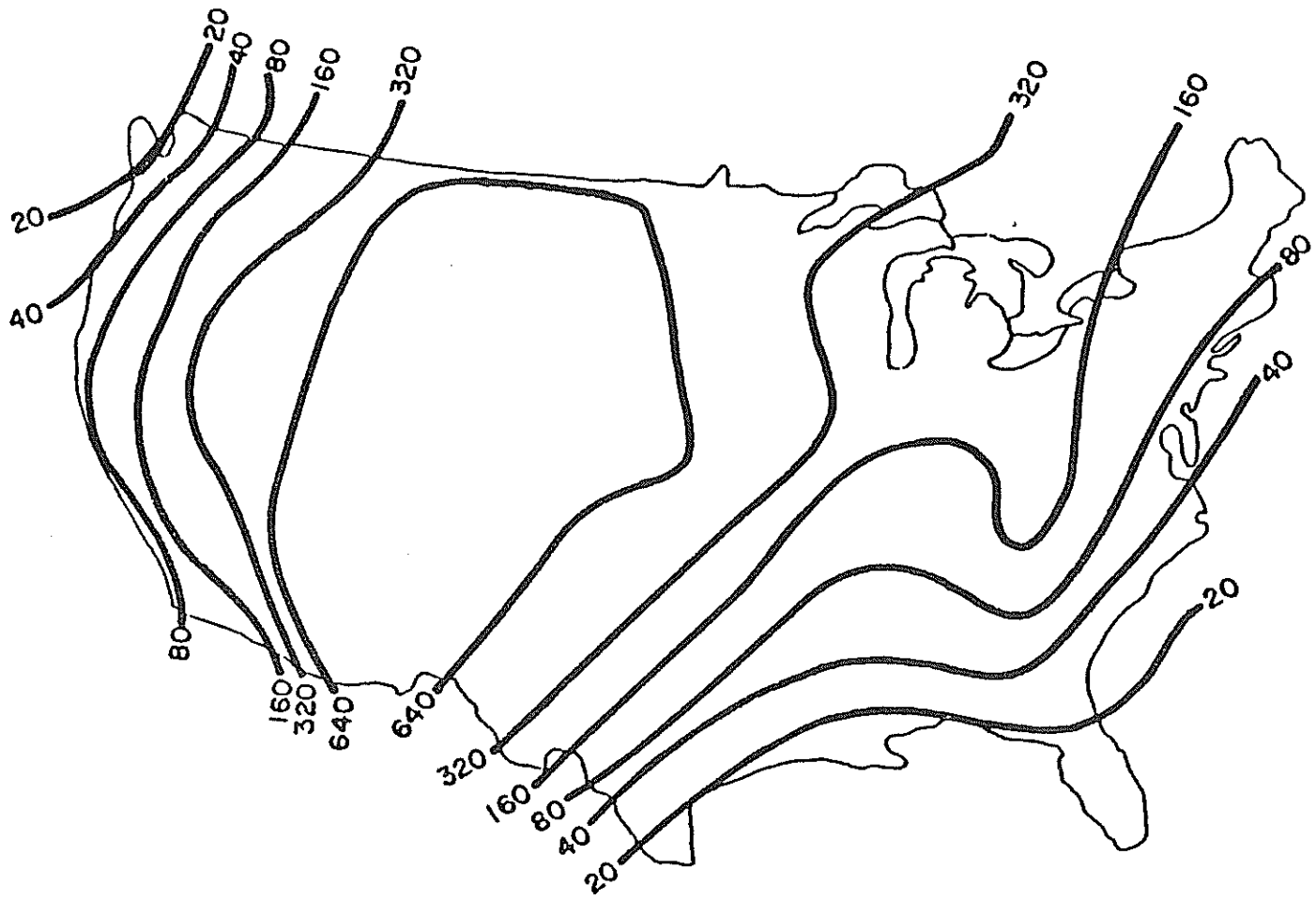

Fig. 3. Calculated pre-bomb $^{36}Cl/Cl$ ($\times 10^{15}$) fallout ratios. From Bentley and Davis (1982).

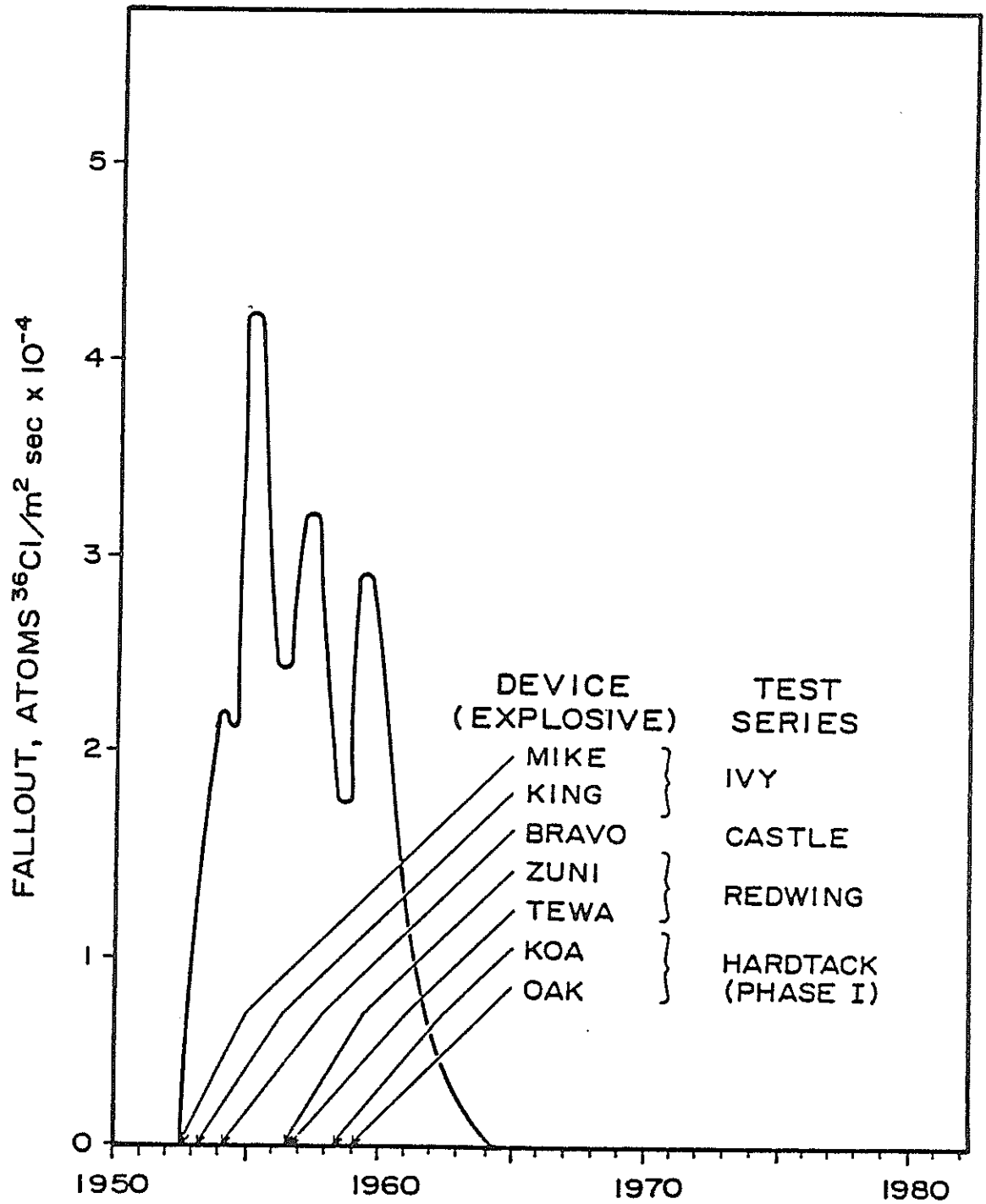

Fig. 4. Bomb-36Cl fallout between 30°N and 50°N latitude. From Bentley et al. (1986).

Tritium Production and Fallout

Tritium is an unstable isotope of hydrogen with a half-life of 12.45 years. It is naturally produced in the atmosphere by the reaction $^{14}_{7}N$ (n, $^{3}_{1}H$)$^{12}_{6}C$. Random collisions between 3H atoms and oxygen atoms occur in the stratosphere to form tritiated-water molecules. Subsequently, they precipitate out of the atmosphere and enter the hydrologic cycle.

Terrestrial nuclear weapons testing in the South Pacific and the USSR during the mid- to late-1950s and stratospheric tests over the arctic circle in the early 1960s increased the concentration of 3H in rainfall by as much as two orders of magnitude over natural background levels of 4 to 25 T.U. (1 T.U. = 1 ^{3}H in 10^{18} H). This anthropogenic 3H is referred to as "bomb-3H". Tritium fallout declined exponentially after atmospheric nuclear weapons tests were banned in 1963 and has reached an annual value of approximately 25 T.U. today. Figure 5 shows the variation of bomb-3H fallout as a function of time and latitude.

Figure 6 is the variation in 3H concentration of precipitation as a function of time for New Mexico. The data were compiled from 3H concentrations in rainfall measured in the Socorro area between late 1956 and 1976 and from measurements made by the U.S. Geological Survey of 3H fallout in Albuquerque, New Mexico. Gaps in the 3H fallout record were filled using data collected in Ottawa, Ontario since there is good correlation between Ottawa and Socorro fallout (Rabinowitz et al. 1977). Figure 7 illustrates the seasonal variation of 3H fallout. Tritium fallout is relatively high during the winter and spring and decreases during the summer.

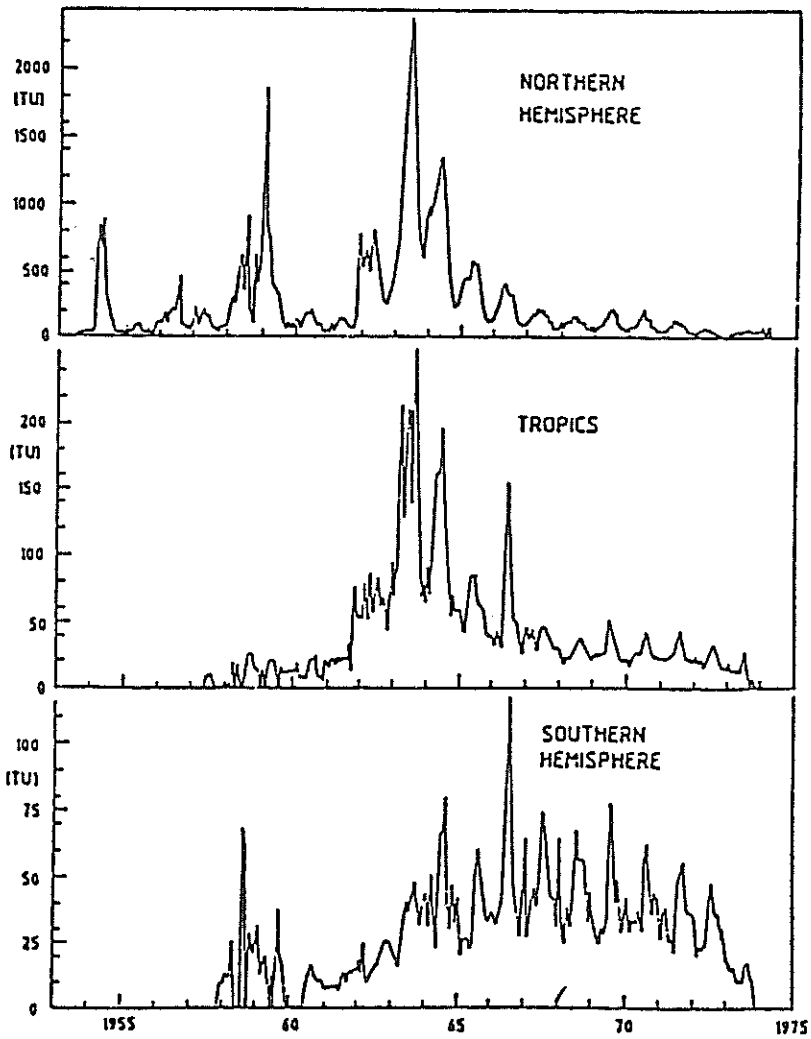

Figure 5. Variation of 3H Fallout as a function of time and latitude (IAEA Tech. Report, 1983).

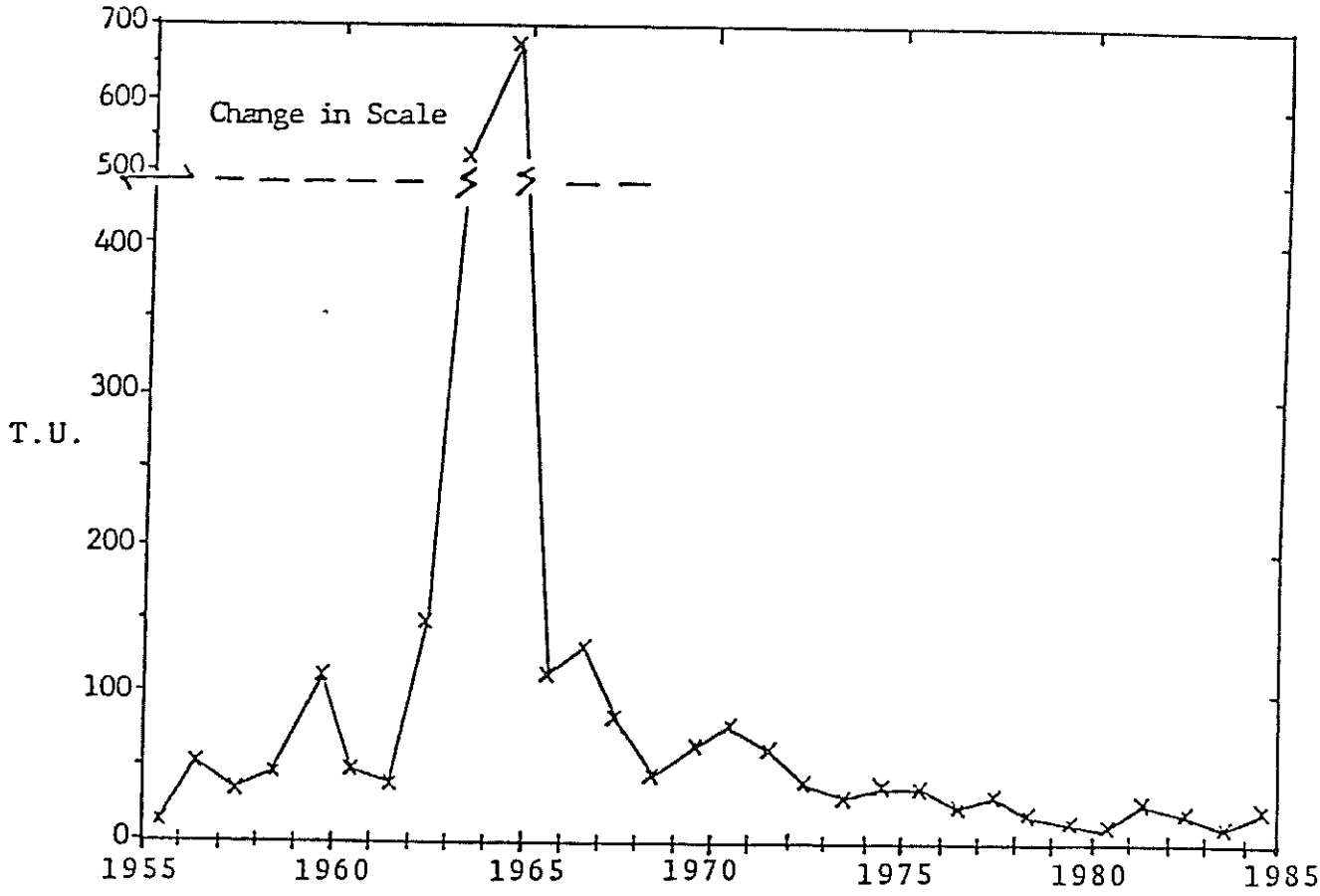

Fig. 6. Annual tritium concentration in New Mexico precipitation. From Duval (1986).

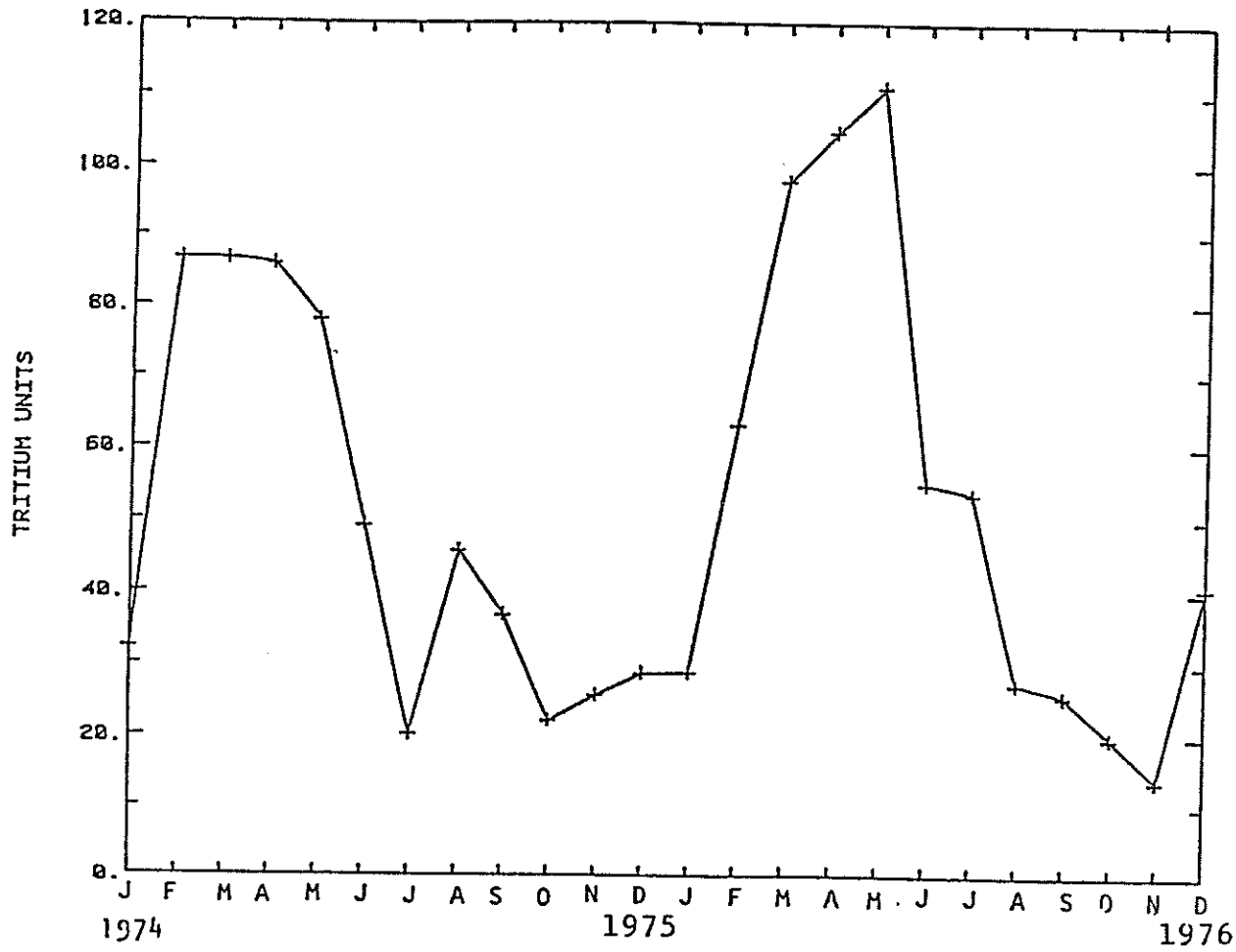

Fig. 7. Monthly variation of tritium concentration in New Mexico precipitation during 1974 and 1975. From Duval (1986).

Tritium and Chlorine-36 as Tracers

Bomb-3H and -36Cl fallout have provided tracers for downward movement of soil water through the unsaturated zone. In arid regions where the pulses have not yet entered the groundwater, they should provide measures of recharge rates.

Although 3H is considered to be an excellent tracer, there are processes which influence the movement of 3H through the soil. One such process is the retention of 3H in an immobile water phase around clay particles. Retardation may be caused by some isotopic exchange of 3H with crystal-lattice hydroxyls of the clay fraction or by replacement of exchangeable cations by 3H (Nielsen and Biggar 1962; Biggar and Nielsen 1962; van Genuchten and Wierenga 1977; Rabinowitz et al. 1971). In addition, Ehhalt (1973) reported that biological activity in the soil may be an additional source of 3H, thus possibly maintaining vadose zone levels of 3H above atmospheric concentrations.

Because of 3H's short half-life, the use of bomb-3H as a hydrologic tracer is relatively temporary. In the southern hemisphere the bomb pulse has already decayed to within 15 tritium units of natural background and in the northern hemisphere, bomb-3H will be difficult to detect in 30 to 40 years (Bentley et al. 1986).

Chloride is considered to be an excellent tracer due to its hydrophylic and unreactive nature. Chloride movement, however, is also affected by processes occurring in the soil. Studies have shown that in soils with high clay contents the rate of chloride movement increases relative to water movement due to anion repulsion by negatively charged soil particle surfaces (Thomas and Swoboda 1970; Krupp, Biggar, and Nielsen 1972; Nielsen and Biggar 1962).

Bomb-36Cl offers certain advantages over bomb-3H as a hydrologic tracer. For example, 36Cl with its long half-life will be easily detected for many

years. Furthermore, there will be no need to separate the effects of radioactive decay from those of dispersion.

Unlike 3H, 36Cl is not subject to vapor transport. In arid climates, where vapor-phase transport may be a significant component of soil-water transport, vapor diffusion will disperse the bomb-3H pulse, resulting in a larger apparent dispersion. Although vapor transport is useful when tracing soil-moisture movement, it will not accurately define solute dispersion or transport.

Finally, the bomb-36Cl input function was simpler. It can be approximated by a square-wave pulse whereas 3H input is multi-pulsed with considerable tailing.

Recharge Estimates Using Soil Chloride, Chlorine-36, and Tritium

Allison (1981) described two different methods available for obtaining values of the mean annual recharge using the bomb profiles. First, assuming piston flow, a steady-state moisture content, and that the isotopes move with the mass fluid flow, recharge may be evaluated by dividing the total amount of water in the profile above the peak by the time elapsed since the fallout peak. In the second method, where the 1962-1965 3H peak can be identified, local mean annual recharge (R) can be evaluated by a mass balance on the tritium:

$$\bar{R}=T/TA \ . \qquad (1)$$

T is the total quantity of 3H stored in the soil profile and is evaluated by the expression

$$T = \int_0^1 Tz\theta z \ dz$$

where l is the depth where virtually no 3H remains (because of radioactive decay) and Tz and Oz are the 3H concentration and volumetric moisture content respectively at a distance z below the surface. TA is given by

$$TA = \sum_{i=1}^{\infty} Wi\ Tpi\ \exp(-i\lambda)$$

where Tpi is the 3H concentration of recharge water i years before sampling, λ is the decay constant for 3H (0.0565/yr) and Wi is a weighting factor which takes year-to-year variations of recharge into account. Allison and Hughes (1978) tested three different weighting schemes based on: (1) the amount of winter rainfall, (2) groundwater fluctuations, and (3) evapotranspirational loss from the soil. They found that although the three different factors gave different weights to each year's recharge, there was little difference in the total 3H added to the soil profile. They therefore considered it unnecessary to use weights other than one.

For comparison with recharge estimates obtained from the bomb peaks, a mass balance on the chloride ion was used to determine net infiltration. The mass-balance argument states that the difference between the chloride concentration of the soil water and the atmospheric input concentration is due to evapotranspirative enrichment. The travel time to the bottom of the ith soil depth interval is given by

$$t = \sum_{i} \frac{\rho_B M_i d_i}{CoP}$$

where ρ_B is the dry bulk density, M the chloride concentration (in mg chloride/kg soil), d the interval length, Co the atmospheric input chloride concentration, and P the annual precipitation (Phillips et al. 1984). Recharge rates determined from the amount of chloride in soil water of the unsaturated zone are considered estimates because it is assumed that: (1) recharge occurs by piston flow (ie. water moves through the soil matrix and not through preferred pathways), (2) flow is one-dimensional and vertical, (3) precipitation is the only source of chloride entering the system, (4) the chloride content of precipitation has remained constant through the time represented by the samples, and (5) average precipitation has remained constant during this time (Stone 1984). Recharge, R, (L/T) is determined from the relationship

$$R=(Co/Clsw) \times P \qquad (3)$$

where Clsw=Chloride concentration in the soil water (mg/l).

RELATED STUDIES

Movement of moisture in the unsaturated zone has been the subject of numerous studies.

Scholl (1976) used soil hydraulic properties and the distribution of moisture in the soil with time and depth to predict the rate of moisture drainage and evapotranspiration under a chaparral stand in central Arizona. The first year of his study was unusually dry and the water balance procedure calculated that ground-water recharge was only 2 percent of the annual precipitation. The second year was unusually wet and approximately 20 percent of the annual precipitation infiltrated below the root zone.

Sammis et al. (1982) compared three methods of estimating infiltration rates beneath the root zone on irrigated land near Phoenix, Arizona. Their three methods included solutions of Darcy's equation, temperature profiles and tracing of bomb-3H which yielded rates of 18, 9 and 40 cm per year respectively.

Stephens et al. (1985) studied the amount of recharge by direct infiltration of precipitation in a desert area near Socorro, New Mexico. Instrumentation was placed in fifteen different locations so that differences in soil moisture movement due to vegetation, topography, and surficial geology could be studied. Instrumentation allowed field measurement of pressure heads, water-content profiles, temperature-depth profiles, water-table elevations and meteorological conditions as a function of time. Groundwater recharge rates calculated using Darcy's equation varied from approximately 5 to 29 percent of the annual precipitation depending upon the method used to average hydraulic conductivities.

Schmalz and Polzer (1969) used bomb-3H to study the movement of water in unsaturated soil. They concluded that approximately 3.5 percent of the 3H which occurred at the southeastern Idaho location remained in the top 200 cm of the

soil profile while the rest was lost by evaporation or transpiration. Using a mathematical model, they calculated hydrodynamic dispersion coefficients which varied within a range of 0.9×10^{-6} and 9×10^{-6} cm^2/sec. Calculated seepage velocities varied between 8 and 10.4 cm per three-month period.

Allison and Hughes (1978) estimated mean annual recharge to a southern Australian aquifer using both the bomb-3H concentration and the chloride concentration of water within the soil profile. They found good agreement between the two methods with local recharge varying between 50 and 250 mm per year.

Dincer et al. (1974) studied infiltration through the Dahna sand dunes in Saudi Arabia using 3H. Their results indicated that approximately 25 percent of the 7 cm of annual precipitation became recharge. In addition, they recognized water transport in both the liquid and vapor phases. The soil profile was divided into two zones, a near-surface zone with relatively low moisture contents and large temperature gradients and a deep zone with relatively high moisture contents and small temperature gradients. Water in the near-surface zone moved under the influence of temperature gradients in both the gaseous and liquid phases. Moisture movement in the deep zone was assumed to be gravity driven.

Sharma and Hughes (1985) monitored the depth distributions of environmental chloride, deuterium and oxygen-18 in deep coastal sands of Western Australia. By using a steady-state model based on conservation of chloride, they estimated the average areal recharge to be 15 percent of the average annual precipitation, which amounts to 80 cm/yr. In addition, based on a mixing model and chloride data, they indicated that some 50 percent of the recharging water may be moving through preferred pathways.

Phillips et al. (1984) used the bomb-36Cl pulse as a tracer for soil-water movement near Socorro, New Mexico. Chloride was leached out of soil samples from a vertical auger hole in a sandy loam. The bomb-36Cl pulse was identified at a depth of about one meter, indicating a net infiltration to that depth of 2.5 mm/yr out of 22 cm/yr precipitation.

For additional studies using chloride and tritium to trace soil-moisture movement, the interested reader is referred to the following: Allison and Hughes (1983); Allison (1981); Hendry (1983); Foster and Smith-Carington (1980); Allison, Stone, and Hughes (1985).

VAPOR TRANSPORT

In addition to mass flow, vapor transfer is a mechanism of water movement in unsaturated soils. Because 36Cl moves only in the liquid phase as a dissolved solute and tritium moves in both liquid and vapor phases, the relative positions of bomb-36Cl and -3H peaks at a given location enable study of vapor transport.

Gurr et al. (1952) attempted to separate liquid and vapor flow due to a temperature gradient by monitoring salt movement in soil columns. At the end of the experiment, in all except the wettest and driest cases, they observed a transfer of water toward the cool end and of chloride toward the warm end of the column. Assuming that chloride is transported in the liquid phase, they concluded that liquid flow due to pressure gradients was in the direction of cold to hot and that the net movement of water in the opposite direction must be due to vapor flow induced by temperature gradients.

Philip and de Vries (1957) pointed out that vapor transport studies by Gurr et al. (1952) and other workers implied that observed water vapor transport under temperature gradients far exceeded that predicted by the theory of vapor diffusion in porous media. In order to explain this, as well as the effect of moisture content on net moisture transfer, and the transfer of latent heat by distillation, Philip and de Vries (1957) developed a theory of moisture movement in porous materials under temperature gradients. Their analysis extended the simple theory of vapor diffusion in porous media to give a separation of the isothermal and thermal components of vapor transfer and the effect of soil-water pressure on vapor transfer. This was then integrated with the theory of liquid movement in porous media under temperature and moisture gradients to provide a general theory of liquid and vapor transfer. The final equation describing moisture and heat transfer under combined moisture and temperature gradients in

porous materials is given by

$$q = -(DTliq + DTvap)\,T - (D\theta liq + D\theta vap)\nabla\theta - Ki \qquad (4)$$

where q =total soil-water flux (liquid and vapor) (L/T)

DTliq=thermal liquid diffusion coefficient (L^2/T^oC)

DTvap=thermal vapor diffusion coefficient (L^2/T^oC)

T =thermal gradient ($^oC/L$)

$D\theta liq$=isothermal liquid diffusion coefficient (L^2/T)

($D\theta liq = K(\partial\Psi/\partial\theta)$)

$D\theta vap$=isothermal vapor diffusion coefficient (L^2/T)

$\nabla\theta$ =volumetric moisture content gradient (L^{-1})

K =hydraulic conductivity (L/T)

i =unit vector in the positive z direction

Conceptually, they explained that for low water contents, the liquid water is discontinuous and forms "liquid islands" between grains. The curvature of the menisci at each end of an island are equal when it is in thermodynamic equilibrium. A thermally-induced vapor-pressure gradient producing a vapor flux results in condensation and decreased curvature of the meniscus at the upstream end of the island and evaporation and increased curvature of the meniscus at the downstream end of the island. This continues until the capillary flow through the island equals the rates of condensation and evaporation. They regard moisture movement under temperature gradients as a "series-parallel process of flow through regions of vapor and liquid". A vapor-pressure gradient

across air-filled pores determines the vapor flux while flow through liquid islands adjusts itself to equal the vapor flux. If the moisture content increases enough, vapor islands exist in a liquid continuum and liquid phase transfer is dominant.

Jackson et al. (1974) analyzed diurnal soil-water fluxes near the soil surface using the theory of Philip and de Vries. When the soil was both relatively wet (.05-.15 g/g) and relatively dry (.02-.04 g/g), isothermal components governed moisture transfer. Under intermediate moisture content conditions (.03-.07 g/g), however, moisture transfer due to temperature gradients reached a maximum value.

Milly (1984) conducted a sensitivity analysis, by means of numerical simulation, to quantify thermal effects on evaporation from soils. He concluded that the effect of thermal liquid flux was least important and neglecting it lead to errors in computed evaporation of only 1 percent. Thermal vapor diffusion suppressed average evaporation by 5 to 15 percent under arid conditions and neglecting thermal vapor diffusion gave rise to errors in the diurnal variation of evaporation. The variation of moisture transport coefficients with temperature also introduced error. In addition, Milly (1984) concluded that the elimination of all thermal effects yielded a more accurate prediction of evaporation from soils than the elimination of only one important thermal effect. This result is because the two most important thermal effects, (thermal vapor diffusion and variation of transport coefficients with temperature) tend to cancel each other out in both the diurnal variations and in the daily average values.

DISPERSION IN POROUS MEDIA

Solute movement is, in large part, attributed to soil-water advection. The rate of transport is equal to the average linear velocity, $\bar{v}$. $\bar{v}=v/\theta$ where $v=-Kdh/dx$ is Darcy's equation and θ is volumetric moisture content. As previously mentioned, however, solutes tend to spread out from the path that they would be expected to follow due to advective flow. This spreading phenomenon, called hydrodynamic dispersion, occurs because of mechanical mixing of fluid parcels and molecular diffusion of solutes.

Mechanical mixing or dispersion results from microscopic nonuniformities in flow velocity in the soil's pores. These nonuniformities are caused by differences in pore sizes, frictional drag along pore walls, and tortuosity and branching of pore channels. Mathematically, the mechanical dispersive flux, Jm, can be expressed as a Fickian-type law

$$Jm = - \theta Dm \frac{\partial c}{\partial x}$$

in which Dm is the coefficient of mechanical dispersion (L^2/T) and $\partial c/\partial x$ is the concentration gradient (Bear 1979). For saturated conditions, this coefficient Dm has been found to be linearly related to the average flow velocity $\bar{v}$ (Freeze and Cherry 1979). Thus,

$$Dm = \alpha \bar{v}$$

where α is a characteristic property of the porous medium called

dispersivity (L) (Freeze and Cherry 1979).

Diffusion processes occur when concentration gradients exist and solutes move from where their concentration is higher to where it is lower. The flux, Jd, due to molecular diffusion in a porous medium can be expressed by Fick's law

$$Jd = -D^* \frac{\partial c}{\partial x}$$

where D* is the coefficient of molecular diffusion in a partially saturated porous medium. D* is strongly dependent upon the volumetric moisture content. According to Hillel (1980) as soil moisture decreases, the volume of water available for liquid phase diffusion decreases while the tortuous path length increases. Thus,

$$D^* = D_o \theta \tau(\theta)$$

where Do is the diffusion coefficient for the solute diffusing in bulk water, θ is the volumetric moisture content and $\tau(\theta)$ is tortuosity of the porous medium (a function of the moisture content).

The effects of mechanical dispersion and molecular diffusion are assumed to be additive and are combined into a single term, the hydrodynamic dispersion coefficient, D.

$$D = Dm + D^*$$

Wilson and Gelhar (1974) investigated several different types of hydrodynamic-dispersion-coefficient behavior. By using laboratory column-experiment results and analytical solutions developed for steady unsaturated flow, they compared the effects of a constant coefficient during one-dimensional adsorption with coefficients that depended on seepage velocities which varied with volumetric moisture content. The constant coefficient represented an integral amount of dispersion which occurred specifically during a field transient-infiltration test. It produced significantly less dispersion than the other coefficients, illustrating the danger of using a constant coefficient representing a particular flow situation in an altogether different situation.

In addition, they examined dispersion during one-dimensional, steady vertical infiltration by investigating the movement of a unit pulse with different surface moisture boundary conditions and different moisture fluxes. They concluded that when velocities are low, molecular diffusion predominates over mechanical dispersion and greater mixing occurs in zones of higher moisture content. But, when velocities are higher, mechanical dispersion is dominant and greater mixing occurs in zones of lower moisture content. As effective saturation increased, the value of Dm initially increased then leveled out and finally decreased. The amount of rise increased with Peclet number. (Peclet number=$\bar{v}l/D^*$, where l is a characteristic pore length).

The differential equation governing one-dimensional solute transport in a variably saturated porous medium is

$$\frac{\partial(\theta c)}{\partial t} = \frac{\partial}{\partial z}\left[D\theta \frac{\partial c}{\partial z} \right] - \frac{\partial(qc)}{\partial z}$$

where

c=solution concentration (M/L^3)

D=hydrodynamic dispersion coefficient (L^2/T)

q=volumetric flux of water (L/T)

θ=volumetric moisture content (L^3/L^3)

Numerous studies have sought to solve this equation both analytically and numerically using both laboratory and field experiments (van Genuchten and Wierenga 1976; Kirda et al. 1973; Gupta and Singh 1980; DeSmedt and Wierenga 1984).

De Smedt and Wierenga (1978) presented an approximate analytical solution for solute transfer during infiltration and redistribution. Their solution included a hydrodynamic dispersion coefficient which varied linearly with velocity. The solution, however, did not account for ion exchange or an immobile water phase. Comparison of numerical and analytical results showed that the approximate solution is best used during the infiltration phase but provides only a rough estimate of the solute distribution during the redistribution phase.

Warrick et al. (1971) studied the transfer of $CaCl_2$ and water during infiltration. By coupling the equations of solute transport and water flow through an unsaturated soil, field results were quantitatively predicted. The simulation indicated hydrodynamic-dispersion coefficients from 8.0×10^{-4} to $1.0 \times 10^{-3} cm^{-2}/s$ best approximated the field data. The dispersion coefficient increased with time or with the distance the solute traveled. In addition, solute travel was found to be nearly independent of the initial moisture content but to vary with the infiltration rate.

Phillips et al. (1984) used bomb-36Cl and an analytical solution of the one-dimensional advective-dispersive equation to determine soil-dispersive properties near Socorro, New Mexico. They approximated an eight-year solute input as a square wave and best matched the observed 36Cl profile using a hydrodynamic dispersion coefficient of $6.0 \times 10^{-7} cm^2/s$.

Andersen and Sevel (1974), at a larger scale, used bomb-3H to determine the dispersive properties of glaciofluvial outwash materials in Denmark. Using a displacement flow model with dispersion, they found a dispersion coefficient equal to $10^{-3} cm^2/s$ best fit measured 3H profiles.

SITE SELECTIONS AND DESCRIPTIONS

The study was conducted at two locations in New Mexico, the Sevilleta National Wildlife Refuge (SNWR) and the New Mexico State University ranch (NMSUR). These sites were selected because they have been intensively investigated with soil-physics instrumentation, thus allowing comparison of geochemically and physically determined infiltration rates.

The SNWR is located approximately 24 kilometers north of Socorro, New Mexico (figure. 8). The research site is approximately 5 kilometers west of Interstate 25, just south of the Rio Salado.

Figure 9 shows the locations of soil-physics instrumentation sites, the isotope-sampling site, topography and soil types. Vegetation includes indigo bush, saltbush, creosote, mesquite, prickly pear, salt cedar and various grasses.

The climate of the Socorro area is arid. The average annual precipitation is 22 cm while annual potential evaporation is 160 cm. Precipitation in the summer is usually from localized convective storms. Moisture for these storms is from the Gulf of Mexico. Winter precipitation originates in the Pacific Ocean as cyclonic storms.

Seasonal variations in temperature are large with summer highs near 40° C and winter lows near 0°C.

The NMSUR is located 40 kilometers northeast of Las Cruces (figure 10). Figure 11 shows the 2700 m transect along which measurement stations were established every 30 m. Rainfall and maximum and minimum air temperature are

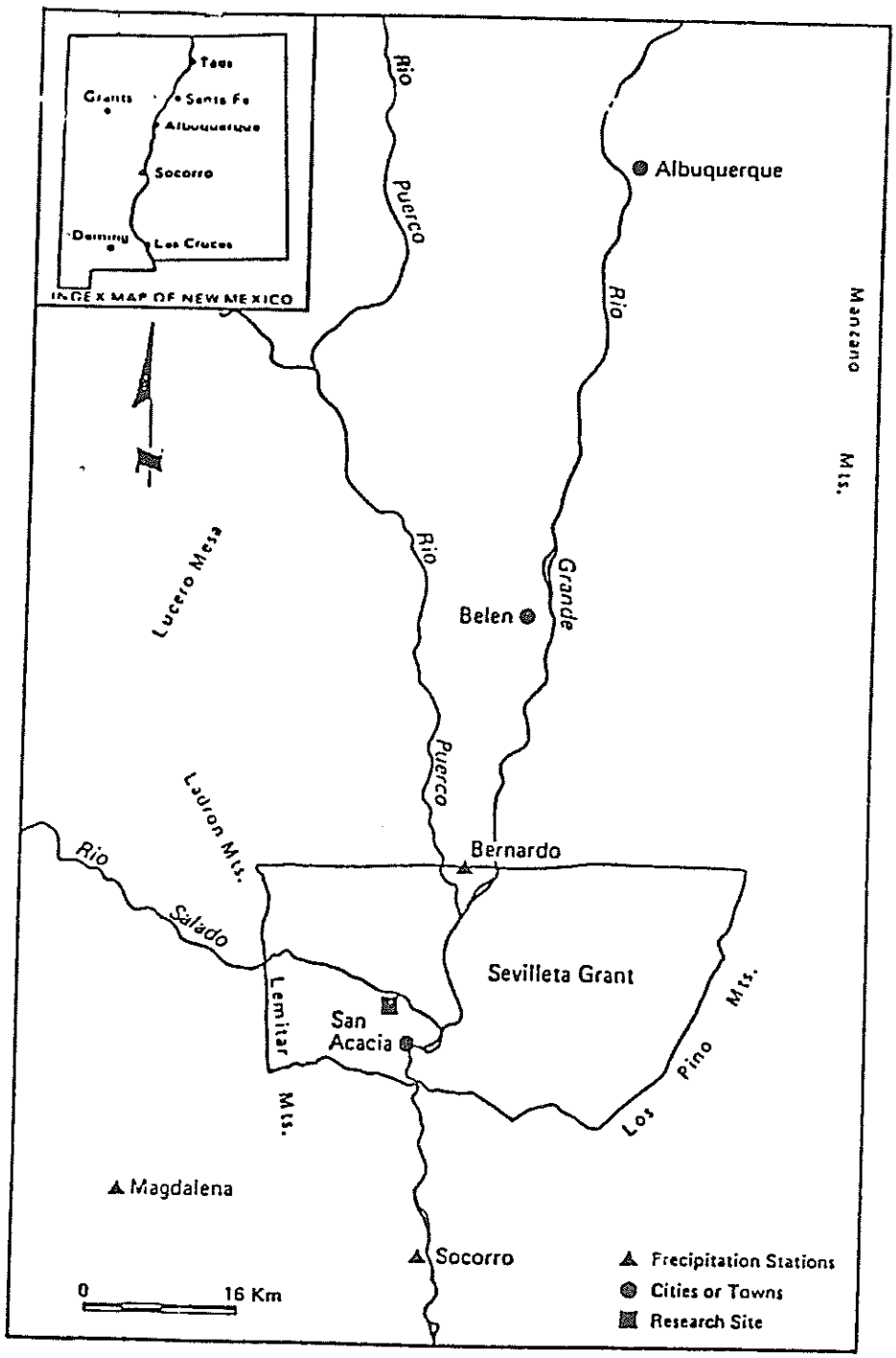

Fig. 8. Location of the Sevilleta National Wildlife Refuge. From Stephens et al. (1985).

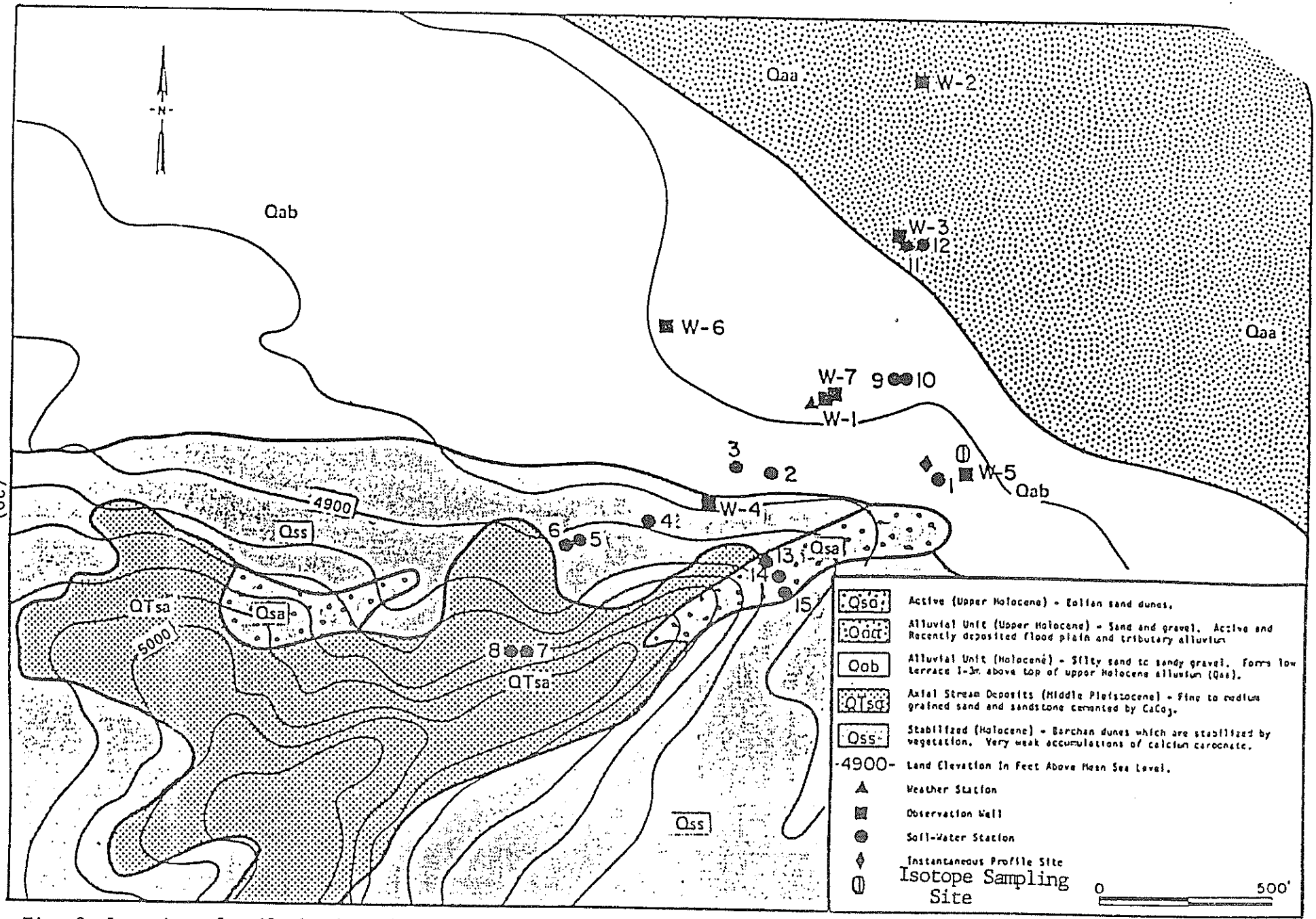

Fig. 9. Location of soil-physics instrumentation at the SNWR. The isotope-sampling site is approximately 15 m northeast of soil-water station 1. From Stephens et al. (1985).

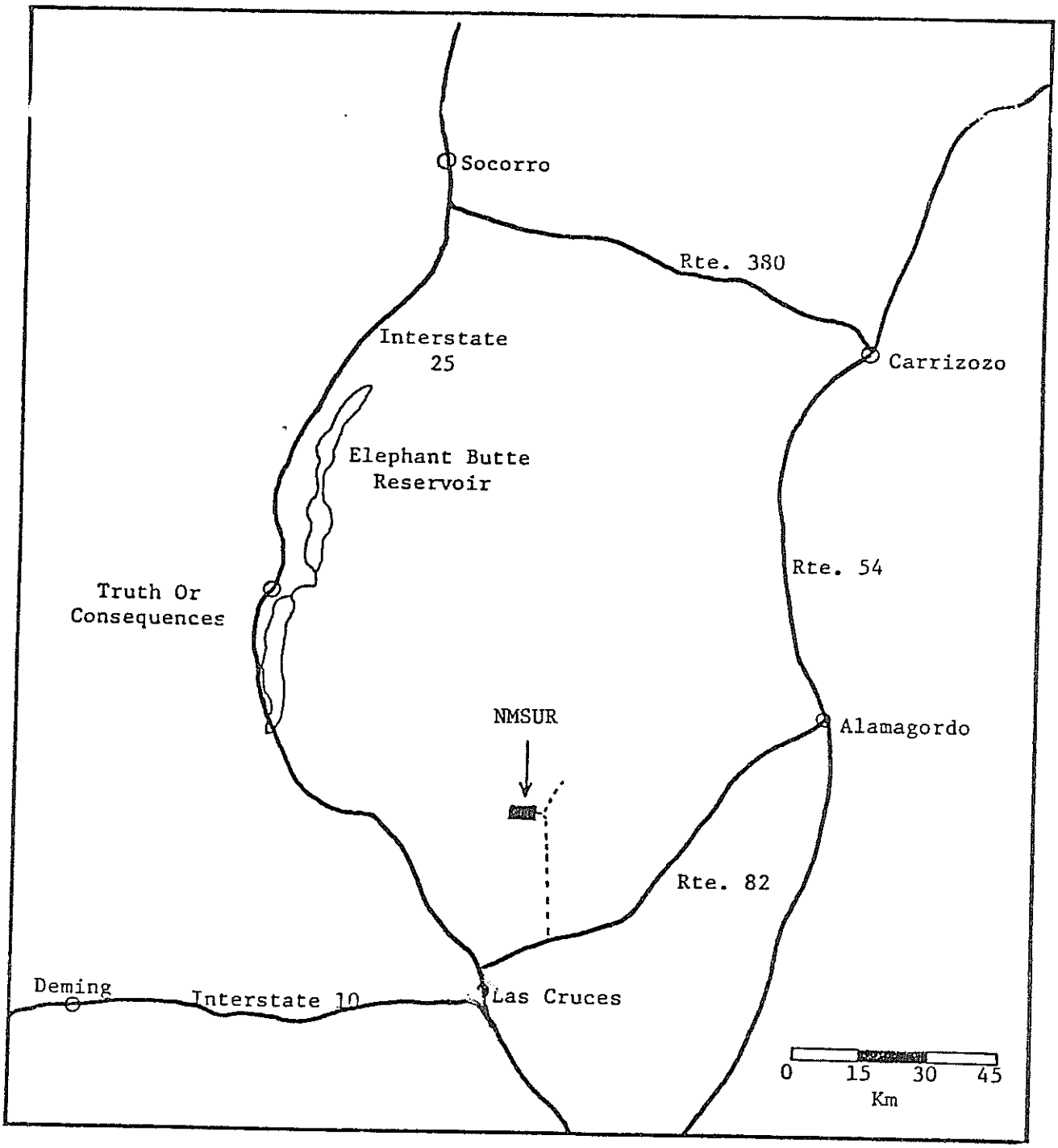

Fig. 10. Location of the NMSUR research site. From Duval (1986).

measured at each station weekly while soil moisture is measured at two week intervals. Near the center of the transect, solar radiation, precipitation, wind speed and direction, relative humidity, and air and soil temperature are measured continuously (Wierenga et al. 1985). The three basic landforms and their associated surfaces traversed by the transect are also shown in figure 11. The isotope sampling site is located approximately 3 m northwest of the transect on the piedmont slopes. Vegetation at the sampling site consists mainly of perennial forbs and grasses and creosote.

The climate in the region is arid. The average annual precipitation is 22 cm while average Class-A pan evaporation is 239 cm. Fifty percent of the rainfall occurs between July and September.

The maximum air temperature is highest in June at 36^{o}C, and lowest in January at 13^{o} C (Wierenga et al. 1985).

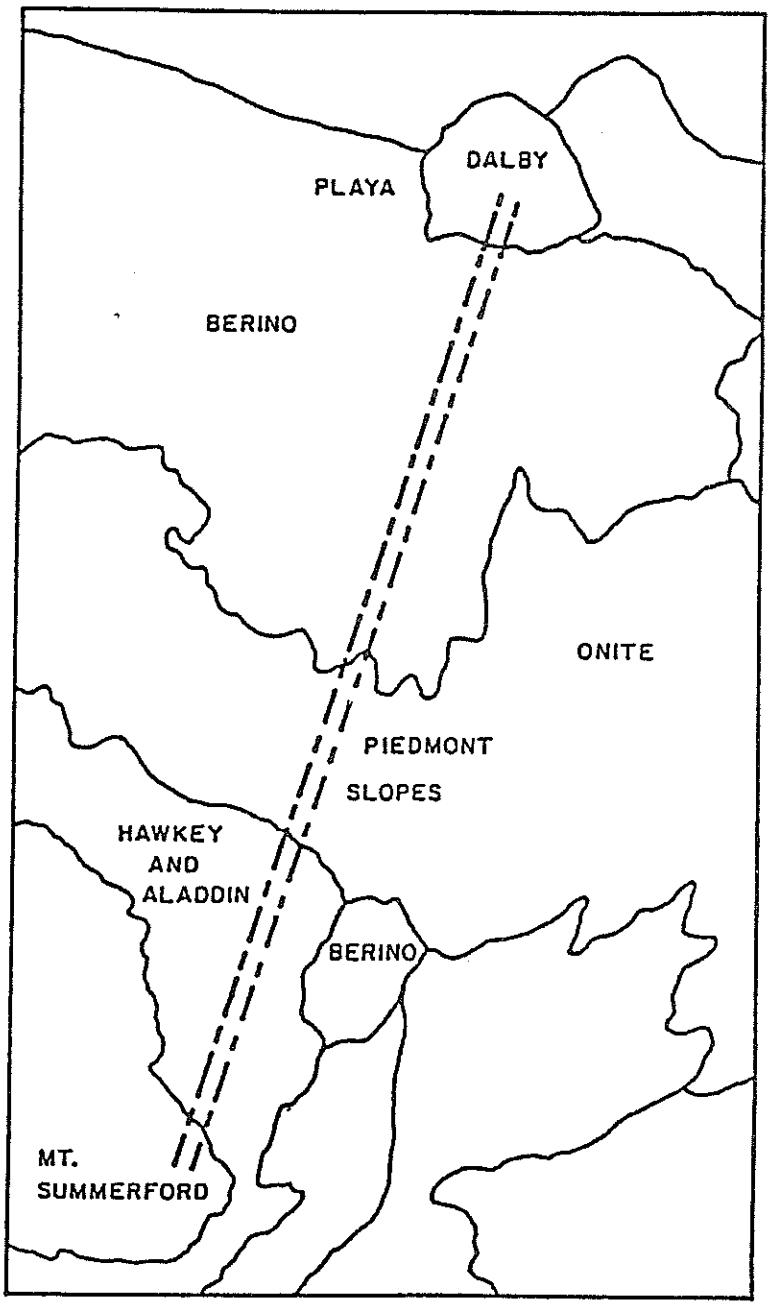

Fig. 11. Landforms and geomorphic features traversed by the long-term monitoring transects on the New Mexico State University college ranch (Wierenga et al. 1985).

PROCEDURES

In order to determine 36Cl concentration, sufficient chloride must be extracted to prepare the sample for 36Cl analysis. At least 10 to 20 mg is preferred. Ideally, soil samples should be large enough to provide this required chloride. In order to determine the required ample size, preliminary soil-chloride concentrations were determined at the SNWR. The chloride concentration of the soil profile was lowest at the surface (less than 5 mg Cl/kg soil) and increased with depth to approximately 20 mg Cl/kg soil at 2 m. Allison et al.#(1985) have shown that chloride concentrations in soil profiles often are lowest at the surface and increase with depth. This characteristic was thus assumed to hold true for both the SNWR and NMSUR sampling locations. Preliminary chloride mass balance calculations indicated that, at the SNWR, both bomb pulses would be found within the top 200 cm of soil. A sampling interval of 25 to 40 cm was therefore chosen to give good depth delineation near the surface. The sampling interval was increased to 50 to 60 cm below 2 m.

Relatively undisturbed soil samples were collected to a depth of 5 m on the SNWR in November, 1984. Samples were taken from a borehole using Shelby tubes. Each thin-walled sampling tube was 3 inches in diameter and 24 inches long. Approximately one kilogram of soil from each sampling tube was required for 3H analysis and was placed into an airtight plastic container designed for soil-water extraction. Each soil container was sealed with parafilm and placed inside two heavy-gauge plastic bags to minimize the risk of contamination and moisture loss. The remaining approximately 2 kilograms of soil were to be used for 36Cl analysis and were stored in plastic bags. Subsamples of soil were placed in two-ounce plastic jars and sealed with parafilm and duct tape for soil-moisture and chloride determinations.

2

$$Clsw = \frac{\dfrac{[Cl^-\text{ in extract (mg/l)}]\ [\text{weight of added DD water (g)}]}{\text{dry weight of soil (g)}}}{\text{moisture content (g } H_2O\text{/g dry soil)}}$$

In the laboratory, soil water for 3H analysis was removed from the samples using a nitrogen-extraction technique (figure 12). Hot nitrogen gas ($100^{o}C$) was passed through the soil-container intake creating an advective flow of nitrogen and water vapor out of the exhaust port (Duval 1986). The gas mixture was collected in a condensation trap and cooled by a NaCl and ice mixture. After an extraction period of approximately 3 days, the condensate was sealed in glass bottles and sent to the University of Waterloo's Environmental Isotope Laboratory for direct liquid scintillation counting. A control experiment was performed to determine if contamination of the soil samples occurred during field work and/or the extraction period. This experiment involved spiking a dry soil sample with water of known tritium content, then putting it through the handling and extraction proceedures along with the actual samples. The measured tritium content of the control was the same as that of the water added, indicating that sample contamination did not occur in the field or during processing (Duval 1986).

Soil-moisture was determined gravimetrically. The oven-dried subsample was then mechanically shaken for six hours with a known amount of distilled, deionized (DD) water to remove chloride originally dissolved in the soil water. The chloride content of this extract was determined by mercuric-nitrate titration (appendix A). Further discussion and evaluation of laboratory procedures for determining soil-water chloride can be found in McGurk and Stone (1985).

The chloride concentration of the original soil-water (Clsw) is calculated according to equation 6.

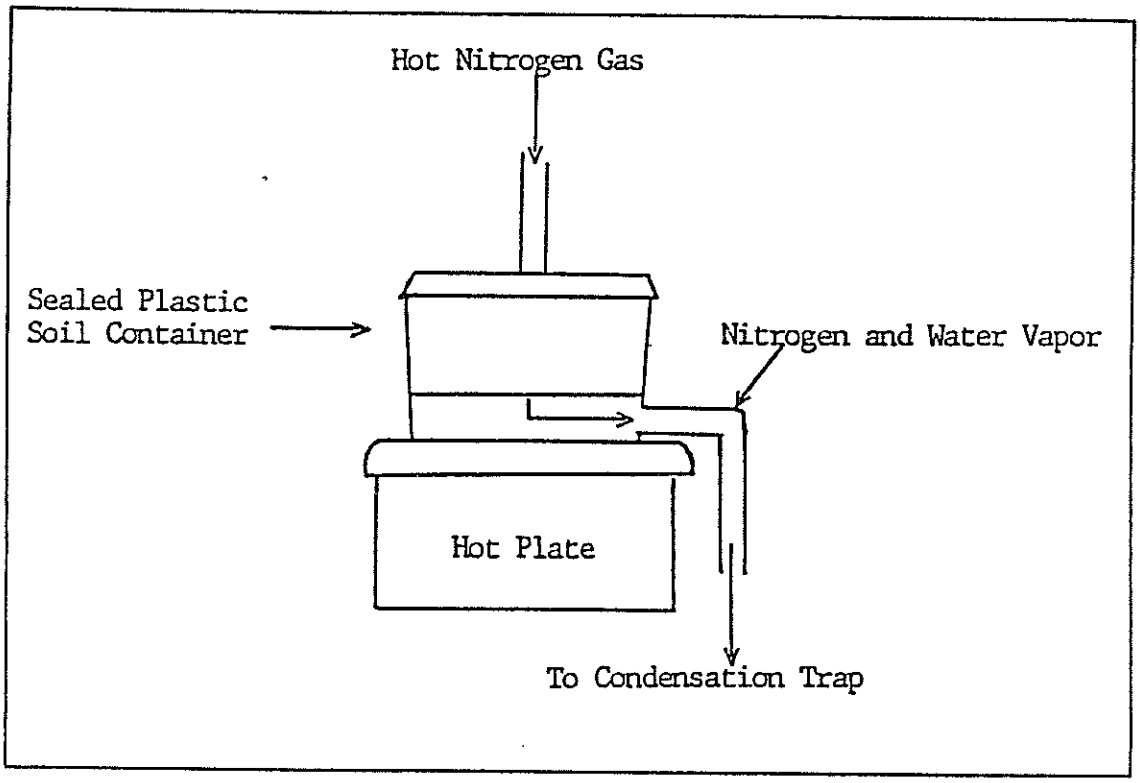

Fig. 12. Nitrogen gas soil-water extraction appartus. From Duval (1986).

Calculated chloride concentrations were less than 3 mg chloride per kilogram of soil throughout the top 2 m of the soil profile. Consequently the 1.5 to 2 kilograms of soil collected with the sampling tubes would not yield sufficient chloride in this zone for 36Cl analysis. The sampling site was therefore reoccupied and a pit was excavated to a depth of 2 m and 13 to 25 kilogram samples were collected at 25 cm intervals. Subsamples were again taken to determine moisture and chloride contents. The large samples were leached of chloride by adding a known volume of distilled deionized water to the soil (approximately 1 part water to 2 parts soil by weight) and mixing to form a fluid slurry. After the slurry settled, the leachate was decanted and vacuum filtered through 0.45 micron filter paper in 300 ml millipore filter funnels. Usually less than 50 percent of the added leach water could be removed by this technique. The efficiency deteriorated as clay content increased and settling and filtration proved to be very time consuming. Flocculants were not used to decrease settling and filtrating times in order to minimize external sources of chloride contamination.

This chloride-extraction method did not have the efficiency required to process low-chloride samples. Consequently, large volumes of leachate with low chloride concentrations often resulted. The chloride was concentrated by slowly evaporating the leachate, being very careful to avoid vigorous boiling of the sample which might result in Cl^- loss. This process was preferred over passing the leachate through prepared anion exchange columns because it minimized external sources of chloride contamination. In cases where the total chloride recovered was less than 10 to 20 mg, a carrier ion was added. In this case, the carrier ion was a weighed amount of dead chloride (chloride containing no 36Cl).

Silver nitrate was then added to all of the leachates, including a blank sample of carrier only, in order to precipitate the chloride as AgCl. The AgCl was purified of 36S (an interfering isobar in the 36Cl analysis) according to procedures outlined in appendix B. The samples were then analyzed for 36Cl on the University of Rochester's tandem accelerator. The 36Cl/Cl ratio measured by the tandem accelerator must first be corrected according to procedures outlined in Elmore et al. (1984). It can then be corrected to the ratio of the actual sample using equation 7.

$$\left[\frac{^{36}Cl}{Cl}\right] = \left[\frac{^{36}Cl}{Cl_{measured}}\right] \left[\frac{Cl_{sample} + Cl_{carrier}}{Cl_{sample}}\right] \qquad (7)$$

Samples from the NMSUR were collected March 15, 1985. Near-surface chloride concentrations were assumed to be low so a 60 cm pit was excavated to obtain adequate amounts of soil (approximately 25 kg) for chloride extraction and 36Cl sample processing. Below 60 cm, samples were taken with a hand auger. Total depth was 220 cm and 25 cm was chosen for the sampling interval in order to give good depth delineation. Soil samples used for 3H analysis were again sealed in plastic containers while samples for 36Cl analysis were stored in plasted bags. Subsamples were taken at intervals ranging from 5 to 25 cm and were sealed in 2-ounce plastic jars for soil-moisture and chloride determinations.

Soil water for 3H analysis was removed from the samples by kerosene distillation. The method involved saturating the soil sample with kerosene and heating the mixture to approximately 100°C. Water and azetropes of kerosene condensed in a moisture trap (figure 13). The water was removed from the trap, sealed in glass bottles and sent to the University of Waterloo for

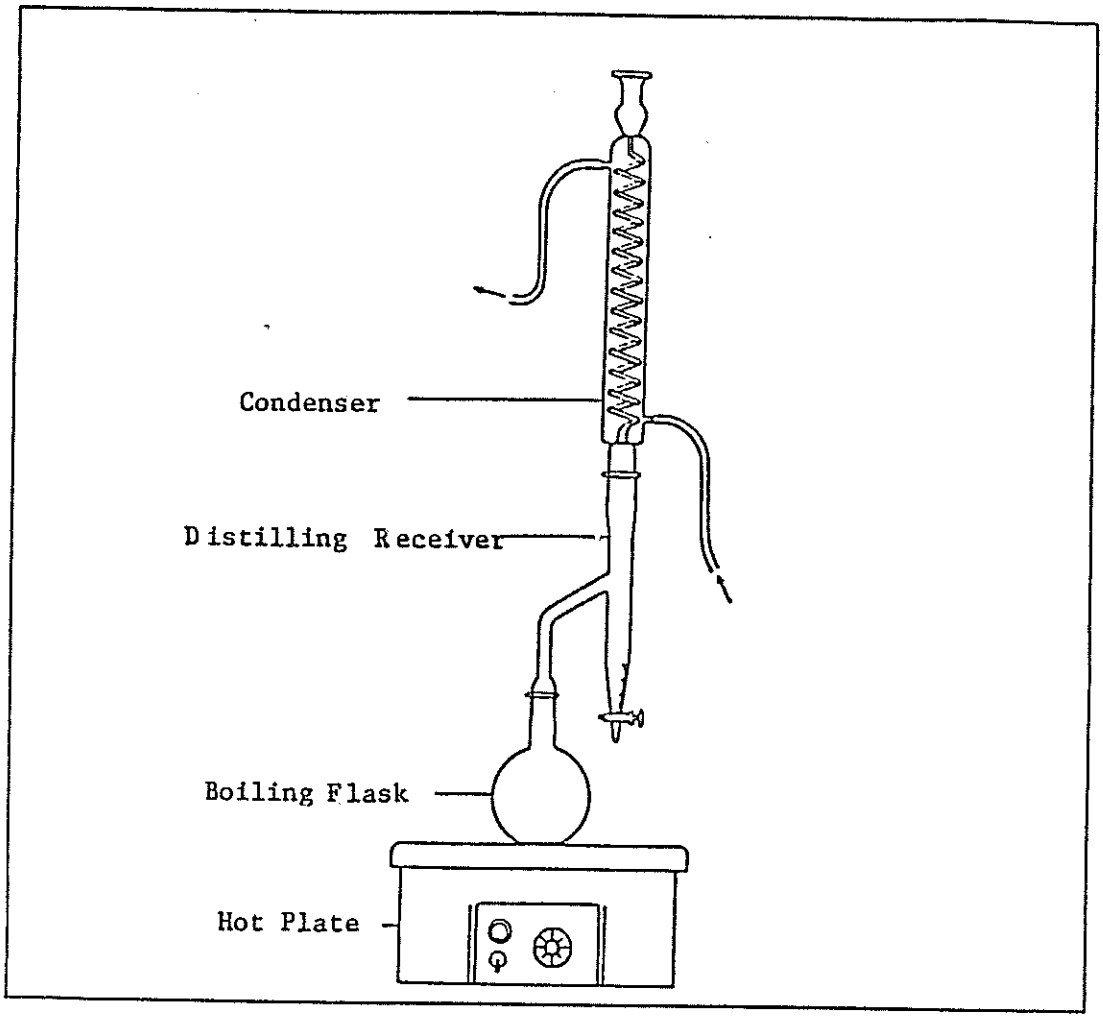

Fig. 13. Kerosene-distillation apparatus. From Hendry (1983).

sealed in glass bottles and sent to the University of Waterloo for liquid-scintillation counting. Kerosene distillation proved to be far more efficient than nitrogen-gas extracton. It saved time and yielded larger volumes of water.

The grain-size distribution of all SNWR and NMSUR soil samples were measured according to procedures outlined in Appendix C. Due to the small percentage of silt and clay in the SNWR samples, hydrometer analyses were not deemed necessary for these samples.

In April, 1985 the saturated hydraulic conductivity of the top 150 cm of soil was determined for the SNWR isotope sampling site. Continuous samples were collected using thin-walled sampling tubes. The tubes were modified and used as permeameters to calculate saturated-hydraulic conductivity. Also, during July, 1985, three ring samples were taken from 150, 200, and 250 cm depths. In the laboratory, the samples were weighed, saturated with water and placed inside a 15-bar pressure-plate apparatus. The equilibrium moisture content at 15 bars was assumed to be the residual moisture content.

A laboratory column experiment was conducted to investigate the possibility of anion retardation during water movement through SNWR soils (figure 14). The lower 20 cm of the column was packed with oven-dried soil and each end of the column was exposed to equal vapor pressures. This was accomplished by connecting each end of the column to vapor released from a reservoir of 0.935 g/liter NaCl solution. This solution maintained a relative humidity of about 0.99944 and a soil mositure tension of 0.77 bars throughout the column. This was designed to ensure water movement by mass flow only and not by vapor diffusion caused by vapor-pressure gradients. In order to determine when the column soil moisture content had equiliberated with the vapor, a separate beaker of oven-dried soil was also exposed to vapor released from a 0.935 g/liter

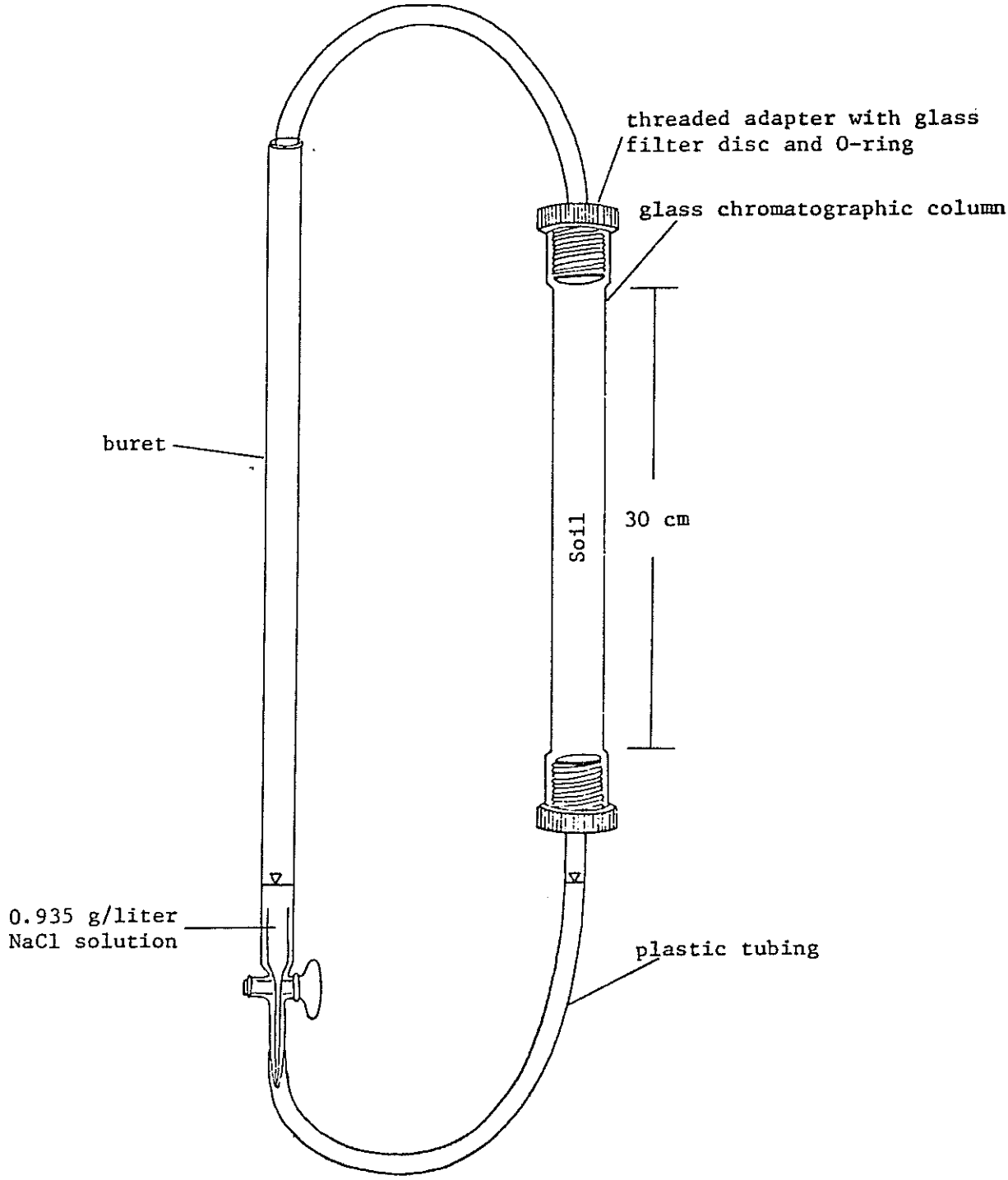

Fig. 14. Column experiment apparatus

reservoir of NaCl solution. The beaker of soil was weighed intermittently and when the weight no longer increased due to acquisition of moisture from the vapor, it was assumed the column had also equilibrated. At this time, the top 10 cm of the column was packed with a plug of wetted soil. The plug was wetted with 0.935 g/liter NaCl solution to a volumetric water content of 20 percent. The column was packed twice to final bulk densities of 1.65 and 1.83 g/cc. In each experiment the moisture front was allowed to move until it had traveled approximately two-thirds the length of the column. The soil was then extracted at 2 cm intervals and soil-moisture and chloride contents were determined.

RESULTS AND DISCUSSION

Grain-Size

Figures 15 and 16 are representative grain-size distributions with depth at the SNWR and NMSUR isotope sampling locations respectively. Data from every sample interval are tabulated and plotted in appendix D.

SNWR grain-size distributions are relatively well sorted and some 65 percent of each soil sample contains grains between 0.1 and 0.4 mm in size. NMSUR samples are poorly sorted and contain a much larger fraction of silt and clay (figure 17). Figure 18 shows percentages of clay, silt and sand and the soil textural class for the SNWR and NMSUR samples.

Figure 19 illustrates the similarity between grain size distributions at the isotope sampling site and soil-water station 1 on the SNWR.

Hydraulic Conductivity

Figure 20 illustrates saturated hydraulic conductivities with depth at the SNWR isotope sampling site. Results from near soil-water station 1 (figure 9) are also included (Byers and Stephens 1983). Results show similar hydraulic conductivities for the adjacent locations.

Soil-Temperature

Soil-temperature readings were taken near soil water station 1 at the SNWR over a 2 year period (Stephens et al., 1985). Temperature gradients were calculated using a time-weighted averaging scheme. Duval (1986) found that seasonal fluctuations tend to cancel each other out but a small net temperature gradient of 0.018 ^{o}C/cm still exists between 61 and 183 cm. The positive gradient indicates temperature decreases with depth. This rather anomalons positive temperature gradient is ascribed to underflow of relatively cool recharge originating from runoff over the nearby bed of the Rio Salado.

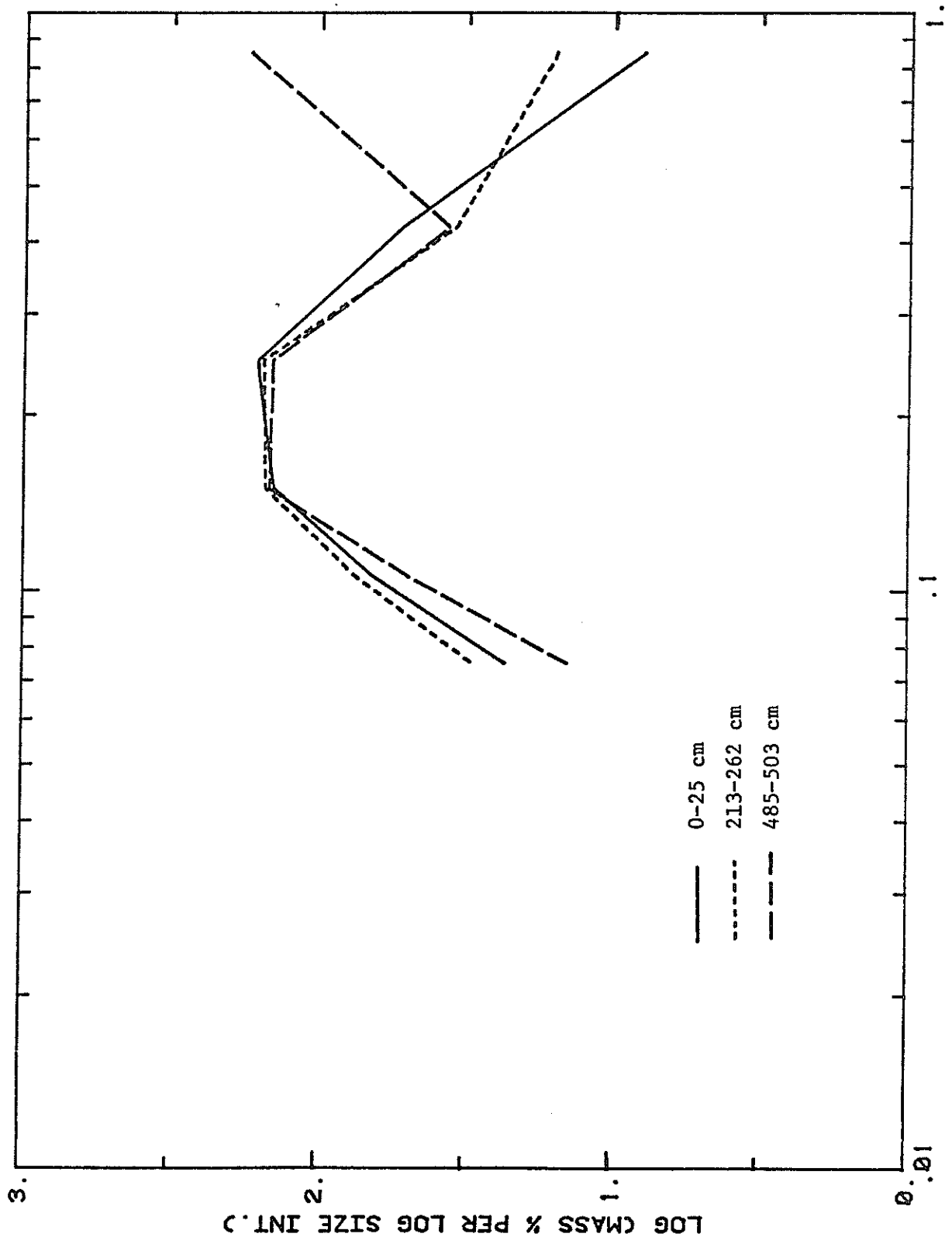

Fig. 15. Grain-size distribution over depth at the SNWR isotope sampling site.

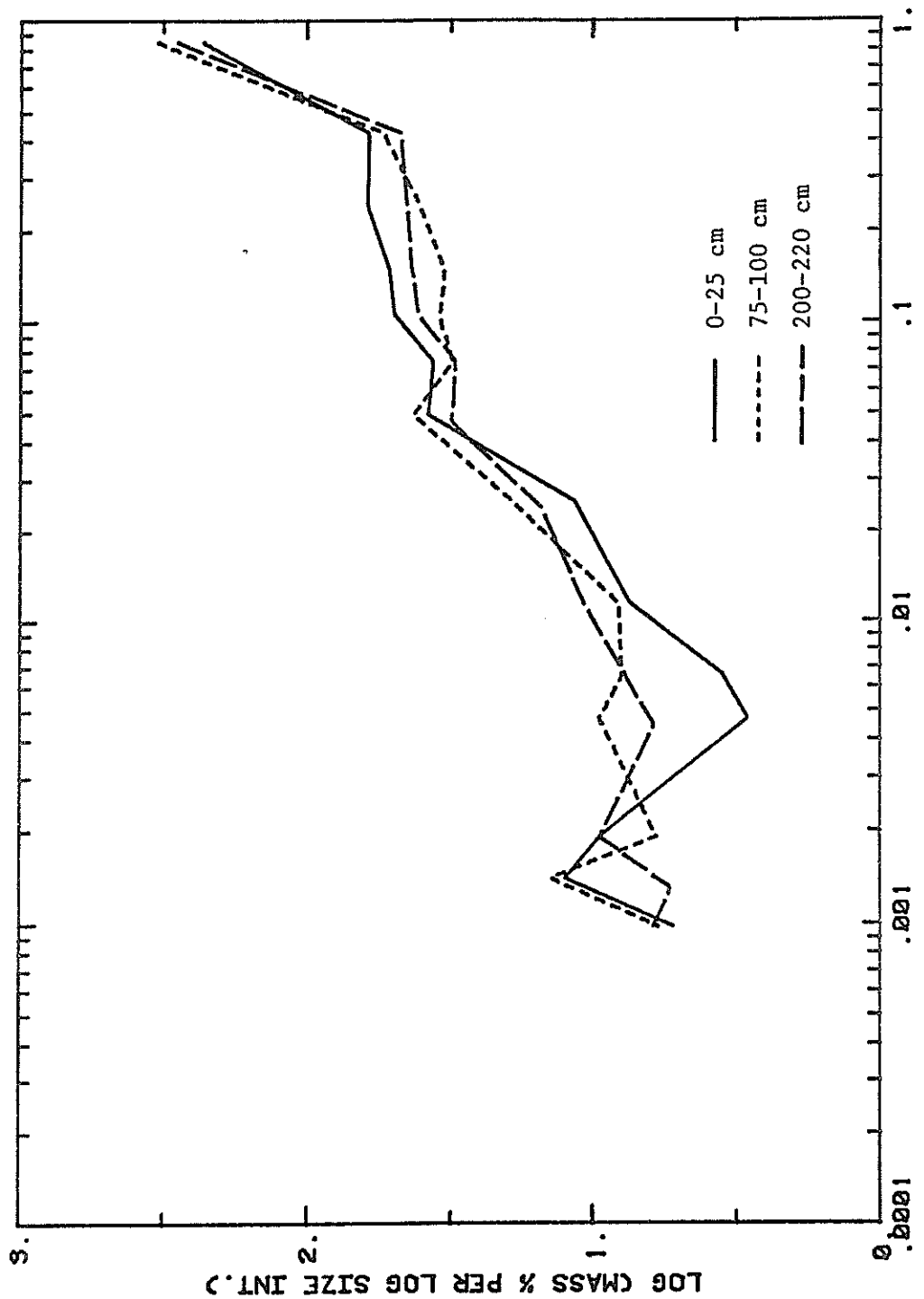

Fig. 16. Grain-size distribution over depth at the NMSUR isotope sampling site.

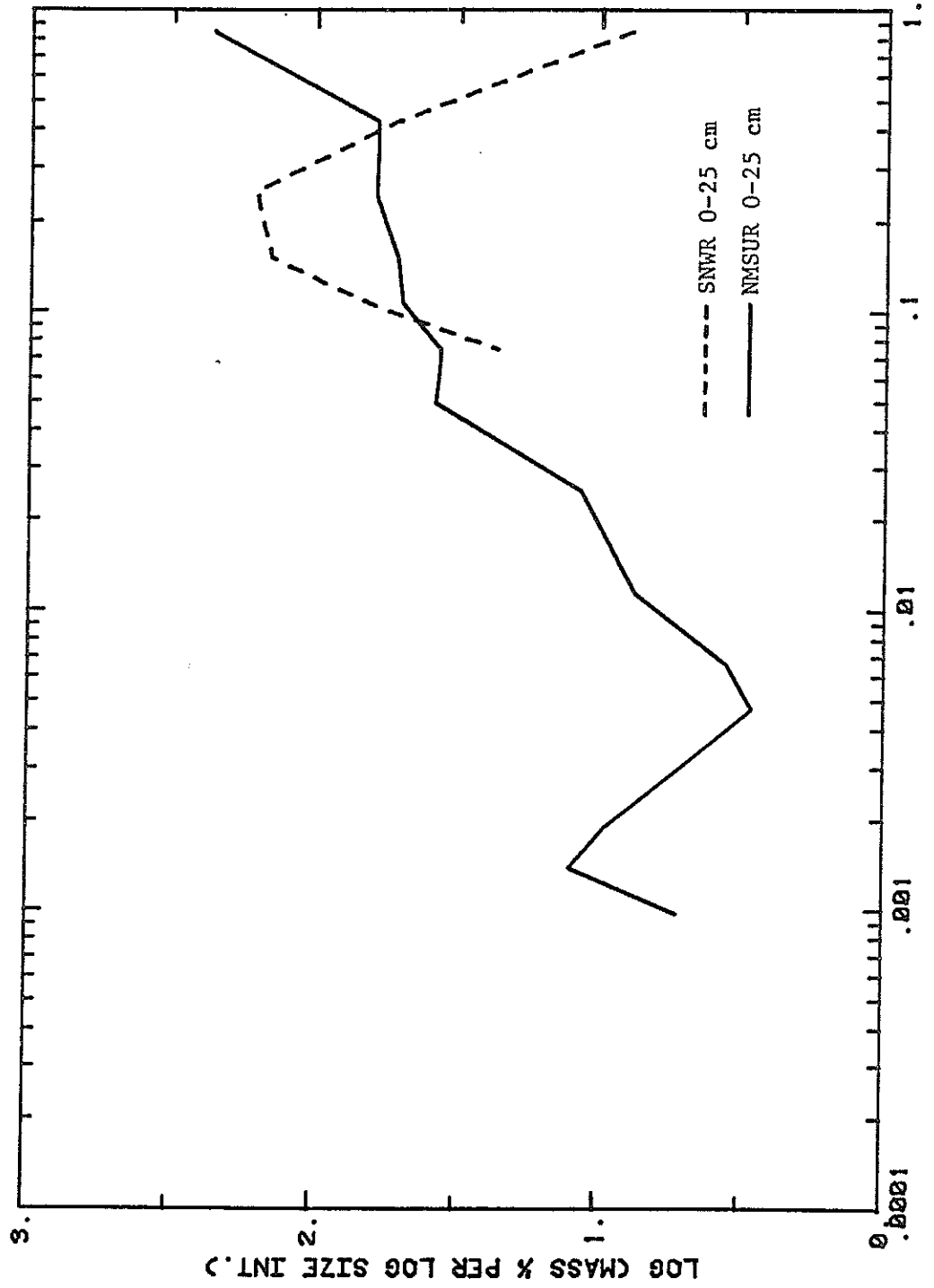

Fig. 17. Comparison of SNWR and NMSUR grain-size distributions

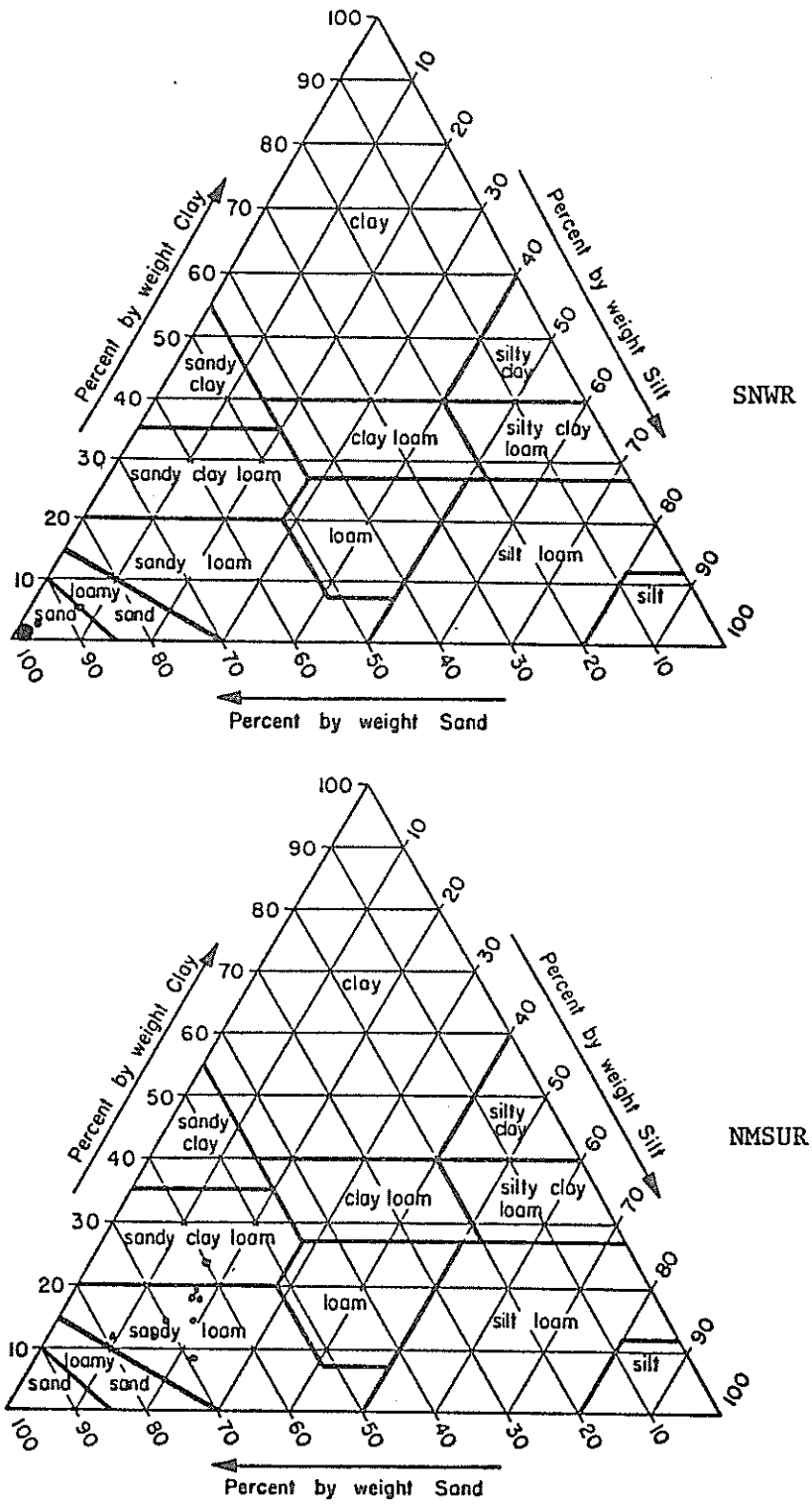

Fig. 18. Textural triangles showing percentages of clay (below 0.002 mm), silt (0.002-0.05 mm), and sand (0.05-2.0 mm) at the SNWR and NMSUR. Dots represent individual samples.

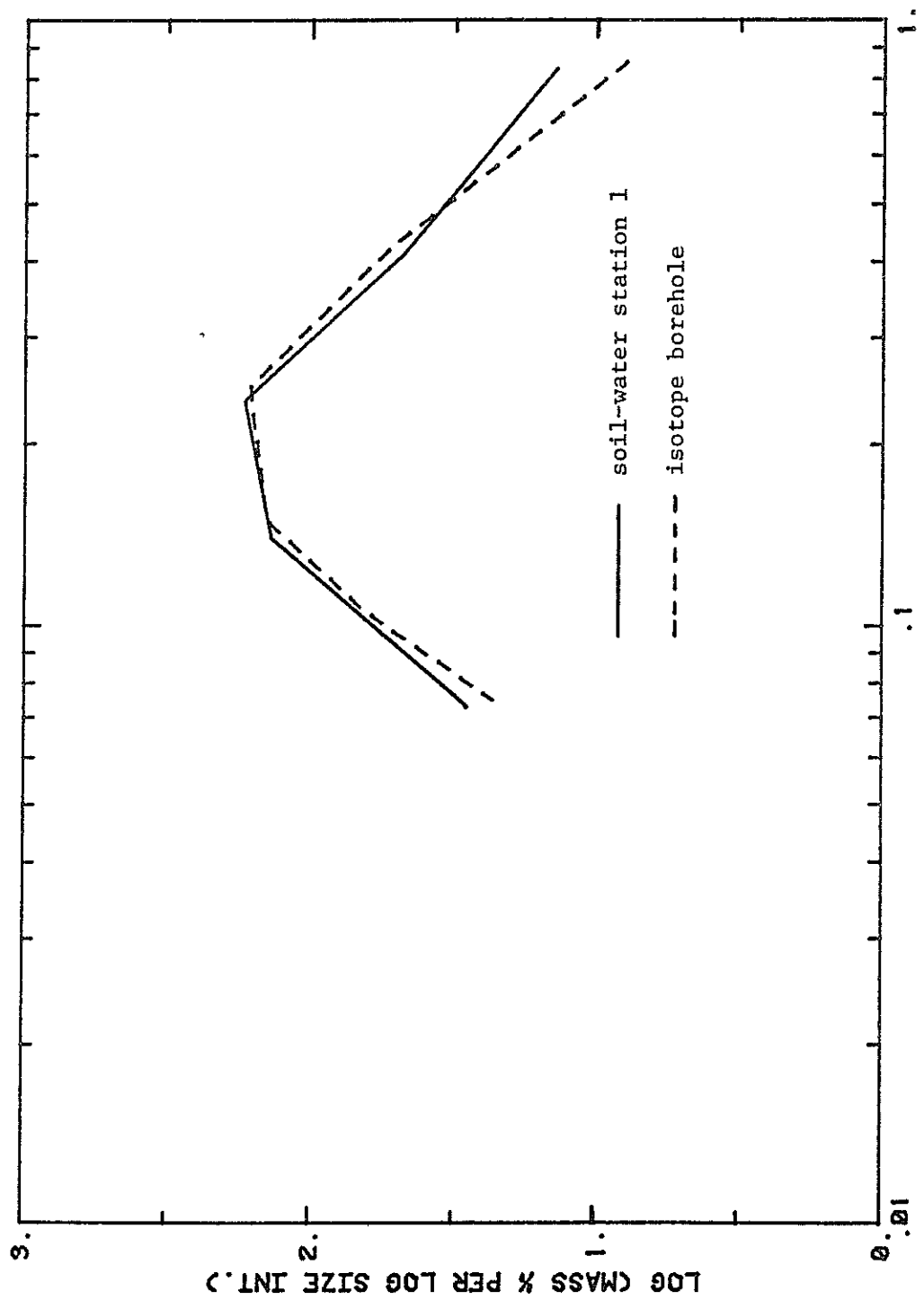

Fig. 19. Comparison of grain-size distributions at soil-water station 1 and the isotope sampling site on the SNWR. From Duval (1986).

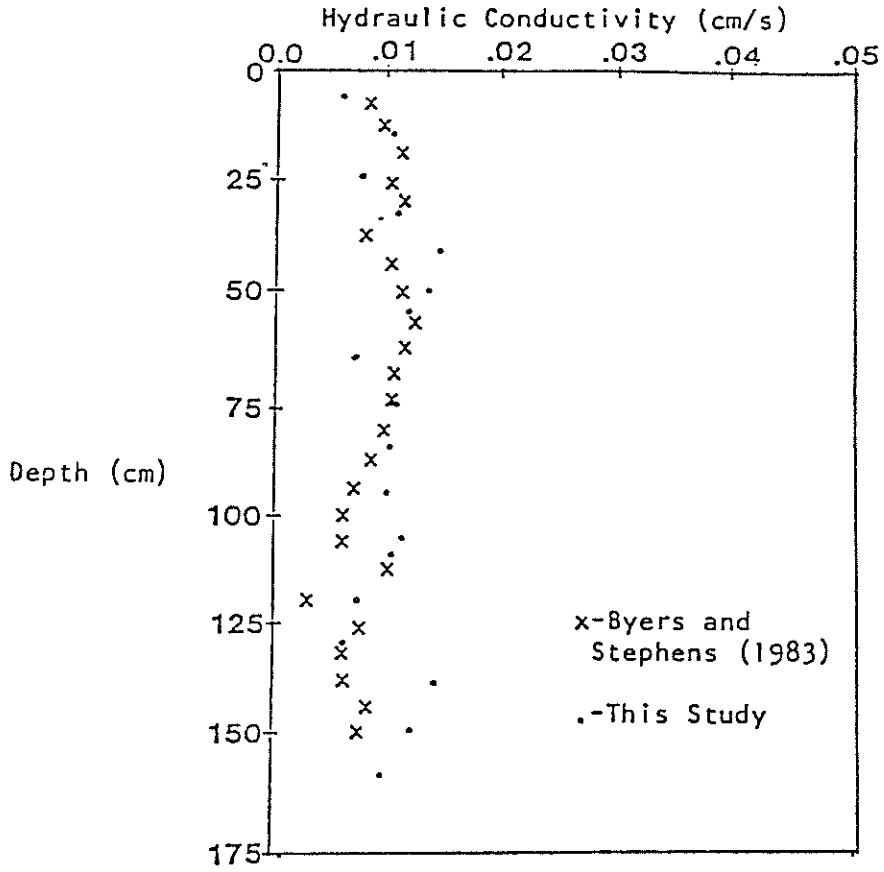

Fig. 20. Hydraulic conductivities with depth at soil-water station 1 and the isotope sampling site on the SNWR. From Duval (1986).

Chloride Method

Recharge was estimated using equation 3 at four settings on the SNWR (figure 9): a relatively unvegetated site some 10 m to the east of the isotope sampling site, soil-water stations 1 and 15, and the isotope sampling site. Such settings represent a variety of geology, slope and vegetation in the study area. Recharge using the chloride method was also estimated for the isotope sampling site at the NMSUR.

Recharge estimates calculated for each of the depth intervals at each location are given in tables 1 through 5. The tabulated values were calculated using a Fortran program listed in appendix E. Co in the Socorro area is 0.375 mg/l (Phillips et al. 1984) and 0.35 mg/l in the Las Cruces area (appendix F). These chloride concentration values are calculated from the measured, prebomb $^{36}Cl/Cl$ ratio in this soil water, using the known fallout of ^{36}Cl as a function of latitude (Bentley et al., 1986). This initial "concentration" is actually the total chloride deposition per unit area divided by the precipitation per unit area and this includes both chloride in precipitation and dry chloride deposition. Average P at both locations is 22 cm/year and Clsw values were calculated using equation 6 and data tabulated in appendix G. Travel times, t, or chloride "ages", calculated from equation 2 are also given in tables 1 through 5.

Chloride and moisture content values for each location are plotted versus depth on arithmetic graph paper, under the descriptions of each sample site. When water containing chloride percolates into a soil, and water loss occurs by transpiration, it is assumed that, at steady state, under piston flow conditions, chloride will increase steadily through the root zone. The maximum value at the base of the root zone should remain constant down to the water

TABLE 1

SNWR Unvegetated Site

SAMPLE INTERVAL CM	AVG. SAMPLE DEPTH CM	d INT. THICK	THETA CC H2O CC SOIL	M MG CL KG SOIL	C MG CL LH2O	R CM YEAR	q CM YEAR	"AGE" YEARS	CUMCL G/M**2	CUMH2O M
0- 13	6.5	6.5	0.0197	5.0	416.8	0.02	1.01	6	0.53	0.00
25- 36	30.5	24.0	0.0344	3.5	167.3	0.05	1.43	22	1.92	0.01
36- 43	39.5	9.0	0.0361	1.9	88.5	0.09	2.58	25	2.20	0.01
51- 58	54.5	15.0	0.0344	1.5	69.6	0.12	3.44	29	2.56	0.02
76- 86	81.0	26.5	0.0361	1.5	68.7	0.12	3.33	36	3.22	0.03
103-112	107.5	26.5	0.0558	1.7	49.1	0.17	3.01	44	3.95	0.04
129-138	133.5	26.0	0.0558	1.6	48.3	0.17	3.07	52	4.65	0.06
146-156	151.0	17.5	0.0656	1.8	44.8	0.18	2.81	58	5.16	0.07
166-175	170.5	19.5	0.0689	1.5	35.0	0.23	3.36	63	5.64	0.08
186-195	190.5	20.0	0.0820	2.7	53.8	0.15	1.87	73	6.52	0.10
204-212	208.0	17.5	0.0590	1.8	49.4	0.17	2.83	79	7.03	0.11
220-230	225.0	17.0	0.0672	2.0	49.8	0.17	2.47	85	7.60	0.12
240-249	244.5	19.5	0.0295	5.3	293.0	0.03	0.95	105	9.29	0.13
258-269	263.5	19.0	0.0541	2.8	85.6	0.10	1.78	115	10.17	0.14
279-289	284.0	20.5	0.0525	1.6	48.9	0.17	3.21	121	10.69	0.15
299-309	304.0	20.0	0.0902	3.4	61.9	0.13	1.48	134	11.81	0.16
317-325	321.0	17.0	0.0443	3.2	118.4	0.07	1.57	144	12.70	0.17
334-344	339.0	18.0	0.0328	2.9	146.8	0.06	1.71	154	13.57	0.18
353-364	358.5	19.5	0.0377	6.6	287.8	0.03	0.76	179	15.68	0.19
371-381	376.0	17.5	0.0262	15.2	949.4	0.01	0.33	231	20.04	0.19
381-389	385.0	9.0	0.0295	24.4	1357.7	0.01	0.21	274	23.05	0.19
389-400	394.5	9.5	0.1230	204.1	2720.7	0.00	0.02	659	55.44	0.20

d = interval thickness (cm)

THETA = volumetric water content

M = measured soil chloride content (mg Cl/kg dry soil)

C = calculated soil water chloride concentration (mg Cl/L soil water)

R = recharge specific flux (cm/yr)

q = recharge pore velocity (cm/yr)

"AGE" = number of years for chloride to reach bottom of the sample interval (yrs)

CUMCL = cumulative soil chloride to bottom of sample interval (g/m^2)

$CUMH_2O$ = cumulative water to bottom of sample interval (m^3/m^2)

TABLE 2

SNWR soil-water station 1

SAMPLE INTERVAL CM	AVG. SAMPLE DEPTH CM	Q INT. THICK	THETA CC H2O CC SOIL	M MG CL KG SOIL	C MG CL LH2O	R CM YEAR	Q CM YEAR	"AGE" YEARS	CUMCL G/M**2	CUMH2O M
0- 5	2.5	2.5	0.0984	3.3	55.0	0.15	1.51	1	0.14	0.00
15- 20	17.5	15.0	0.0314	3.2	154.0	0.05	1.55	10	0.94	0.01
40- 45	42.5	25.0	0.0394	4.1	171.0	0.05	1.22	30	2.62	0.02
60- 65	62.5	20.0	0.0459	2.9	102.0	0.08	1.75	41	3.57	0.03
80- 85	82.5	20.0	0.0541	3.0	91.8	0.09	1.66	53	4.56	0.04
100-105	102.5	20.0	0.0476	2.1	73.0	0.11	2.36	61	5.26	0.05
120-125	122.5	20.0	0.1296	2.2	27.8	0.30	2.29	69	5.98	0.07
140-145	142.5	20.0	0.0705	2.2	51.5	0.16	2.27	77	6.71	0.09
165-170	167.5	25.0	0.0738	5.3	117.8	0.07	0.95	103	8.83	0.11
190-195	192.5	25.0	0.0886	3.3	60.4	0.14	1.54	119	10.22	0.13
215-220	217.5	25.0	0.0640	3.3	85.8	0.10	1.50	135	11.59	0.14
235-240	237.5	20.0	0.0836	3.0	58.2	0.14	1.70	146	12.56	0.16
255-260	257.5	20.0	0.0935	5.0	88.3	0.09	1.00	166	14.22	0.18
275-280	277.5	20.0	0.1214	3.0	40.4	0.20	1.68	177	15.20	0.20
295-300	297.5	20.0	0.0918	4.6	82.9	0.10	1.08	195	16.72	0.22

TABLE 3

SNWR soil-water station 15

SAMPLE INTERVAL CM	AVG. SAMPLE DEPTH CM	d INT. THICK	THETA CC H2O CC SOIL	M MG CL KG SOIL	C MG CL LH2O	R CM YEAR	q CM YEAR	"AGE" YEARS	CUMCL G/M**2	CUMH2O M
0- 5	3.0	3.0	0.0212	0.8	59.6	0.14	0.55	0	0.04	0.00
24- 33	28.5	25.5	0.0494	0.9	30.6	0.27	5.45	4	0.42	0.01
44- 55	49.5	21.0	0.0502	1.1	34.7	0.24	4.74	8	0.79	0.02
67- 79	73.0	23.5	0.0776	1.3	26.9	0.31	3.95	13	1.28	0.04
95-106	100.5	27.5	0.0515	0.9	29.9	0.28	5.36	18	1.70	0.06
117-127	122.0	21.5	0.0599	0.9	24.3	0.34	5.08	21	2.02	0.07
136-149	143.5	21.5	0.0549	1.3	38.2	0.22	3.93	26	2.47	0.08
158-167	162.5	19.0	0.0503	0.9	27.7	0.30	5.30	29	2.76	0.09
178-188	183.0	20.5	0.0490	1.3	43.2	0.19	3.89	34	3.20	0.10
198-208	203.0	20.0	0.0676	0.9	21.0	0.38	5.66	37	3.49	0.12
218-228	223.0	20.0	0.0795	1.0	20.0	0.41	5.19	40	3.81	0.13
237-246	241.5	18.5	0.0677	1.3	30.9	0.27	3.94	44	4.19	0.14
254-264	259.0	17.5	0.0702	1.5	36.0	0.23	3.27	49	4.64	0.16
274-284	279.0	20.0	0.0863	1.3	33.4	0.25	3.73	54	5.08	0.17
293-303	298.0	19.0	0.0674	1.7	46.2	0.21	3.05	60	5.59	0.19
313-325	319.0	21.0	0.0630	1.2	30.9	0.27	4.24	64	6.06	0.20
331-343	338.5	19.5	0.0620	1.0	27.2	0.30	4.89	67	6.33	0.21
353-362	357.5	19.0	0.0626	1.2	30.9	0.27	4.20	71	6.70	0.22
373-383	378.0	20.5	0.0638	1.3	34.0	0.24	3.80	76	7.14	0.23
383-393	388.0	10.0	0.0718	1.0	22.8	0.36	5.04	77	7.31	0.24
393-402	397.5	9.5	0.0746	1.3	29.0	0.28	3.81	79	7.51	0.25

TABLE 4

SNWR isotope sampling site

SAMPLE INTERVAL CM	AVG. SAMPLE DEPTH CM	d INT. THICK	THETA CC H2O CC SOIL	M MG CL KG SOIL	C MG CL LH2O	R CM YEAR	J CM YEAR	"AGE" YEARS	CUMCL G/M**2	CUMH2O M
0- 25	12.5	12.5	0.0886	2.5	46.3	0.18	2.01	6	0.51	0.01
25- 50	37.5	25.0	0.0968	2.0	34.2	0.24	2.49	16	1.34	0.04
50- 75	62.5	25.0	0.0984	2.0	33.2	0.25	2.53	25	2.16	0.06
75-100	87.5	25.0	0.1115	2.2	32.0	0.26	2.31	35	3.05	0.09
100-125	112.5	25.0	0.1279	2.1	28.8	0.31	2.41	45	3.90	0.12
125-150	137.5	25.0	0.1263	2.0	28.1	0.32	2.50	55	4.73	0.15
150-175	162.5	25.0	0.0951	4.2	72.3	0.11	1.20	75	6.45	0.18
175-200	187.5	25.0	0.0525	3.9	121.7	0.07	1.29	94	8.05	0.19
213-262	237.5	50.0	0.0443	3.8	142.4	0.06	1.31	132	11.20	0.21
262-310	286.0	48.5	0.0492	1.9	63.7	0.13	2.63	150	12.72	0.23
310-358	334.0	48.0	0.0525	5.4	169.4	0.05	0.93	201	16.98	0.26
358-404	381.0	47.0	0.0344	7.4	354.2	0.02	0.68	270	22.72	0.28
404-432	418.0	37.0	0.1968	229.5	1912.2	0.00	0.02	1957	161.96	0.35
432-457	444.5	26.5	0.0492	30.1	1004.9	0.01	0.17	2115	175.06	0.36
485-503	494.0	49.5	0.1197	32.1	439.5	0.02	0.16	2430	201.10	0.42

TABLE 5

NMSUR isotope sampling site

SAMPLE INTERVAL CM	AVG. SAMPLE DEPTH CM	d INT. THICK	THETA CC H2O CC SOIL	M MG CL KG SOIL	C MG CL LH2O	R CM YEAR	Q CM YEAR	"AGE" YEARS	CUMCL G/M**2	CUMH2O M
0- 5	2.5	2.5	0.1335	5.3	65.9	0.12	0.88	2	0.22	0.00
5- 20	12.5	10.0	0.0733	3.8	85.0	0.09	1.24	10	0.84	0.01
20- 30	25.0	12.5	0.1066	5.0	87.0	0.09	0.83	25	2.00	0.02
30- 40	35.0	10.0	0.1185	3.4	46.9	0.16	1.39	32	2.56	0.04
40- 55	47.5	12.5	0.1304	3.0	38.0	0.20	1.53	40	3.19	0.05
60- 73	66.5	19.0	0.1407	3.2	37.7	0.20	1.45	53	4.19	0.08
73- 77	75.0	8.5	0.1440	2.8	32.0	0.24	1.67	58	4.58	0.09
75-100	87.5	12.5	0.1620	2.2	22.4	0.34	2.12	63	5.04	0.11
100-125	112.5	25.0	0.1879	3.6	31.8	0.24	1.29	82	6.53	0.16
120-150	135.0	22.5	0.2028	10.3	83.7	0.09	0.45	131	10.35	0.20
150-175	162.5	27.5	0.1546	47.2	503.9	0.02	0.10	409	31.77	0.25
175-200	187.5	25.0	0.0903	37.3	681.8	0.01	0.13	608	47.16	0.27
200-220	210.0	22.5	0.0860	35.2	676.5	0.01	0.13	777	60.24	0.29

table (Allison et al. 1985). Where chloride content decreases at depths below the base of the root zone, Allison et al. (1985) suggest a possible source of water at some depth beneath that of the peak in chloride concentration. Where water tables are deep and it is unlikely that there could be a source of water beneath the root zone, it is assumed that water is reaching the lower part of the profile by other than piston flow or that conditions were more favorable for recharge during the time represented by the lower part of the profile (Stone 1984).

Alternatively, precipitation, chloride input, and/or recharge can be assumed to have changed with time (Stone 1984). Where chloride content decreases with depth below a maximum value, plots of cumulative chloride (g/m^2) vs. cumulative water (m) are used to identify periods of change. Cumulative chloride is calculated from equation 8.

$$\sum_i (\theta_i \times (Clsw_i) \times d_i \qquad (8)$$

where θi=volumetric water content (m^3/m^3) at depth i (θi=gravimetric water content x bulk density; bulk density approximately equals 1.65 g/cc at both locations), Clswi=chloride content (g/m^3) at depth i, and di=sample interval length at depth i. Cumulative water is given by $\sum_i (\theta i \times di)$ (Stone 1984). These plots result in straight lines if there has been no change in precipitation rates, chloride input or recharge. Curved lines result if any of these conditions have changed over time. Recharge rates for straight-line segments of these curves can be calculated using equation 3 where Clsw is the

weighted mean chloride content (mg/l) of the soil water in the samples corresponding to the segment. Cumulative chloride and cumulative water values are given in tables 1 through 5.

Unvegetated site. This site was selected to represent topographically flat alluvium with sparse grasses. Soil-moisture at this site (figure 21) increases rather uniformly from .01 g/g at the surface to .05 g/g at 195 cm. It then fluctuates between .01 and .05 g/g until a noticeable increase to .075 g/g occurs at a depth of approximately 400 cm. Although grain-size analyses were not performed at the unvegetated site, a relatively large percentage of silt- and clay-sized grains were encountered at this depth some 10 m to the west at the isotope sampling site. This high moisture content probably corresponds to an increase in the percentage of silt and clay. The low surface value may be due to evaporation.

Chloride content (figure 21) drops off below a peak of 417 mg/l at 6.5 cm depth and remains relatively low until it increases rapidly at about 360 cm toward a value of 2700 mg/l. The surface peak may result from evaporative chloride enrichment. The increase at 360 cm could possibly be explained by chloride enrichment due to evaporation from the water table. The chloride concentration of groundwater at the SNWR is 297 mg/L (Stephens et al. 1983). The water table at this location is approximately 550 cm below ground surface. This level may vary by as much as a meter. During periods of high water levels, evaporation from the water table surface would enrich chloride in the capillary fringe. Declining water levels would allow entrapment of this concentrated capillary fringe water in the zone containing a higher percentage of silt and clay.

A cumulative chloride vs. cumulative water plot (figure 22) suggests relatively constant environmental conditions during the period represented by

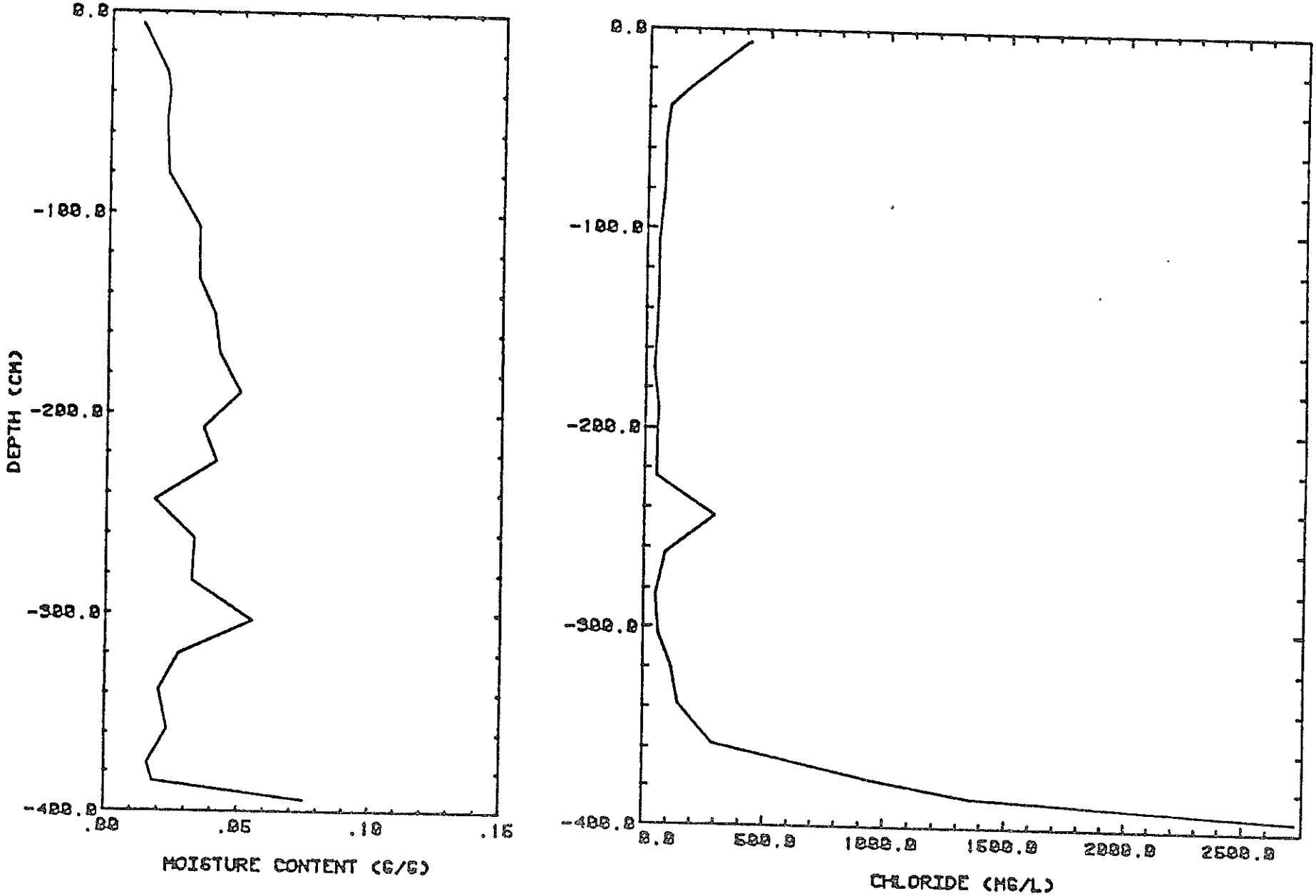

Fig. 21. Results from the SNWR unvegetated site

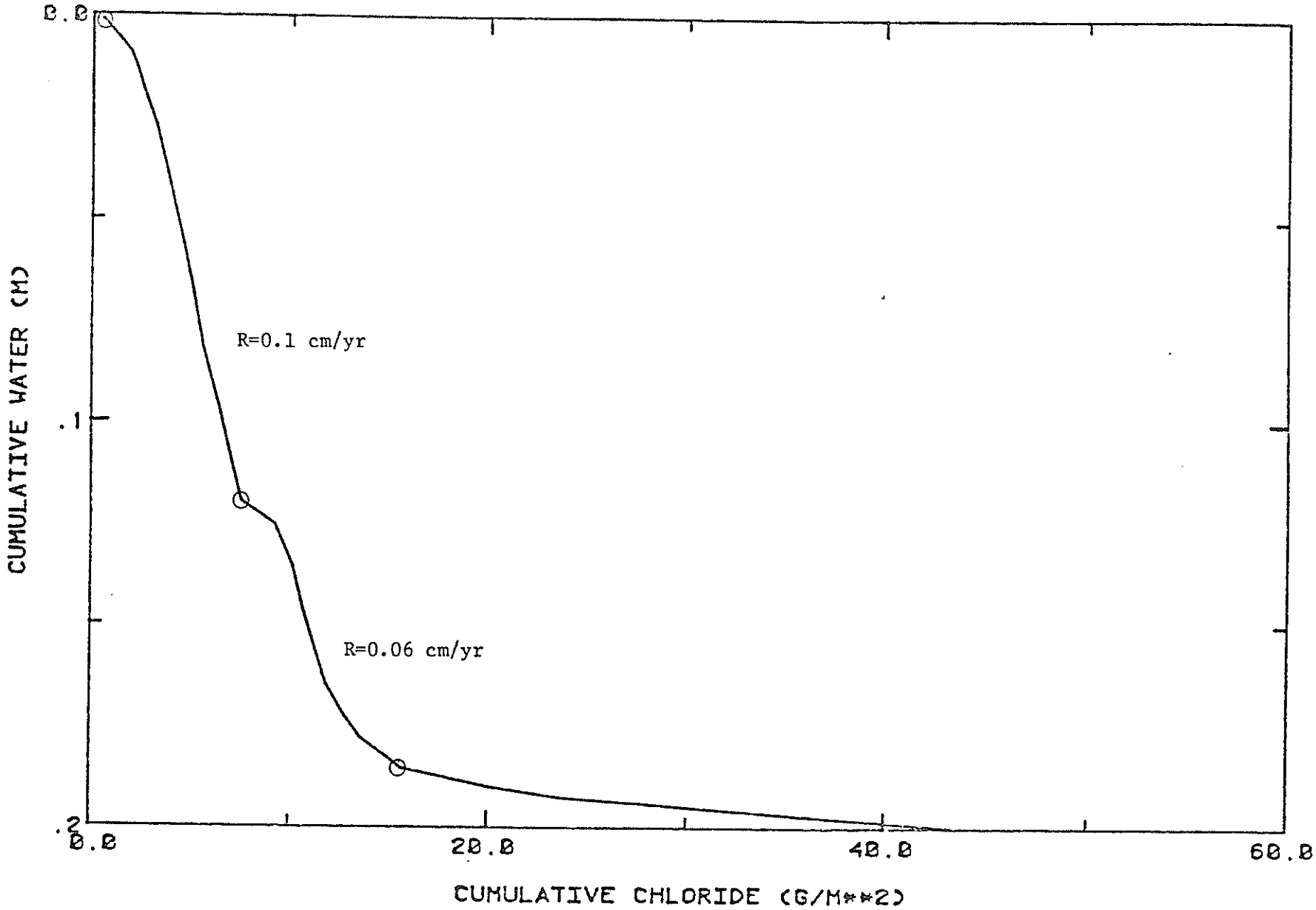

(09)

Fig. 22. Chloride vs. water, SNWR unvegetated site

the upper portion of the plot. The increased cumulative chloride value at the base of the plot is due to the anomalously high chloride content at 400 cm depth and probably is not explained by a change in precipitation, chloride input, and/or recharge at this location. Using a weighted mean Clsw value, average recharge calculatedfor the profile above the peak is about .1 cm/yr or less than 1 percent of the average annual precipitation becomes recharge.

Soil-water station 15 This site represents a swale on an active eolian sand dune. The station is unvegetated although shrubs grow nearby.

Soil moisture (figure 23) increases from approximately .01 g/g at the surface to .045 g/g at 400 cm. Such low surface values are likely due to the effects of evaporation.

Chloride concentration (figure 23) is highest (60 mg/l) at the surface then decreases and fluctuates between 20 and 40 mg/l throughout the remainder of the profile. The higher surface value is probably due to evaporative chloride enrichment.

Cumulative chloride vs. cumulative water (figure 24) shows constant environmental conditions through the time represented.

The weighted mean value of Clsw is 31 mg/l. Recharge for this setting is .3 cm/yr or just over 1 percent of the average annual precipitation becomes recharge.

McCord (1986) analyzed soil-moisture data from stations 13, 14 and 15 on the active unvegetated sand dune. By determining the change in volumetric moisture storage at each location after a precipitation event, he found that station 15, located in a swale on the dune, gained approximately 15 percent more water into storage than actually fell in the precipitation event. This gain in moisture storage was 60 percent greater than that at station 13 (slope on dune) and 800 percent greater than the moisture gain at station 14 (crest of dune).

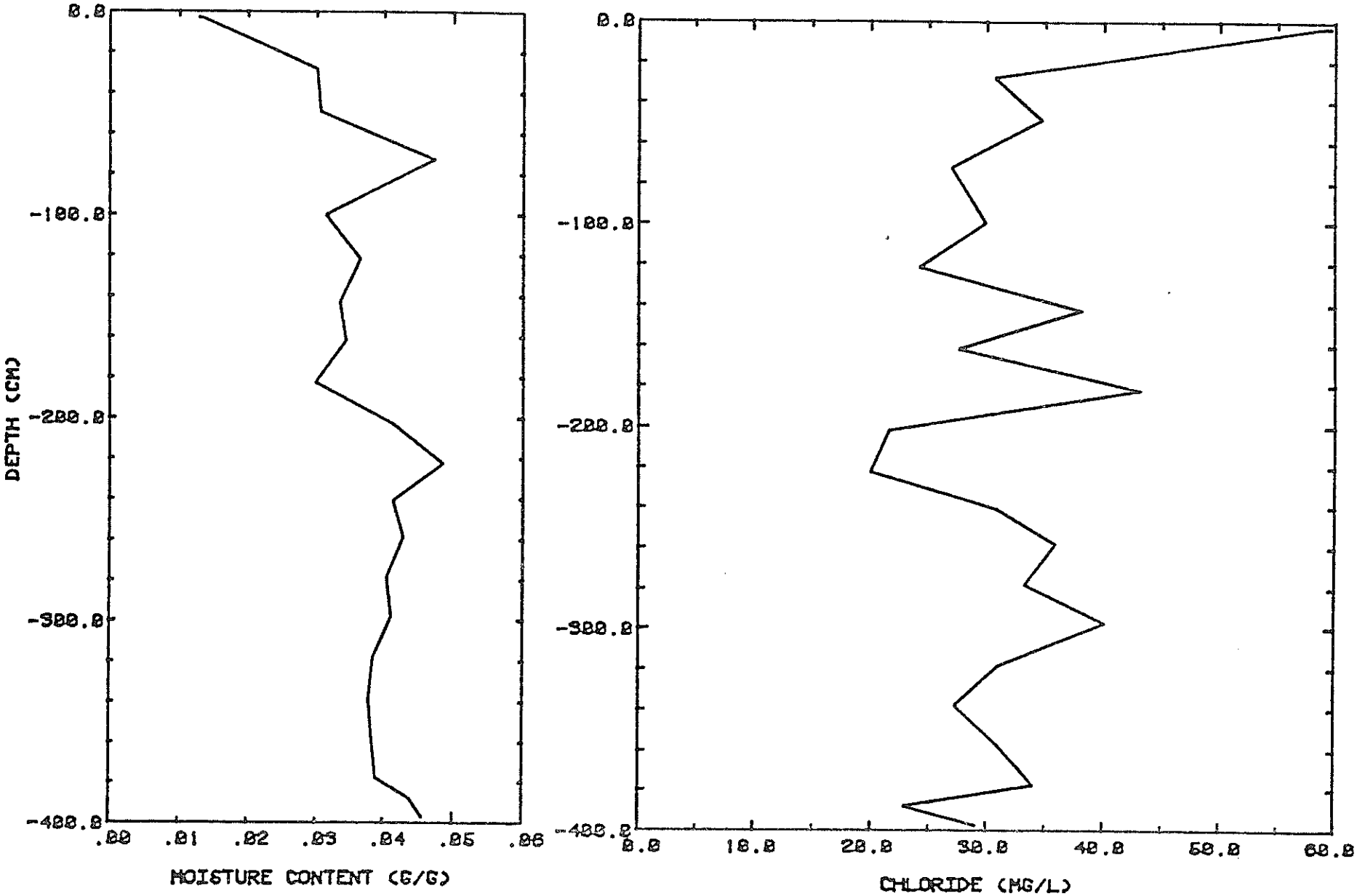

Fig. 23. Results from soil-water station 15, SNWR

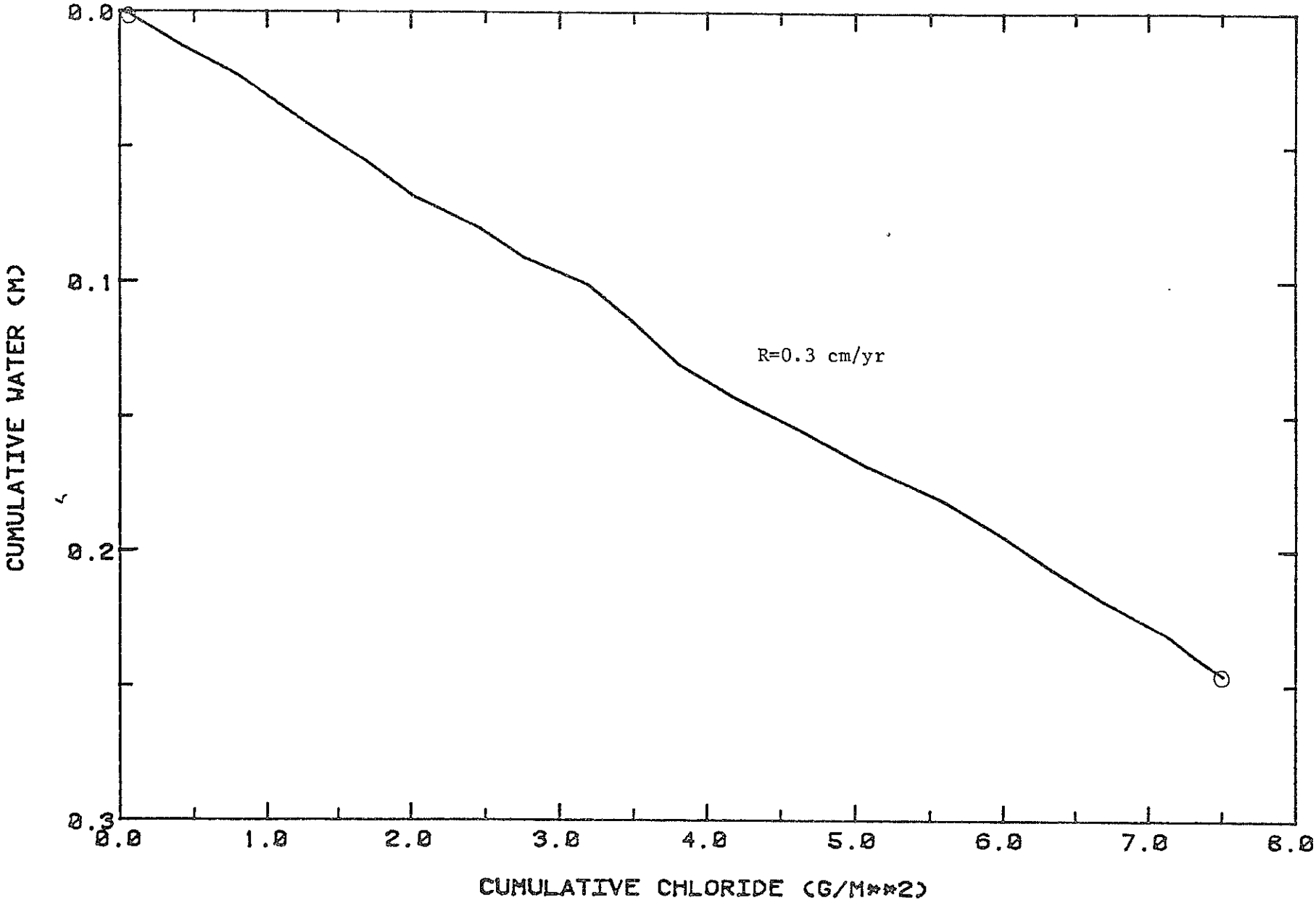

Fig. 24. Chloride vs. water, SNWR soil-water station 15

Since no evidence of surface runoff was observed, McCord (1986) concluded that unsaturated lateral flow best explained these results. Moisture appears to have moved laterally away from station 14 (convex station) since it gained the least moisture. He infered, based on the significant soil-moisture increase, that lateral flow converges on station 15, which is located in a swale. In addition, he pointed out that the effects of lateral flow became increasingly apparent over time since station 15 continued to gain moisture long after the rainfall event.

One would expect, therefore, that convergence of lateral flow and concentration of moisture would enhance the amount of recharge occurring at station 15. Fluxes calculated below the root zone, using Darcy's Law, proved this to be the case. For the dry year 1984, McCord (1986) calculated a deep flux equal to 3 percent of the average annual precipitation at station 15 versus 1 percent at stations 13 and 14. For the period January 1984 to May 1985, which included the wet winter of 1985, he calculated a deep flux equal to 152 percent of the average annual precipitation at station 15 versus 13 and 1 percent for stations 13 and 14 respectively. This recharge flux (33 cm) is larger than the flux of 0.3 cm/yr obtained from the chloride mass balance. However, the chloride mass balance actually reflects the relative amounts of precipitation vs evapotranspiration and gives accurate values for <u>local</u> infiltration only if the infiltration is areally uniform. The assumption of one-dimensional vertical flow is invalid at this location. Recharge values determined using the chloride method will consequently be less than actual local value. However, the chloride method may give realistic values for the average recharge over the entire collection area of the swale.

<u>Soil-water station 1</u>. This site was selected for direct comparison between recharge estimates using geochemical and physical methods. The area is

predominantly alluvial sand and is topographically flat. A moderate increase in slope occurs about 4m to the south of station 1. Station 1 is sparsely vegetated, including shrubs and grasses.

Soil moisture (figure 25) fluctuates between .025 and .08 g/g and consistently increases with depth over the measured interval. The chloride concentration (figure 25) reaches a peak of 172 mg/l within 42 cm of the ground surface. The concentration then decreases to an average 72 mg/l near 300 cm depth. This decrease in concentration is not likely to be due to a water-table rise. The water table at this location is approximately 550 cm below ground surface and fluctuates by only about one meter. There are several possible explanations for the variability of the chloride profile. The net decrease could possibly be explained by non-piston-flow conditions providing a source of water beneath the peak. Alternatively, unsaturated lateral flow from the higher slope to the south of station 1 could also possibly provide an additional source of water. However, the fact that the chloride peak is accompanied by a very low soil moisture content (2 percent gravimetric) suggests that it may simply be due to intense evaporation. The more uniform chloride and moisture contents deeper in the profile may be a result of mixing between water accumulated during evaporative episodes and more dilute water from occassional recharge events.

A cumulative chloride vs. cumulative water plot (figure 26) suggests little change in environmental conditions during the period represented. This also supports the hypothesis of an evaporative origin for the chloride peak.

Using a weighted mean Clsw value, recharge for the time represented by the profile below 42 cm is .1 cm/yr. Less than one percent of the average annual precipitation becomes recharge.

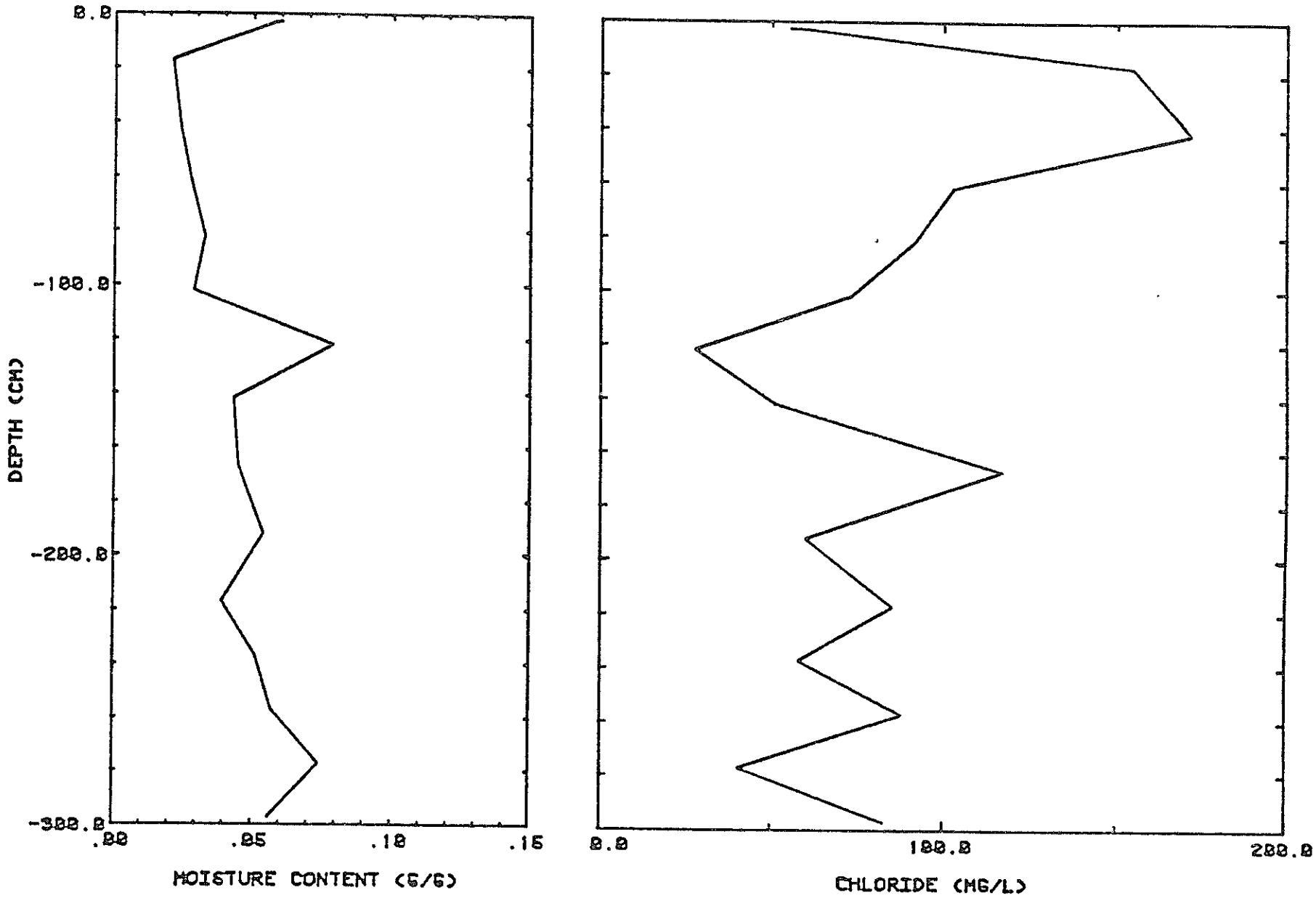

Fig. 25. Results from soil-water station 1, SNWR

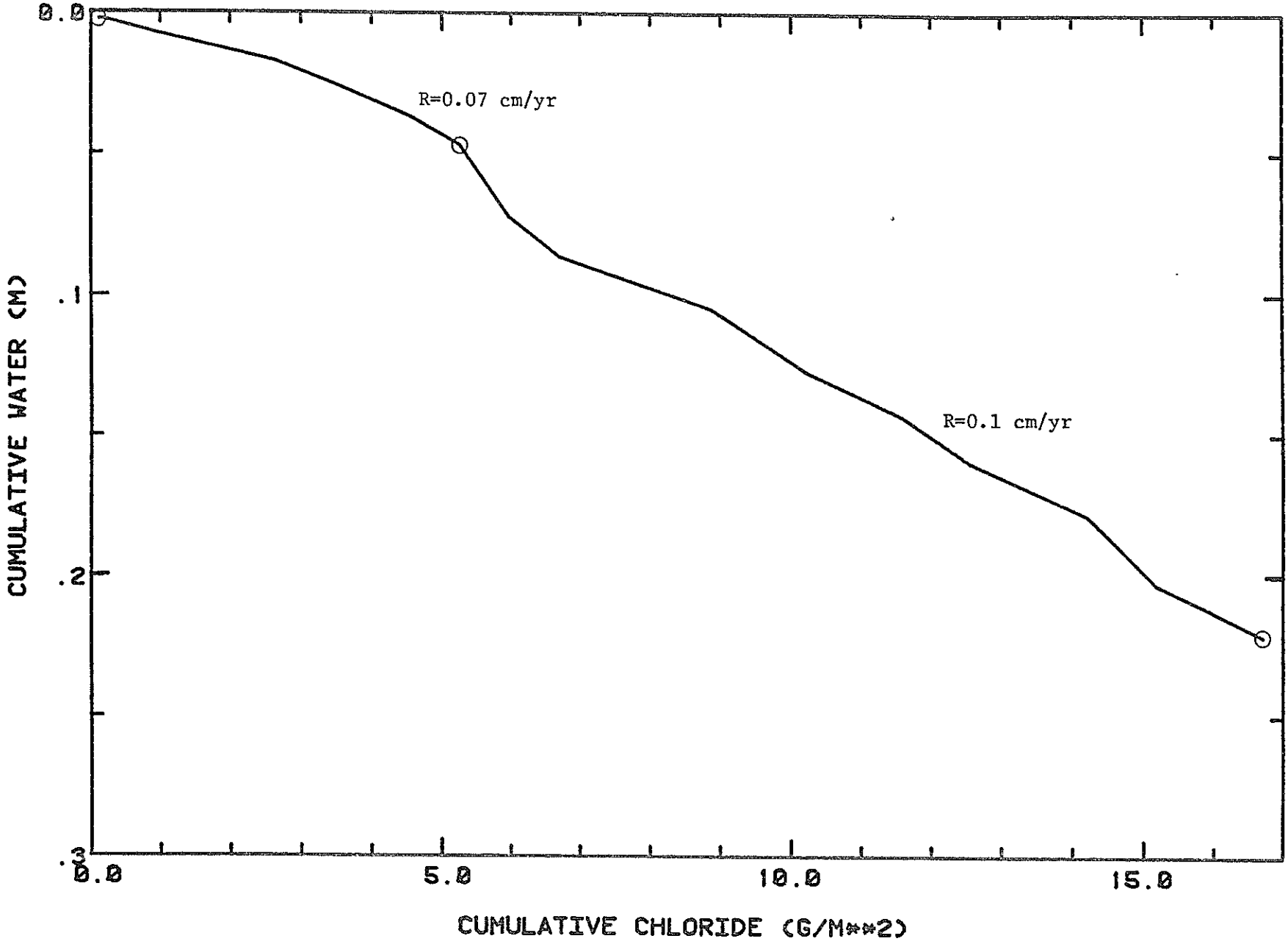

Fig. 26. Chloride vs. water, SNWR soil-water station 1

SNWR isotope sampling site. This site was selected for comparison between geochemically and physically determined recharge estimates. The area is relatively flat topographically and represents sparsely vegetated alluvial sand.

Soil moisture (figure 27) increases from .05 g/g at the surface to .08 g/g at 125 cm. It then decreases to .03 g/g and remains consistently low until 420 cm where it increases to .12 g/g. Soil heterogeneities are probably not responsible for the observed moisture profile. Figure 28 illustrates the relationship between percent silt and clay and moisture content at this location. There is no correlation with the exception of soil from the interval 404 to 432 cms depth. The high moisture content in this sample corresponds to the relatively high percentage of silt and clay sized particles. The peak at 125 cm could be due to a recent precipitation event while the increase in moisture at 500 cm is probably due to the influence of the capillary fringe since the water table was encountered at approximately 550 cm.

Chloride content (figure 27) remains uniformly low throughout the profile until it increases sharply at 400 cm. Such an increase could be due to evaporative enrichment of chloride at the water-table surface as previously discussed. The decrease below 400 cm could be attributed to the mixing of less saline groundwater with more saline soil water.

A cumulative chloride vs. cumulative water plot (figure 29) suggests little change in environmental conditions during the period represented by the upper portion of the plot. The increase at the base of the plot, as at the unvegetated site, is due to the anomalously high chloride content at 400 cm depth and not necessarily explained by a change in precipitation, chloride input and/or recharge at this location. The average recharge rate calculated from this plot, down to the point of major chloride concentration increase (about 3.5m) is 0.1 cm/yr. However, for the top meter it is 0.25 cm/yr.

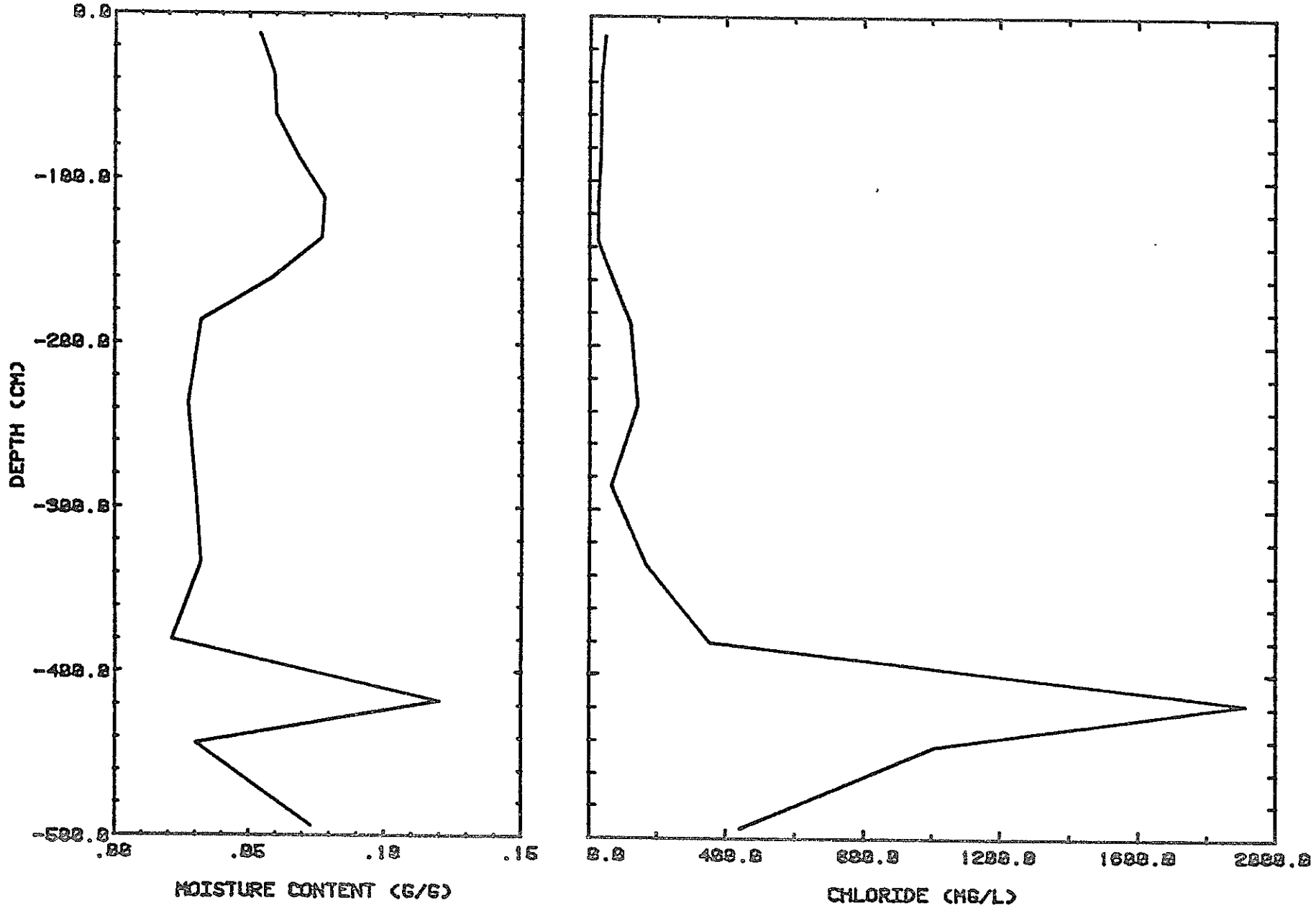

Fig. 27. Results from the isotope sampling location, SNWR

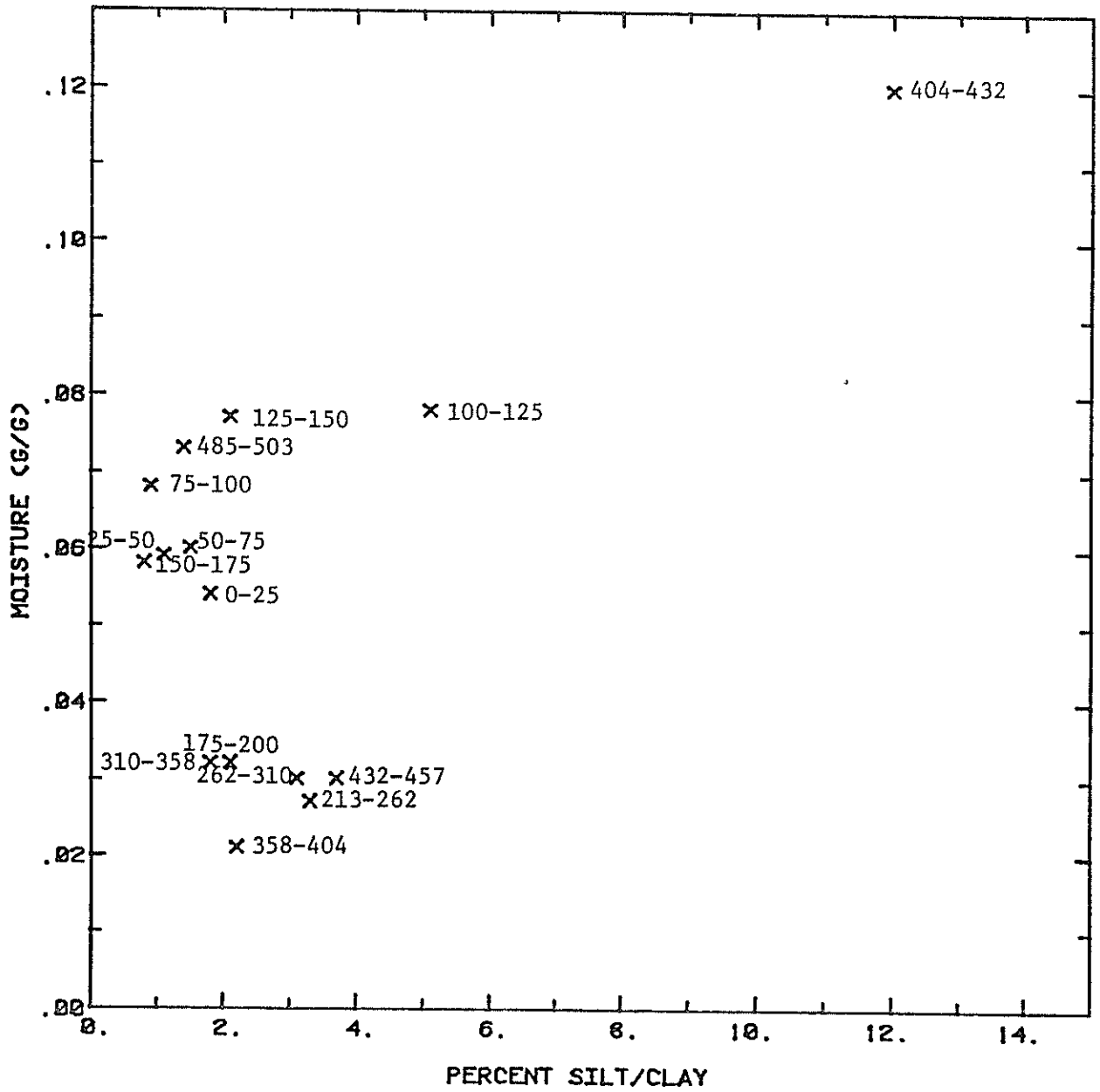

Fig. 28. Grain size vs. moisture content, SNWR isotope sampling site

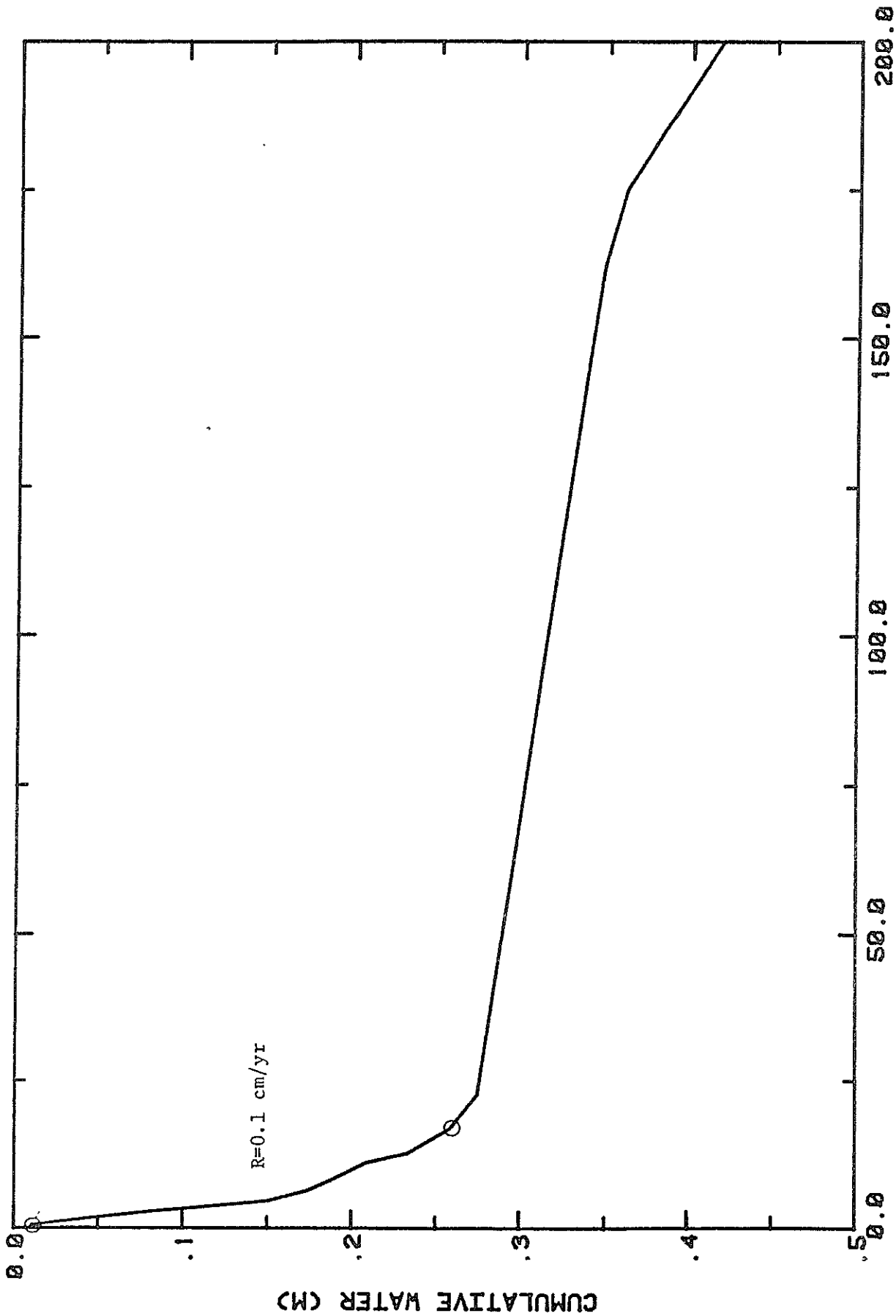

Fig. 29. Chloride vs. water, SNWR isotope sampling location

The weighted mean value of Clsw above the peak is 83 mg/l. Recharge for this setting is .1 cm/yr or less than one percent of the mean annual precipitation becomes recharge.

Results from the pressure-plate analyses are given in table 6. These measurements were performed to evaluate the possible influence of matric potential gradients on liquid and vapor flow of soil water. Residual moisture contents determined at 200 and 250 cm depths are greater than those observed at these depths in the field. Matric potentials in the field must thus be in excess of 15 bars. Moisture extraction by plant roots could decrease moisture contents below the 7 to 9 percent residual volumetric moisture content.

NMSUR isotope sampling site. This site is topographically flat and sparsely vegetated. Moisture content from 10 to 130 cm (figure 30) increases from .045 g/g to .12 g/g. Below 130 cm, moisture content decreases sharply to 0.05 g/g. Soil heterogeneity probably accounts for the variation in moisture content at this site. Figure 31 illustrates the correlation between moisture content and percent silt and clay. In general, higher moisture contents are associated with higher percentages of silt and clay. The two samples collected below 175 cm were from a moderately indurated caliche which probably inhibited the downward movement of water through this zone. This factor would account for the low moisture contents associated with the relatively high percentages of silt and clay sized particles.

Chloride concentrations (figure 30) remain relatively uniform around an average value of 50 mg/l from land surface to a depth of about 130 cm where chloride increases to near 700 mg/l. This increase could represent the effects of the root zone although a less abrupt increase in chloride concentration throughout the root zone would be expected. Chloride concentration remain at

TABLE 6

Results of the 1.5 and 15 bar pressure plate experiment.

Depth (cm)	Residual Vol. Moisture Content at 1.5 Bars	Residual Vol. Moisture Content at 15 Bars
150	0.080	0.080
200	0.073	0.067
250	0.096	0.096

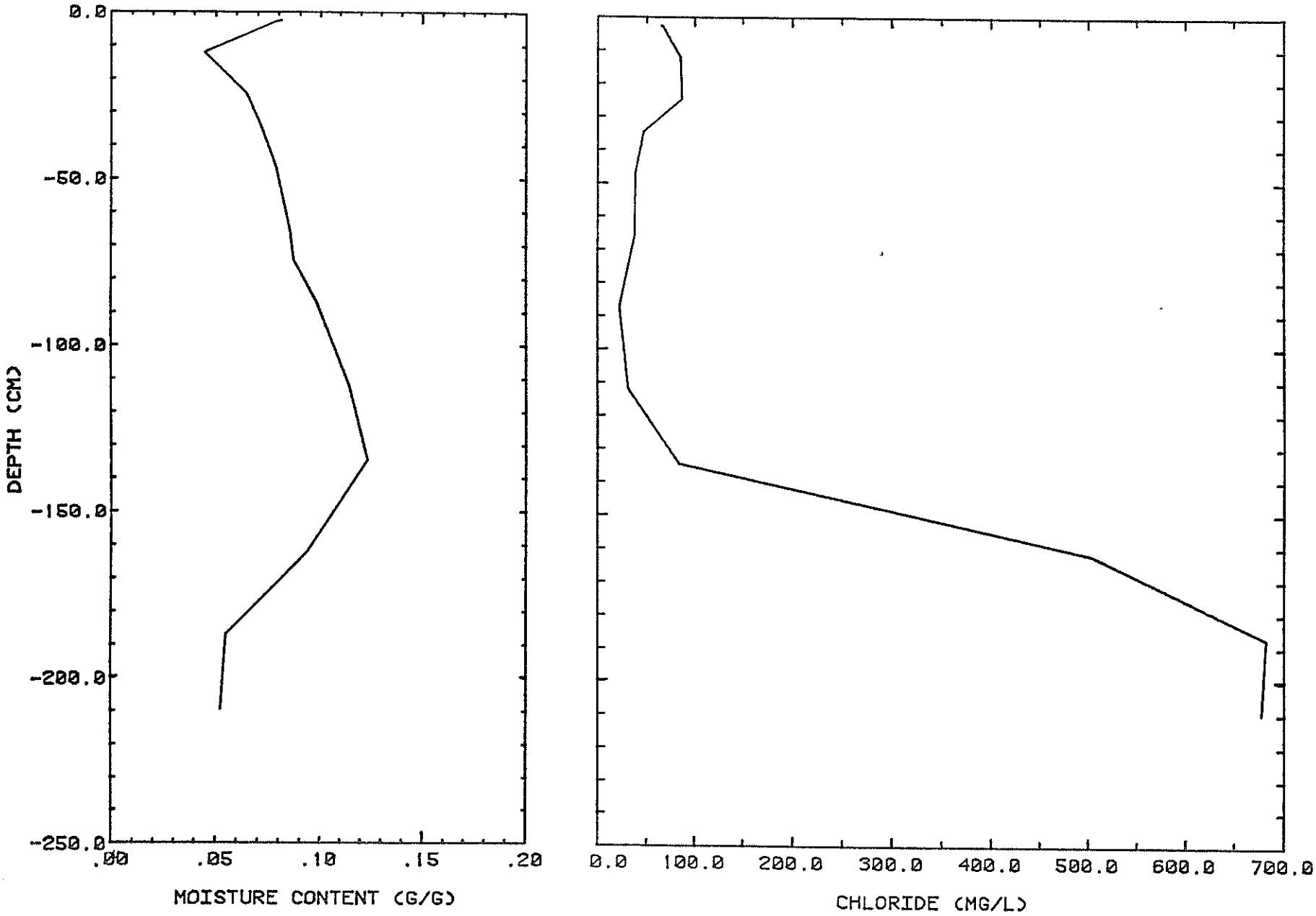

Fig. 30. Results from the NMSUR isotope sampling site

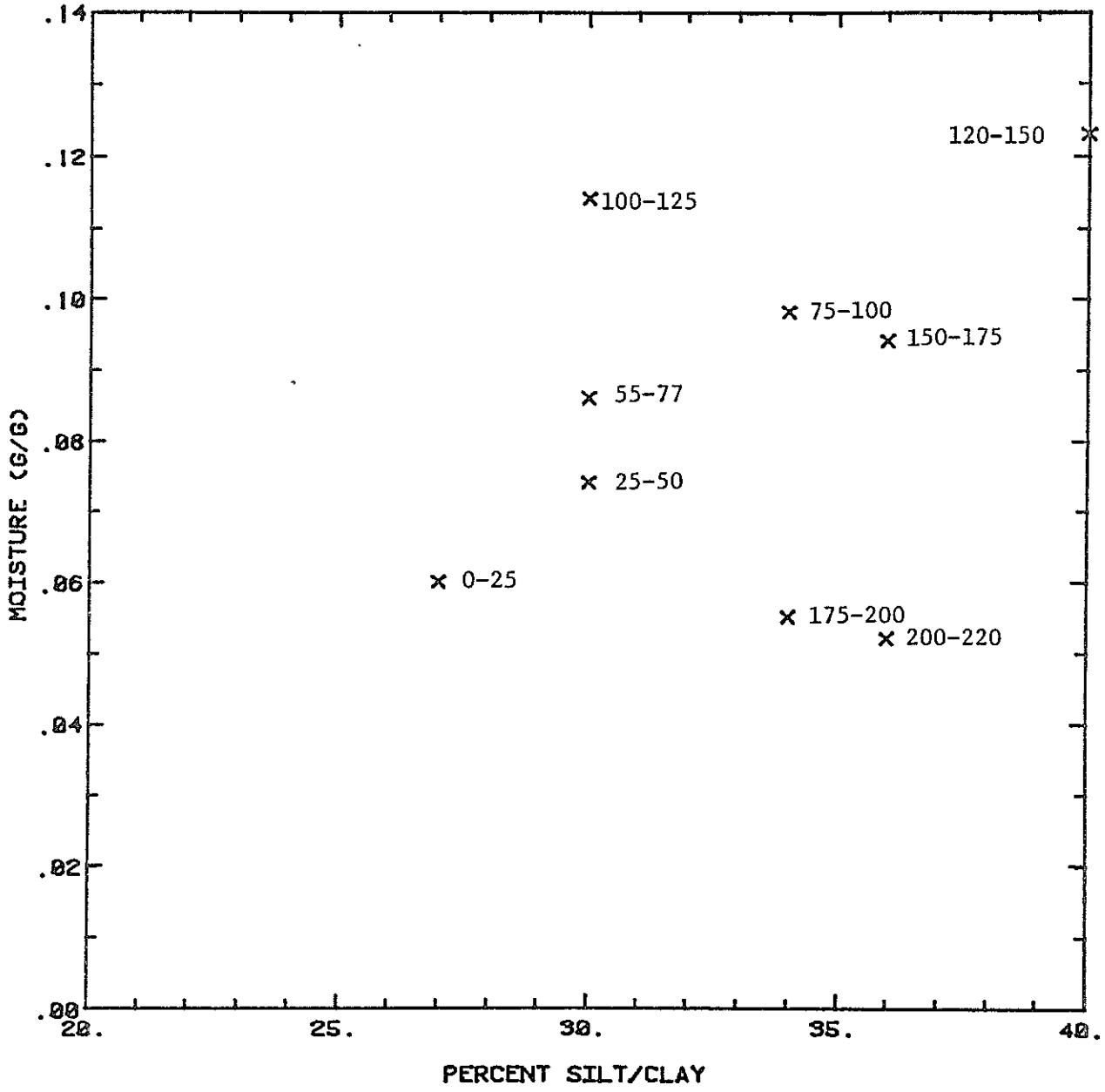

Fig. 31. Grain size vs. moisture content, NMSUR isotope sampling site

Numbers indicate the sampling depth interval, in cm.

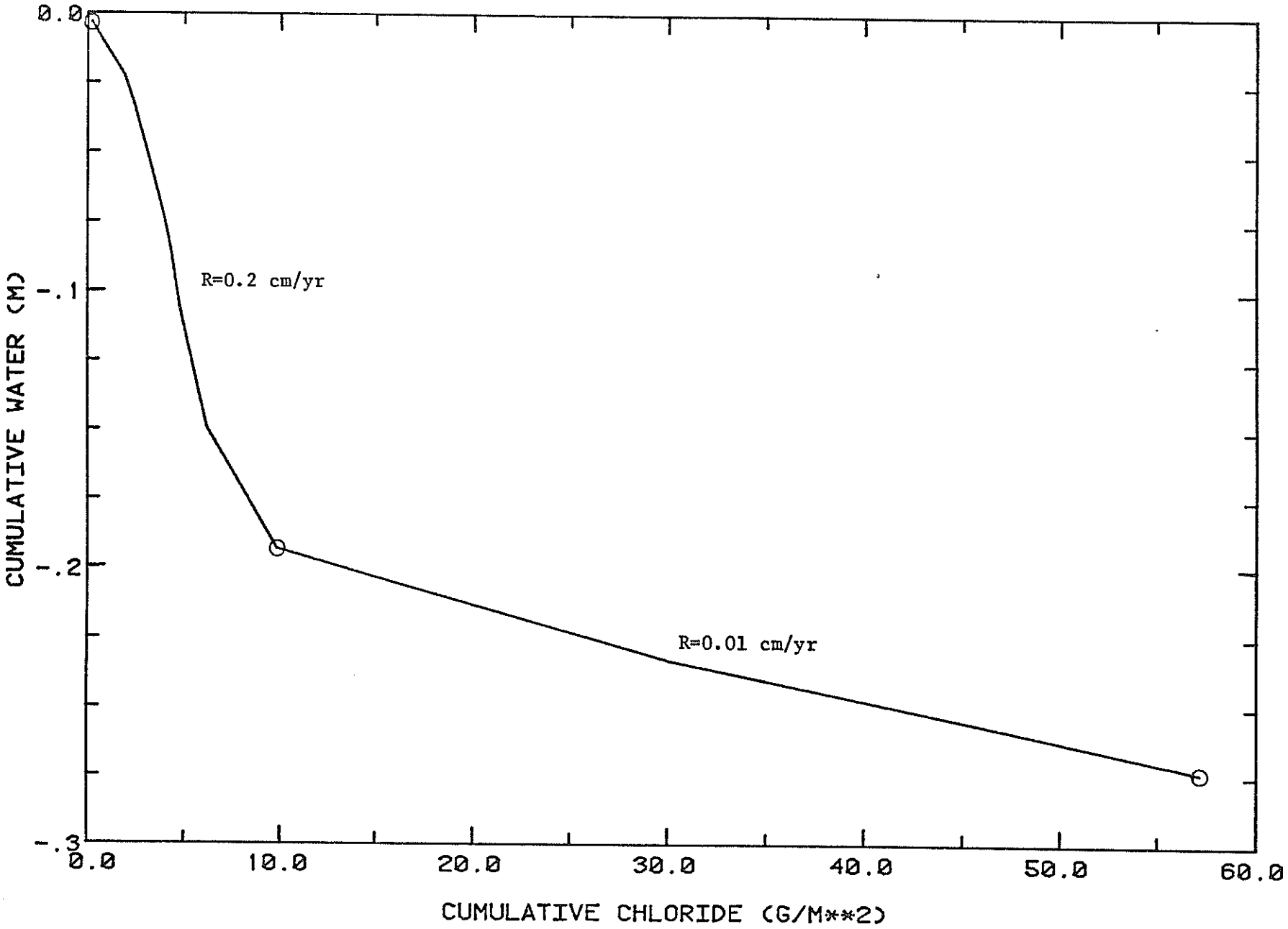

Fig. 32. Chloride vs. water, NMSUR isotope sampling site

peak levels for at least 25 cm. A decrease in chloride concentrations below the peak, similar to that seen at the SNWR isotope sampling site, is not evident. The water table is approximately 100 m below ground surface and could not affect chloride concentrations in the top 2 m of soil. Further sampling would be required to accurately delineate chloride concentrations below 210 cm. Assuming concentrations maintain this peak value, recharge below the root zone is only .01 cm/yr. If, however, concentrations decrease below the peak, either fresh water is reaching the lower part of the profile by other than piston flow, or conditions were more favorable for recharge at the time represented by the lower part of the profile. Recharge above the peak, using a weighted average Clsw of 45 mg/l, is .2 cm/yr or almost one percent of the average annual precipitation.

A cumulative chloride vs. cumulative water plot (figure 32) indicates two periods of relatively constant environmental conditions, with recharge in the upper portion greater than that in the lower.

Discussion of Chloride-Mass-Balance Results

Stephens et al. (1985) calculated recharge based on Darcy's equation at soil-water station 1 on the SNWR. During the period November, 1982 through May, 1984, they estimated a mean annual flux of 0.902 cm/yr and 4.73 cm/yr using harmonic and geometric mean hydraulic conductivities respectively. Using a mean annual precipitation of 17.9 cm/yr during that period, recharge is 5.0 percent and 26.5 percent of annual precipitation, using harmonic and geometric mean hydraulic conductivities respectively.

The chloride method estimates that recharge is less than 1 percent of the average annual precipitation at soil-water station 1, considerably lower than that estimated by the soil-physics study of Stephens et al. (1985). This difference could be, in part, a result of chloride movement only in the liquid phase. Even a small component of vapor-phase transport could retard chloride

relative to the movement of water. In addition, because the topographic slope increases to the south of station 1, lateral flow components may exist. Stephens et al. (1985) studied the effects of topography on unsaturated flow direction by tracing bromide movement on a hillslope near station 7. They found that bromide moved with a significant lateral component in the direction of the topographic slope even when all stratification was destroyed. These lateral flow components are probably largely responsible for the discrepancies between chloride determined recharge estimates and those based on Darcy's Law on those sites close to steep topography. This is because the chloride mass balance reflects the average amount of evapotranspiration over whatever area the soil water is derived from whereas the soil physics measurements determine vertical flux at one specific location. If the vertical flux is not areally uniform the local flux may be greater or less than the average.

At station 15, on the active dune, where the sands are very permeable and vegetation is sparse, recharge estimates based on the chloride method are still only about one percent of the average annual precipitation. The discrepancy between this value and those calculated using a soil-water mass balance is not surprising. The chloride method assumes one-dimensional vertical flow while three-dimensional flow actually occurs.

Recharge rates estimated using the chloride method for the SNWR isotope sampling site and the unvegetated site are also quite low, averaging about 1 percent of the annual precipitation. There is no apparent effect of vegetation, as indicated by comparing the vegetated sites with the site growing only sparse grasses. Surficial vegetation distribution, however, may not be a good indicator of recharge. Plant root systems may be much more laterally extensive below land surface and consequently affect areas that appear only sparsely

vegetated. Both locations are topographically flat and no evidence for lateral flow exists at this time.

It is important to emphasize that the chloride method assumes one-dimensional vertical flow. This assumption is incorrect on sloping locations and leads to erroneously low local recharge estimates. Estimates on topographically flat locations, however, are probably good, providing the remaining assumptions of the chloride method are valid.

3H AND 36Cl PROFILES

-Sevilleta National Wildlife Refuge Site

Final 36Cl/Cl sample ratios and 3H values for the SNWR and the NMSUR are listed in tables 7 and 8, and plotted vs. depth in figures 33 and 34.

The SNWR 3H profile consists of three peaks, two smaller peaks towards the surface at approximately 30 and 90 cm depths and a large pulse between 175 and 300 cm. The peak closest to the surface has a concentration of 48 T.U. and probably represents rainfall from the last precipitation event to have a similar concentration. Rainfall during April-June, 1981 was the last to have approximately the same concentration, indicating that surface soil water is nearly 3.5 years old (Duval 1986). The pulse between 175-300 cm corresponds to 1962-1965 input. Average seepage velocities to the surface and 1964 peaks are 9 and 11 cm/yr respectively (Duval 1986). Seepage velocities were calculated by dividing the distance between the ground surface and the peak by the travel time. According to these calculations, the peak at 90 cm was input during 1975, a wet year with a decay corrected input of 40 T.U. (Duval 1986). The trough in the 3H profile (8 T.U.) at 160 cm would normally indicate pre-1957 3H levels. The 1962-1965 pulse is, however, directly below the trough. Assuming an average flow velocity of 10 cm/yr, and correcting for decay, soil moisture at this depth should have been input during 1971-1972. The average 3H concentration in

TABLE 7

Data from SNWR soil samples

Depth (cm)	Tritium (T.U.)	Depth (cm)	$^{36}Cl/Cl \times 10^{15}$
5-25	48±8	0-25	16870±8%
45-65	20±8	25-50	5140±17%
70-90	40±8	50-75	2538±7%
100-120	27±8	75-100	9749±21%
145-160	8±8	100-125	2797±28%
180-200	70±8	125-150	2556±8%
231-251	59±8	150-175	2234±15%
282-302	68±8	175-200	2095±17%
333-353	none detected	213-262	1253±30%
380-400	24±8	262-310	2530±7%
422-442	27±8	358-404	172±9%
505-525	31±8	404-432	113±14%
		485-503	279±10%

TABLE 8

Data from NMSUR soil samples

Depth (cm)	Tritium (T.U.)	Depth (cm)	$^{36}Cl/Cl \times 10^{15}$
0-25	16±8	0-25	19853±7%
20-30	49±8	25-50	2672±8%
30-40	28±8	55-77	15484±7%
40-50	16±8	75-100	3398±8%
55-70	44±8	100-125	4995±6%
75-100	45±8	120-150	9260±4%
100-112	24±8	150-175	3504±4%
112-135	45±8	175-200	677±6%
135-156	90±8	200-220	465±6%
175-180	43±8		
195-205	34±8		

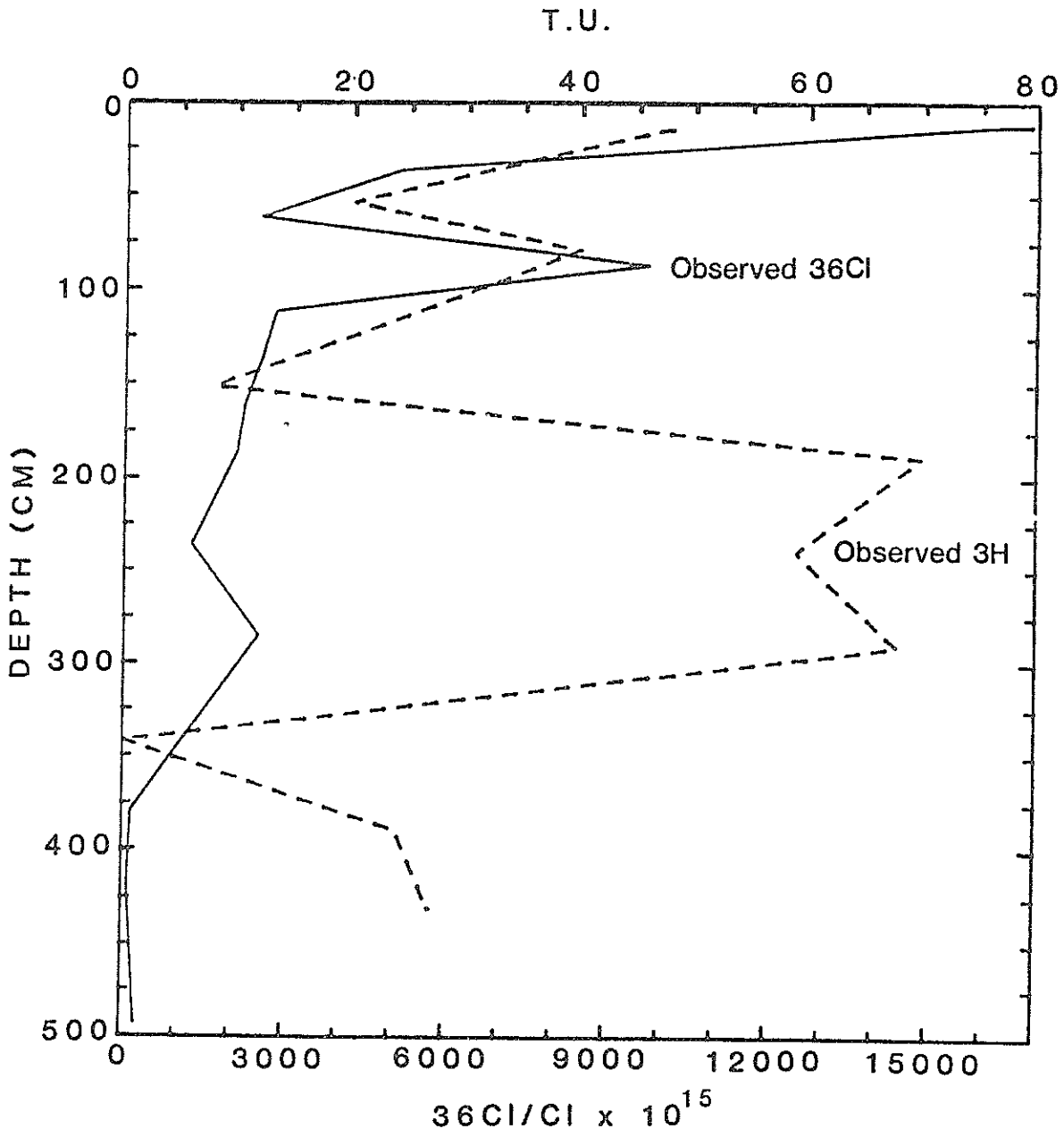

Fig. 33. 3H and 36Cl vs. depth at the SNWR, November, 1984. The broken line indicates 3H concentration.

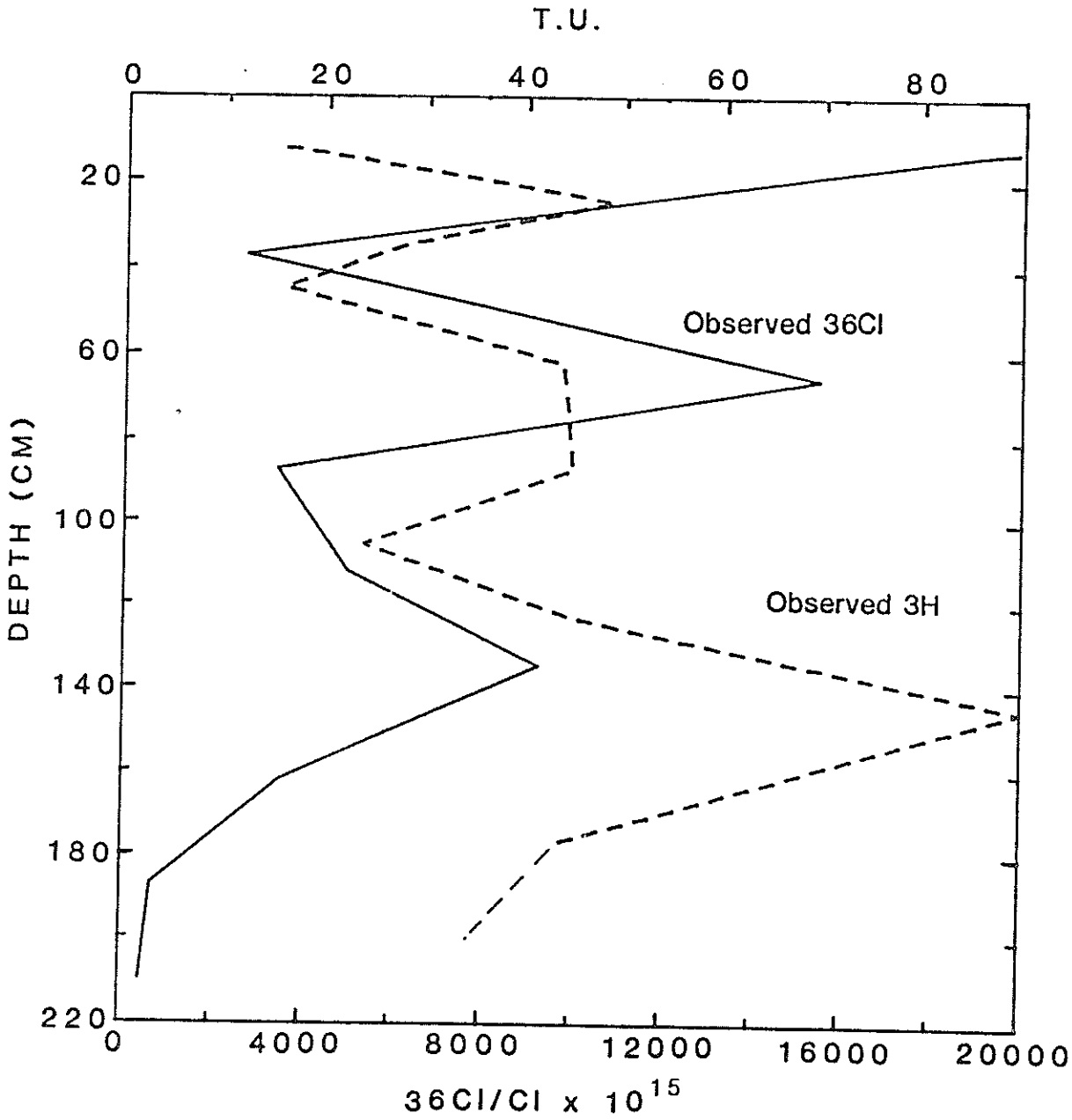

Fig. 34. 3H and 36Cl vs. depth at the NMSUR, March, 1985. The broken line indicates 3H concentration.

rainfall for those years was 40-50 T.U., too high to account for the trough at 160 cm. However, rainfall during the last quarters of 1971 and 1972 had decay-corrected concentrations of 20.6±10 T.U. and 17.9±10 T.U. respectively. October of 1972 was very wet (13.6 cm of rain) and could possibly account for the observed concentration. Much of the balance of the 1972 precipitation may have been lost to evapotranspiration and consequently did not contribute higher levels of 3H to the soil water (Duval 1986). The calculated seepage velocity to 160 cm is 12.4 cm/yr which correlates well with the average seepage velocity of 10.8 cm/yr.

The 3H concentration between 333 and 353 cm is below detectable levels. This sample represents the maximum penetration of bomb-3H. The increase in 3H concentration below 353 cm can be attributed to soil water low in 3H mixing with high 3H (31 T.U.) groundwater (Duval 1986).

Since the 36Cl input function can be closely approximated by a square wave, it is expected that, under piston flow conditions, the 36Cl profile found in the soil would be identified by a well-defined peak. Because of its different shape, the 36Cl profile at the SNWR cannot by explained in terms of this simple model. The profile consists of three peaks, the depths of which correspond closely to the depth locations of the three peaks observed in the 3H profile. Most of the bomb-36Cl is retained in the upper portion of the soil profile although some has traveled to depths as low as the 1962-1965 bomb-3H pulse. Under piston-flow conditions, most of the bomb-36Cl should have moved deeper into the soil profile than the 3H pulse since bomb-3H was input after bomb-36Cl. Anion exclusion effects, if present, would also drive 36Cl ahead of 3H.

The 36Cl/Cl ratio at 375 cm represents the maximum penetration of bomb-36Cl indicating the extent of the last 30 years of solute movement. Below 375 cm,

the ratio is relatively constant, averaging 175 x 10^{-15} and represents the prebomb production of 36Cl. This value does not correspond well with the predicted range in figure 3 and may indicate addition of low $^{36}Cl/Cl$ ratio sedimentary chloride. This low ratio is present only in the groundwater-influenced capillary zone (4 to 5m) and this was probably introduced by underflow originating from the Rio Salado (Salt River).

This 36Cl profile is difficult to explain. Since much of the 36Cl is retained in the upper portion of the soil profile above the 1962-1965 bomb-3H pulse, it appears that chloride movement may somehow be restricted. Such a phenomenon, however, would be the opposite of that commonly observed. Generally, negatively charged silicates repel anions from the mineral surfaces, resulting in chloride movement ahead of tritium.

As previously explained, column experiments were undertaken to determine if indeed some chloride retardation mechanism existed in SNWR soils. Results in figures 35 and 36 indicate no such mechanism. High concentrations of chloride were not maintained in the upper portion of the column above the wetting front. Instead, chloride moved relatively uniformly along with the moisture, indicating that the tracer had little chemical interaction with the porous material.

The answer to this dilemma may be the greater volatility of HTO comared to $36Cl^-$. Since chloride travels only in the liquid phase, it can move only through interconnected liquid pathways. Where liquid continuity is broken, 36Cl may be trapped in liquid water pockets between grains while 3H continues to move across the gaps in the vapor phase. Such a mechanism would allow 3H to move ahead of 36Cl. Some liquid pathways probably remain continuous or become continuous during intense recharge events which would allow some 36Cl to travel to lower depths.

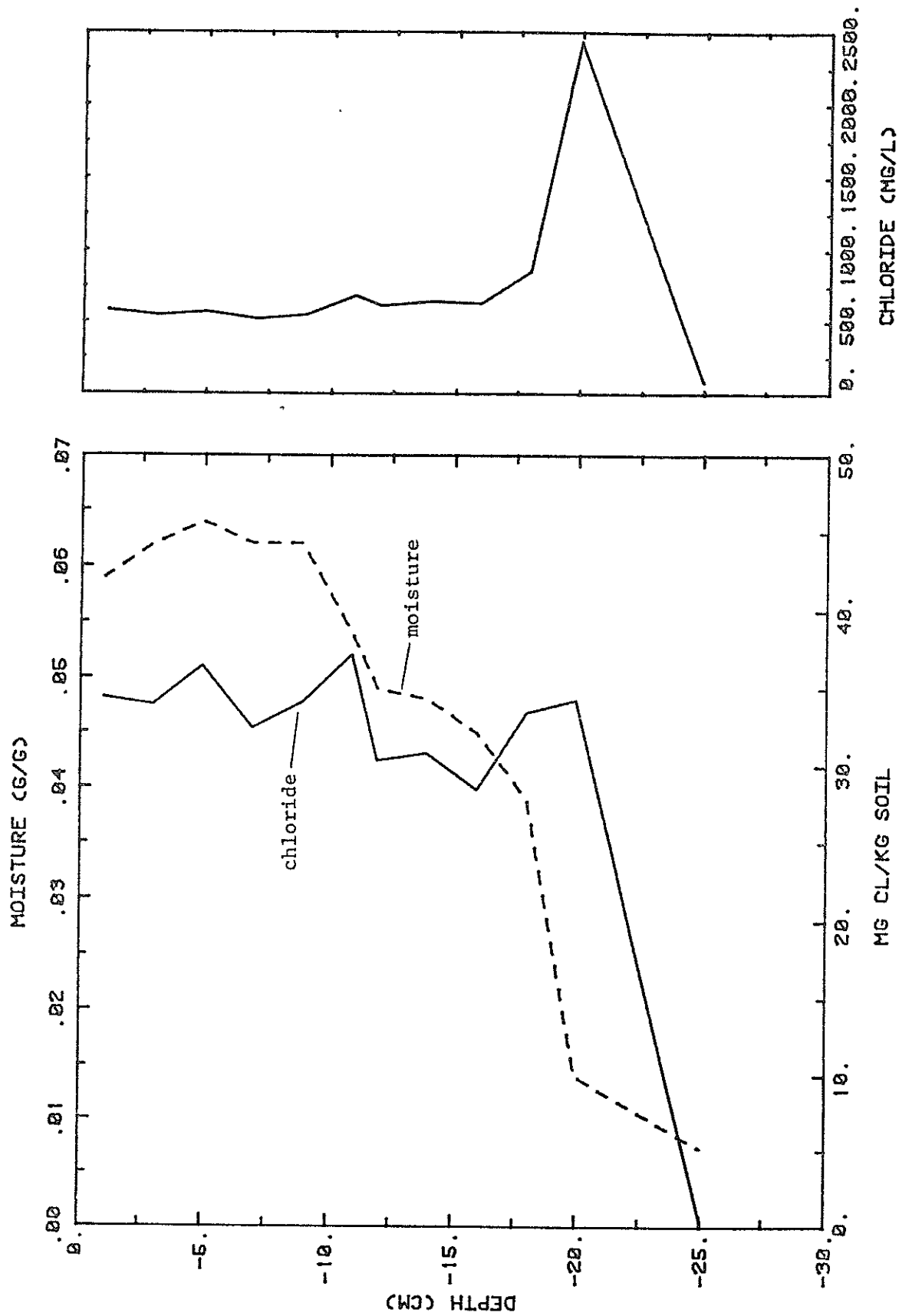

Fig. 35. Moisture and chloride vs. depth. Column experiment 1. Density equals 1.65 g/cc.

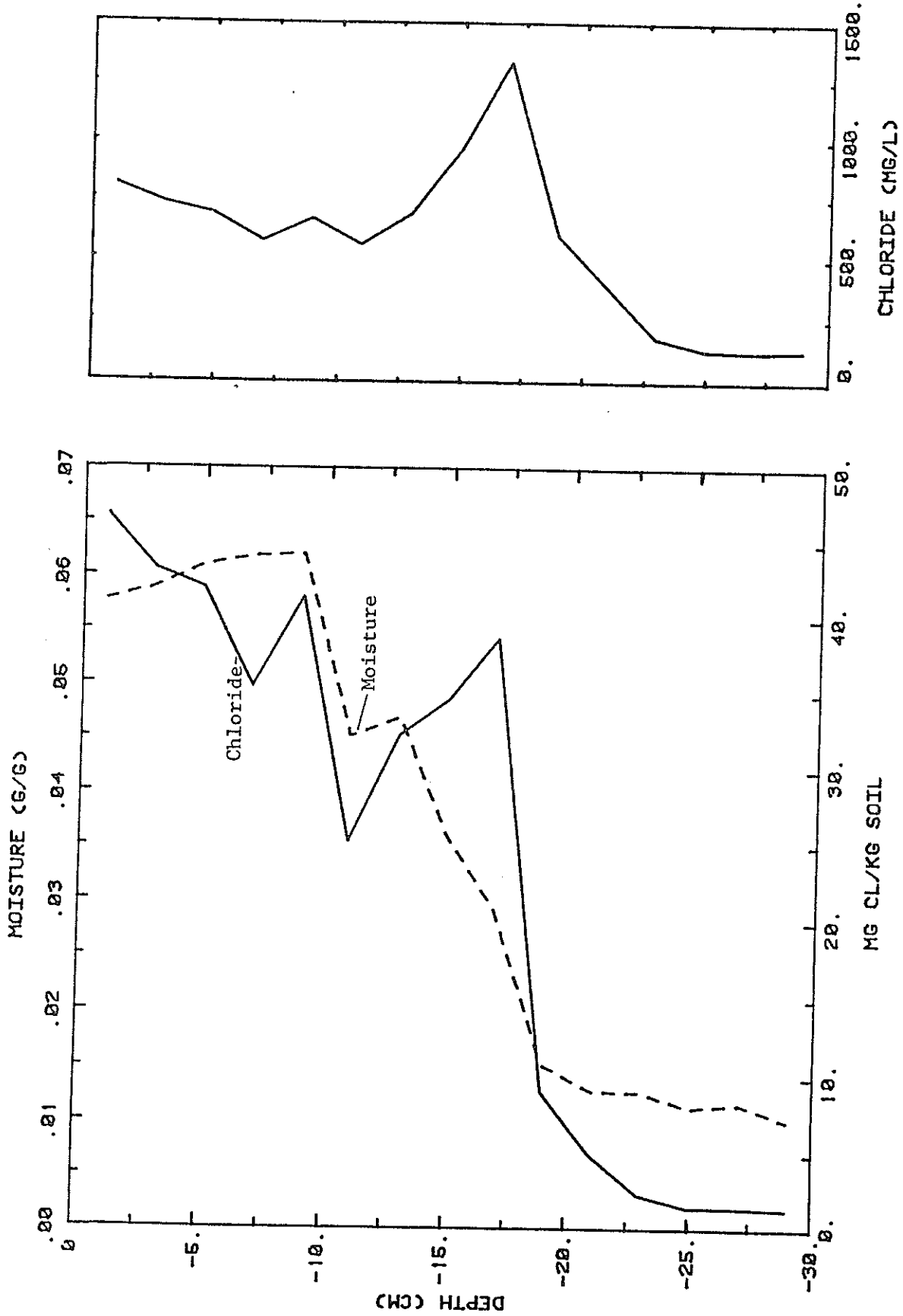

Fig. 36. Moisture and chloride vs. depth. Column experiment 2. Density equals 1.83 g/cc.

The corresponding depths of 3H and 36Cl peaks may be a manifestation of "catastrophic" recharge events which open more interconnected pathways and pulse water downward. However, the troughs between peaks are difficult to explain using this mechanism.

Another possible mechanism by which these peaks may occur is flow through preferential pathways. Allison and Hughes (1983) proposed that rainfall intercepted by the foliage of plants is concentrated by stemflow and directly input to the soil, inducing rapid percolation. According to their study, stemflow has been observed to occur in a number of species of vegetation growing in semi-arid conditions in Australia. This water is then transported to depth through the channels of living roots. They point out that the diameter of roots may change diurnally in response to water stress and that dry matter produced by roots is shed and decomposes, leaving a gap around the mature root. In order for moisture to reach greater depths, the movement of water through the annuli between soil and roots must occur under high antecedent moisture conditions or be rapid enough to allow only small amounts of wetting up of the shallow soil surrounding the root. The water which has moved down the root annuli may then spread laterally at depth. Organic matter shed by roots may help to produce a relatively impermeable annulus around the roots (Allison and Hughes 1983).

The actual mechanism by which water moves to depth is open to conjecture but the above provide possible explanations.

-New Mexico State University Ranch Site.

The shape of the NMSUR 3H profile is similar to the SNWR profile. The 1962-1965 peak lies at 145 cm and two smaller peaks occur closer to the soil surface. The surface soil water in this profile, however, has a relatively low 3H concentration, 16 T.U.. Las Cruces field work was conducted in March 1985 and

apparently the heavy but presumably low 3H precipitation from the previous fall penetrated the top 25 cm of soil (Duval 1986). Tritium concentrations in fall precipitation during the 4 previous years varied between 10 and 25 T.U. which compares well with the 16 T.U. observed in the top 25 cm of soil (Duval 1986). In November 1984 the top 25 cm of soil at the SNWR isotope sampling site had 3H concentrations equal to 49 T.U. In March, 1985 3H concentrations between 20 and 30 cm at the NMSUR also equaled 49 T.U. Since 3H concentrations do not vary appreciably over the state, precipitation that fell between November and March may have displaced high-3H soil water with low-3H fall-winter precipitation. The unusually wet fall and winter (22 cm of precipitation between October and March) makes this hypothesis quite plausible (Duval 1986).

The 3H concentration at 145 cm represents the 1963-1966 pulse but not the maximum penetration depth of post-1955 recharge. The average seepage velocity to 145 cm equals 6.9 cm/yr which is significantly less than the average seepage velocity calculated for the SNWR. This reduction in velocity may be attributed to the larger fraction of silt and clay size grains at the NMSUR, resulting in greater moisture retention in the soil profile and thus a smaller depth of infiltration. The specific recharge flux averaged to the maximum bomb 3H penetration depth (160cm) is 0.95 cm/yr, very similar to that at the SNWR site.

The shape of the NMSUR 36Cl profile is similar to the SNWR profile. The profile consists of three peaks, the depths of which correspond closely to the depths of the three peaks observed in the 3H profile. The 36Cl/Cl ratio at 190 cm represents the maximum penetration depth of solute input since 1953. This depth is significantly less than that observed at the SNWR and may, again, be attributed to the larger fraction of silt and clay at the NMSUR. Below 190 cm the ratio averages 575×10^{-15} and represents the pre-bomb production of 36Cl.

This pre-bomb value corresponds to that predicted in figure 2 more closely than the SNWR pre-bomb value and indicates little or no chloride contamination.

This multi-peaked profile indicates discontinous or non-piston flow conditions, possibly explained by previously discussed mechanisms.

At the SNWR, the 1964 3H peak indicates an average seepage velocity of 10.8 cm/year. The weighted average volumetric moisture content between 0 and 325 cm equals 0.078. Multiplying the average seepage velocity by the average volumetric moisture content gives a mean recharge specific flux to the peak of 0.84 cm/yr, or 3.8 percent of the average annual precipitation becomes recharge. Equation 1, based on the total amount of 3H stored in the profile, gives a slightly lower value equal to 3 percent of the average annual precipitation. Recharge calculations based upon the 1963-1964 bomb peak at the NMSUR show that 4.7 percent of the average annual precipitation recharges to 145 cm.

The multi-peaked nature of the 36Cl profiles at both locations make recharge estimates difficult.

Phillips et al. (1984), as previously mentioned, used the bomb-36Cl pulse as a tracer for soil-water movement on a Pleistocene terrace on the SNWR. Chloride was leached from soil samples taken from a vertical auger hole in a sandy loam. Results are given in figure 37. Unlike the multi-peaked profile found in the current study, water that infiltrated during 1953-1964 is easily identified by the peak at 1 m depth. The average prebomb 36Cl/Cl ratio below two meters is 717×10^{-15} which corresponds well with the predicted range in figure 3.

Recharge estimates are easily calculated from such results. They estimated the net infiltration to 1 m depth to be 1.2 percent of the annual precipitation.

The recharge fluxes estimated by Darcy's Law, the 3H and 36Cl peaks, and the chloride mass balance are listed in table 9. All of the isotope profiles and

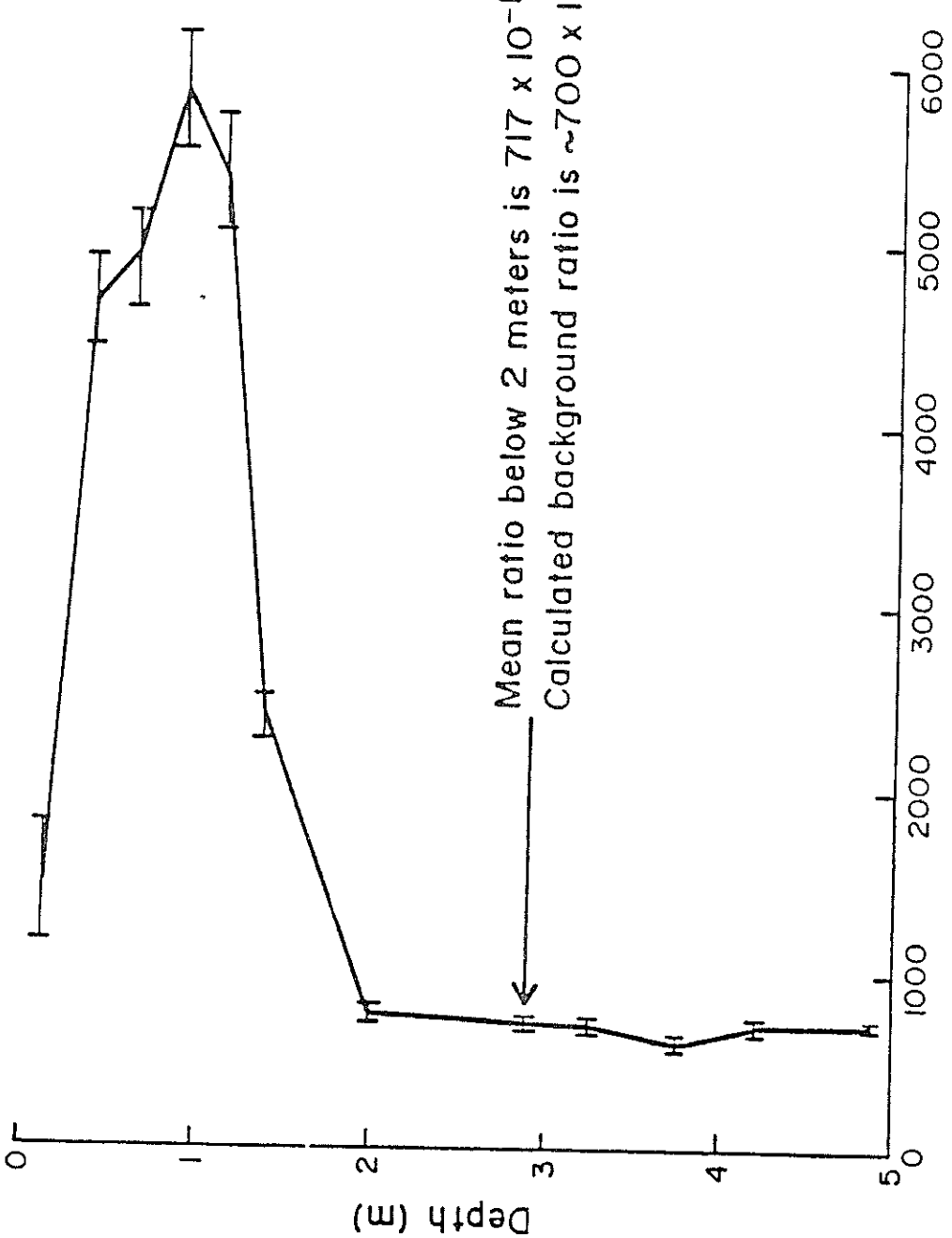

Fig. 37. The 36Cl/Cl ratios of soil samples from the Phillips et al. (1984) study.

Table 9. A comparison of recharge specific fluxes calculated by various methods

Site	Soil Texture	Darcy's Law: Geometric Mean K	Darcy's Law: Harmonic Mean K	Tritium Peak Method	^{36}Cl Peak Method	Chloride Mass Balance
SHWR Holocene floodplain	fine sand	4.73 cm/yr	0.90 cm/yr	0.84 cm/yr	0.3 cm.yr (0.8 cm/yr)**	0.25 cm/yr
SHWR Pleistocene terrace	sandy loam	-	-	-	0.26 cm/yr	0.2 cm/yr
NMSUR	sandy loam	-	-	0.95 cm/yr	0.25 cm.yr (0.9 cm.yr)**	0.15 cm/yr

* to depth of ^{36}Cl peak

** recharge value if deepest penetration of bomb-^{36}Cl is used

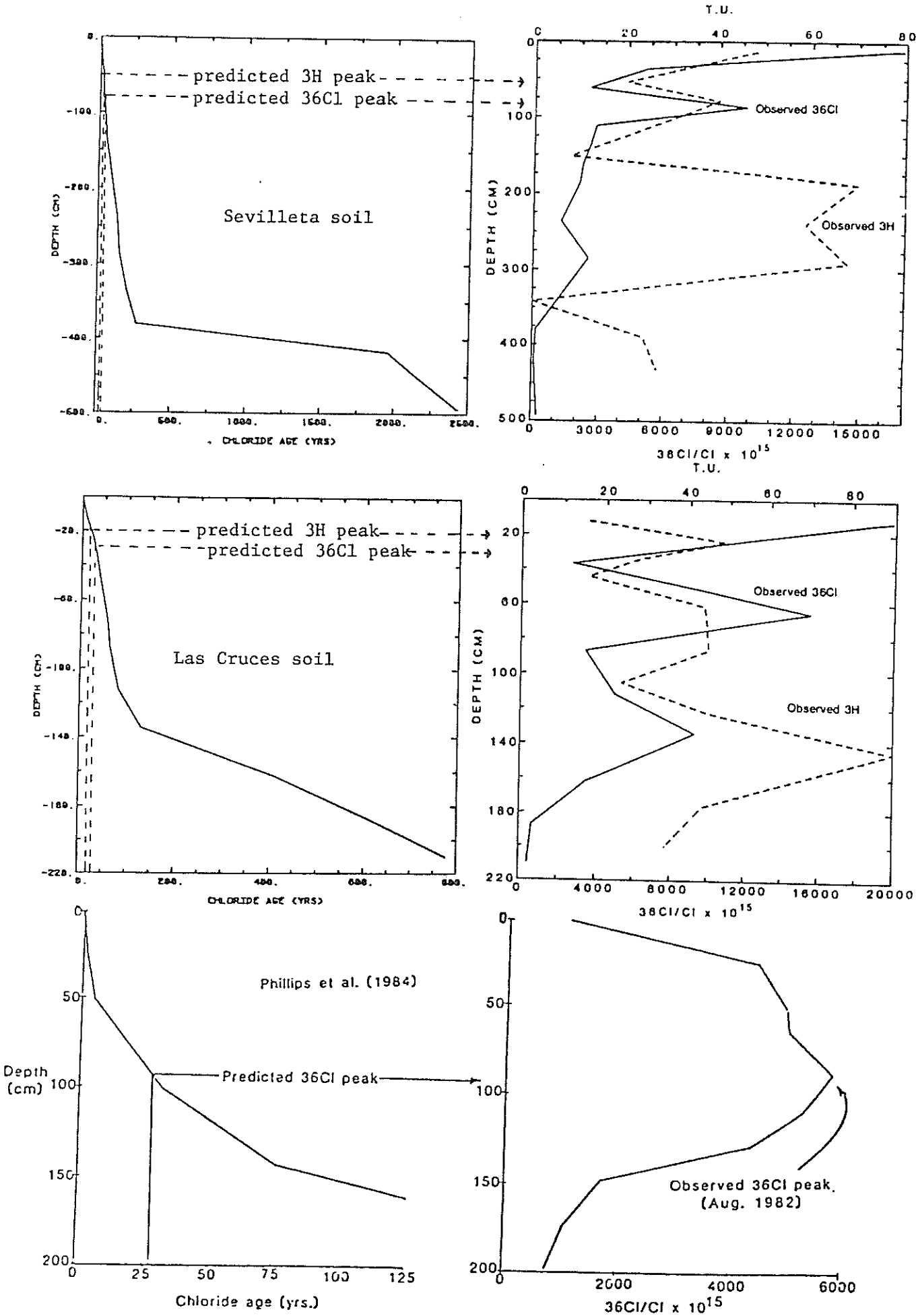

Fig. 38. Travel time calculation results

chloride mass balance results are shown together for comparison in Figure 38. Several observations can be made by comparing these data. First, if the mass centroid of the 36Cl ratio is used to calculate the recharge specific flux, the results from the three sites are in remarkable agreement, varying from 0.25 cm/yr to 0.3 cm/yr. Furthermore, these rates are also in substantial agreement with the independent chloride mass balance calculations, which range from 0.15 cm/yr to 0.25 cm/yr. A second observation is that these 36Cl and chloride mass balance results are not in agreement with the 3H peak results (0.84 cm/yr and 0.95 cm/yr). However, the 3H peak recharge fluxes are supported by the SNWR Darcy's Law calculations using the harmonic mean K.

Examination of the shape of the SNWR and NMSUR 36Cl profiles helps to resolve this discrepancy. Unlike the 3H profile, which can be explained by piston-flow translocation (plus dispersion) of the 3H input to the soil surface, the 36Cl profile tends to decrease from a maximum at the soil surface to pre-bomb values at depths, in a roughly exporential fashion. If the deepest penetration of bomb 36Cl is used to calculate recharge, rather than the centroid, the fluxes agree well with those determined from the 3H peak. The following conclusions may be drawn:

1. The recharge specific fluxes at the SNWR and NMSUR sites are both about 0.9 cm/yr.
2. The soil water movement may be approximated by a piston-flow displacement process.
3. Both the 36Cl and the stable chloride do not move with the soil water, but rather move at an average rate about one-third that of the water.
4. The advection of the chloride is not a piston-flow process, but rather one in which the amount of chloride retarded appears to be proportional to the travel distance.

The retardation of the chloride compared to the water is quite anomalous, given the well-known anion exclusion phenomena which tends to accelerate chloride relative to bulk water flow. The column moisture redistribution experiments (described above) provide evidence that interactions with the soil particles are probably not responsible for the retardation. The most likely explanation is thus one involving the fact that chloride can only be transported as a solute in the liquid phase, whereas 3H can move along with water vapor. Vapor-phase transport is discussed below.

Vapor Transport

The evidence discussed above suggest that 3H moves by a combined liquid and vapor flux. The combined liquid and vapor flux is given by equation 9.

$$q(l+v)=q(l)+q(v) \qquad (9)$$

where $q(v)$=vapor flux (L/T)

$q(l)$=liquid flux (L/T)

A first approximation of the vapor flux can be determined from equation 9 by using the mean liquid seepage velocities calculated from the values in tables 4 and 5, and the average seepage velocities calculated from the displacement of the 3H peaks.

From table 4, the weighted average liquid seepage velocity to 300 cm at the SNWR isotope sampling site is 2.0 cm/yr while the average seepage velocity calculated from the displacement of the 3H peak is approximately 10.8 cm/yr. Assuming that the difference between these velocities can be explained by additional vapor-phase movement, equation 9 may be solved to give a q(v) equal to 8.8 cm/yr. Similar calculations at the NMSUR give a q(v) equal to 6 cm/yr.

Equation 4 can be simplified to account only for vapor-phase transport. Assuming that thermal vapor flux dominates and that Ki is negligible, equation 4 can be reduced to

$$q(v)=DTvap\ T\ .$$

The "DTvap" coefficient incorporates the effects of porosity, tortuosity, and the "enhancement factor" on the free-air thermal diffusion coefficient.

The assumed vapor flux and the temperature gradient between 61 and 183 cm are known at the SNWR, and thus the thermal vapor diffusion coefficient can be back calculated for this interval. Using q(v) equal to 8.9 cm/yr and T equal to 0.018 $^{o}C/cm$, DTvap would have to equal 494 $cm^2/yr^{o}C$. This apparent effective diffusion coefficient is five to thirty times the values calculated from the physical properties of the soil, based on the works of Philip and de Vries (1957) and Cass et al. (1984). Thus the greater penetration of 3H than 36Cl cannot be explained solely on the basis of a thermally-induced vapor enhancement of the total flux.

Matric potential gradients can also induce vapor fluxes. The moisture content of the soil at the SNWR isotope site does decrease to quite low levels (3 to 5 volume percent) between 150 and 350 cm. Although the matric potentials associated with these moisture contents cannot be measured with the instrumentation available at the site, the pressure plate measurements described previously indicate that the potentials must be considerably less than -15 bars. Thus the downward matric potential gradient must be inducing a downward vapor flux. However, using an approach similar to that described above for the thermal vapor flux, an isothermal vapor diffusion coefficient at least six times

the values determined by Jackson (1964) for similar soils would be required. Thus neither thermally-induced nor matric-potential induced vapor diffusion alone, nor even the two combined, are of sufficient magnitude to explain the difference in water and chloride transport. Instead, we hypothesize that a much more limited form of vapor transport is responsible.

According to Philip and de Vries (1957), the state of water in very dry soils may be visualized as liquid "islands" linked by vapor transfer. As the water content is increased liquid regions become more interconnected. However, even when most of the water transport is by liquid flow, there may still exist some pores across which full liquid interconnection does not exist and across which the transport is in the vapor phase. These vapor "gaps" constitute a barrier to solute transport. We propose that the roughly exponential ^{36}Cl profiles at the SNWR and NMSUR sites are a result of the decreasing number of continuous liquid pathways with increasing flow distance. (The number of continuous pathways decreases, not because the number of vapor gaps increases with depth, but simply because the probability of encountering a gap increases with increasing flow distance.) This hypothesis has the advantage of requiring relatively small proportions of vapor transport across limited distances rather than massive vapor fluxes.

Solute Transport

A numerical solution of equation 5, developed by van Genuchten and Alves (1982), was used to simulate the transport of 3H through the SNWR sands. The solution is based on a linear finite element approximation of the spatial derivatives and a third-order finite difference approximation of the time derivative.

In order to model 3H transport and calculate a hydrodynamic dispersion coefficient, it was necessary to approximate the solute input. Duval (1986)

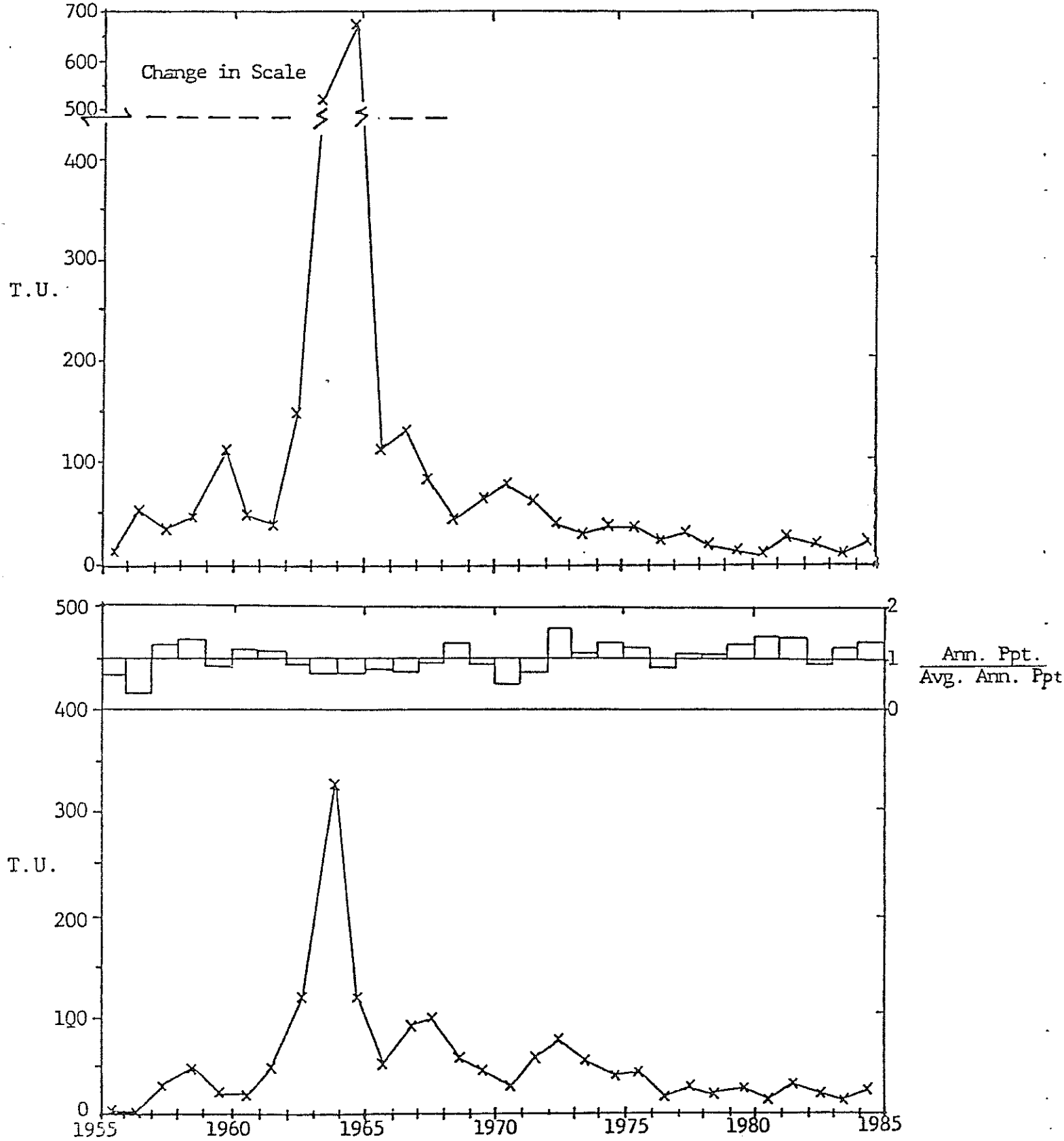

Fig. 39. Annual 3H concentration in New Mexico precipitation (top) and calculated 3H concentration using the TIF (bottom). Histogram shows the deviation of precipitation from the mean at Socorro, 1955-1985. All 3H values are corrected for decay. From Duval (1986).

developed a tritium input function (TIF) to account for temporal variations in tritium fallout (equation 10). The TIF is a first approximation of the potential 3H input and was calculated to maintain a mass balance between the observed and computed curves.

$$ATI = \frac{AP \; \Sigma \; TM(MP-ME)}{P \; \Sigma \; (MP-ME)} \qquad (10)$$

where
- ATI = potential annual tritium input (T.U.)
- AP = annual precipitation (L)
- TM = monthly tritium concentration in precipitation (T.U.)
- (MP-ME) = effective precipitation (L) (monthly precipitation minus estimated monthly evapotranspiration)
- P = average annual precipitation (L)

The TIF weights more heavily years with above average precipitation since they are most likely to contribute to recharge.

Equation 11 was used to estimate monthly evapotranspiration rates for 1983 and 1984 using SNWR corrected pan evaporation data and estimated crop coefficients (Duval 1986). If rainfall did not exceed potential evaporation, effective precipitation was given a zero value.

$$ME = EPan \; (kco) \qquad (11)$$

where ME =monthly evapotranspiration (L)

EPan=corrected monthly pan evaporation (L)

kco =crop coefficient (McWorter and Sunada 1977)

Figure 39 shows the temporal distribution of 3H concentration in rainfall and the calculated 3H input. Since most potential recharge occurs during the low 3H months from August through December, the calculated 3H input is lower than the annual precipitation 3H concentration (Duval 1986).

The numerical code was modified to handle this calculated 3H input and to calculate the hydrodynamic dispersion coefficient according to equation 12.

$$D = \alpha\bar{v} = 1/3\ (\theta/\text{porosity})^2 D_o \qquad (12)$$

The second term on the right of equation 12 is a relationship for the molecular diffusion coefficient developed by Wilson and Gelhar (1974). Duval (1986) used this relationship, with a porosity of 30 percent and a free-water diffusion coefficient for 3HHO of 790 cm^2/yr, to calculate an average molecular diffusion coefficient of 11.5 cm^2/yr at the SNWR.

Model input parameters included a dispersivity value, an average seepage velocity calculated from the 3H profile, a decay constant for 3H (0.056 yr^{-1}), and the calculated average molecular diffusion coefficient. Initial and boundary conditions are

$t \leq 0,\ x>0 \quad C=Co$

$t>0,\ x=0 \quad -D\partial c/\partial x + vc=vc$

$x=L \quad \partial c/\partial x=0$

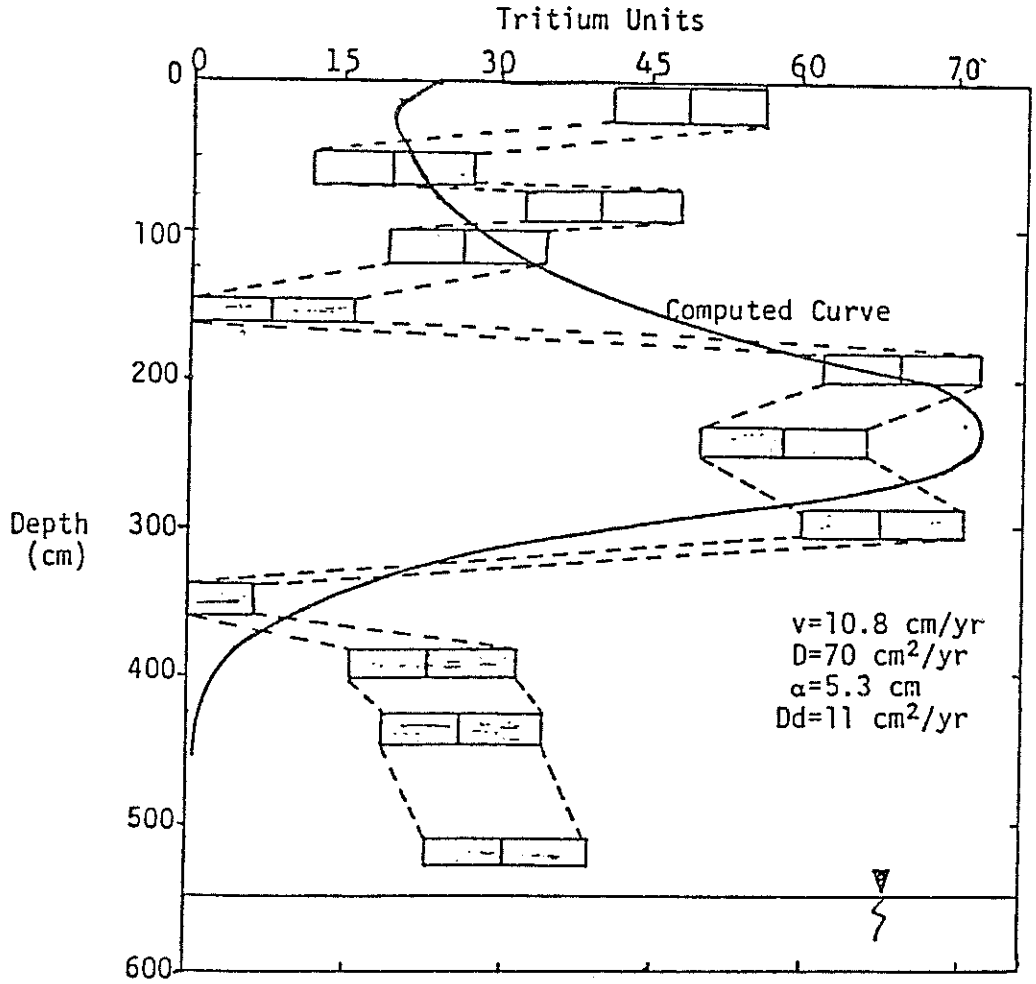

Figure 40 . Variation of the observed 3H concentration versus the computed concentration as a function of depth at the SNWR . The solid line represents the calculated profile. The shaded area of each box represents the analytical measurement error. From Duval (1986).

Results of the numerical simulation are given in figure 40. Boxes in the figure best describe the 3H distribution in the soil because the soil moisture was extracted over depth intervals. The solid curve represents calculated concentrations.

Duval (1986) found that a hydrodynamic dispersion coefficient equal to 70 cm^2/yr provided the best fit of the computed curve to the observed profile. Since the actual flow field is neither unidirectional nor constant, as required by the model equation, the calculated hydrodynamic dispersion coefficient is only an apparent value. The soil dispersivity equals approximately 5.3 cm assuming an average seepage velocity of 10.8 cm/yr. Freeze and Cherry (1979) give laboratory-determined dispersivity values of .1 to 1 cm under saturated conditions. They also point out that many investigators have concluded that dispersivities in field systems are significantly larger than values obtained in laboratory experiments. Using a statistical model, Wilson and Gelhar (1974) demonstrated that dispersivity increases as θ decreases. Such an increase is attributed to the more complicated flow path through which a fluid particle must travel as moisture content is lowered.

The computed curve does not fit the observed profile within 150 cm of the surface. One possibility for this discrepancy is the simplistic assumption of an average seepage velocity. Seepage may occur only for short periods after a precipitation event. After this time, soil water probably becomes nearly static until the next recharge event (Duval 1986). In addition, the 3H input function averages fallout over the year and consequently smoothes the data.

The observed 3H concentration increases below 350 cm which, as previously mentioned, may be due to mixing of groundwater with soil water. The numerical

simulation does not account for this and consequently the computed curve does not fit the lower three data points.

Because the multi-peaked nature of the 36Cl profiles at both sampling locations indicates discontinuous chloride movement or non-piston flow conditions, simulation of bomb-36Cl movement using equation 5 is impossible.

As previously mentioned, piston flow conditions do appear to exist in the Phillips et al. (1984) study.

The straight-line segments in figure 41 show the observed 36Cl concentrations over depth intervals on the Pleistocene terrace at the SNWR. The 36Cl/Cl ratio data were taken from Phillips et al. (1984) and were converted to concentrations as outlined in appendix H. The concentration peaks at a depth of approximately 135 cm. The mean input age of this pulse is 25 years, indicating an average vertical seepage velocity of 5.4 cm/yr. The bomb peak is deeper than that in figure 37 because of variation in sample chloride concentrations with depth.

A numerical solution of the advective-dispersive equation was used to simulate 36Cl transport. Galerkin's finite element method was applied to equation 5. One-dimensional linear elements were used (2 nodes/element) and the equation was solved subject to initial and boundary conditions previously given. Appendix I includes a listing of the Fortran program which details input variables required for program execution.

The hydrodynamic dispersion coefficient was calculated according to equation 12, using an average molecular diffusion coefficient of 0.015 cm^2/day and the seepage velocity determined from the observed 36Cl profile. This molecular diffusion coefficient falls within a range of values typical of non-reactive chemical species in clayey deposits (Freeze and Cherry 1979).

The predicted bomb fallout (figure 4) was multiplied by 0.14 to normalize areas under the observed profile and the predicted fallout curve. The observed profile at the SNWR isotope sampling site is also approximately 14 percent of the total predicted 36Cl fallout. Because precipitation is the major mechanism by which material is transferred to the surface of the earth, precipitation differences probably influence these values the most. Peterson (1970) estimated that 30-50°N "dry" area deposition is 0.5 times the average deposition 30-50°N while 30-50°N "wet" area deposition is 1.25 times the average deposition 30-50°N. Because New Mexico is considered a dry area (Federal Radiation Council Report No. 6, 1964), it is not surprising that observed total 36Cl fallout is reduced by approximately an order of magnitude. Appendix I illustrates the shape of the fallout curve used as input to the model and the necessary calculations to arrive at the input values.

The smooth curve in figure 41 is the modeled concentration profile. A hydrodynamic-dispersion coefficient equal to 0.13 cm^2/day provided the best fit of the computed curve to the observed profile. This yielded a soil dispersivity equal to approximately 8 cm. Again, the hydrodynamic-dispersion coefficient is only an apparent value.

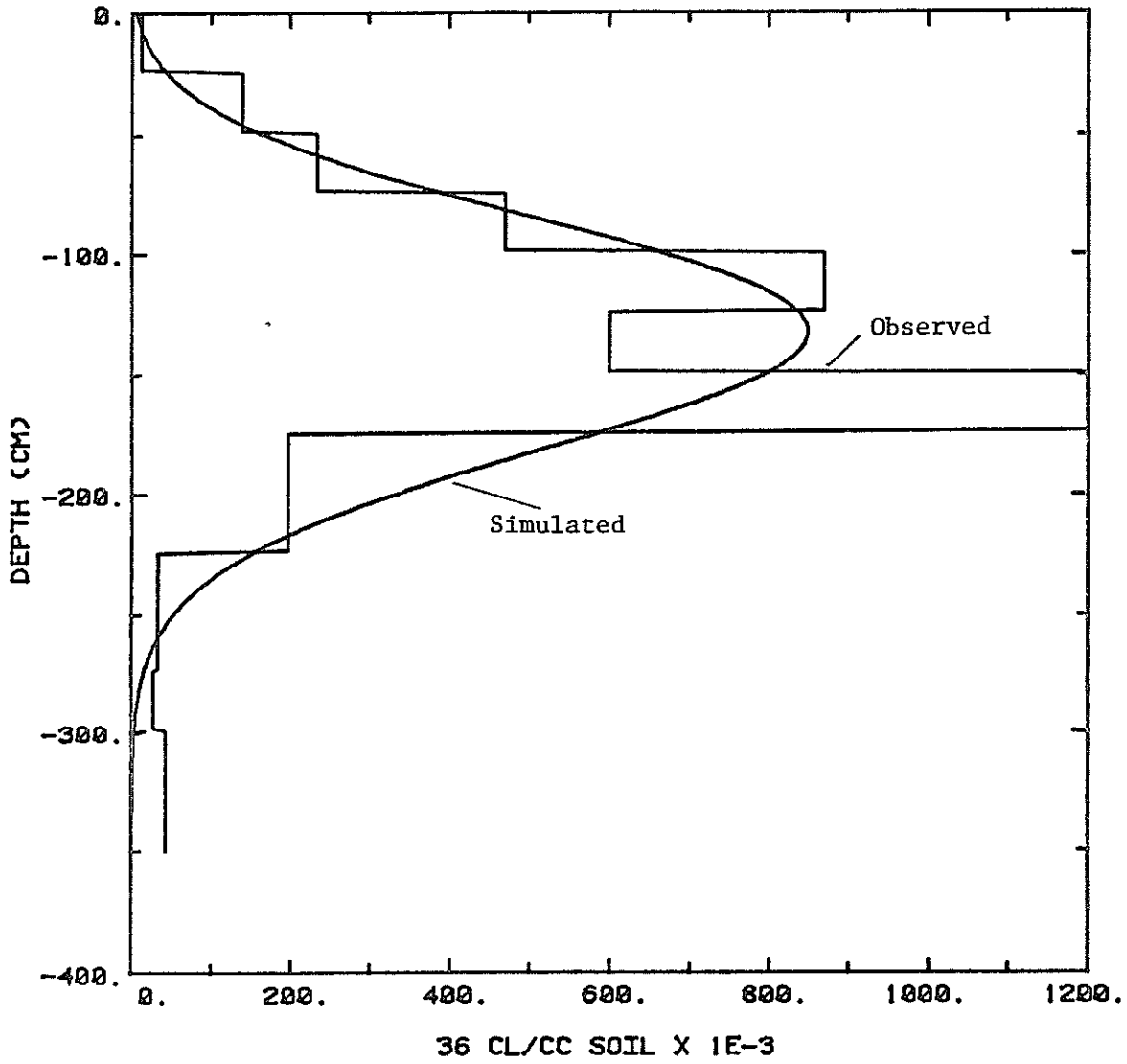

Fig. 41. Observed and simulated 36Cl concentrations as a function of depth on the Pleistocene terrace at the SNWR.

APPLICATION TO VADOSE ZONE CONTAMINATION PROBLEMS

The vadose zone in arid regions is frequently used as a place for disposing of hazardous wastes. This use is often justified by the assertion that, inasmuch as potential evapotranspiration far exceeds precipitation, there is no movement of soil water below the root zone and the wastes will thus be immobilized in the vadose zone. The radiosotope tracing and chloride mass balance studies reported here clearly indicate that this assumption is not justified. In the New Mexico desert, at any rate, there is measurable deep penetration of soil water, which has the potential to carry soluble contaminants to the water table.

However, these same techniques also demonstrate that the net rates of downward soil-water movement are slow, with pore velocities on the order of 5 to 10 cm/yr. Thus in areas with deep water tables, very long time periods would elapse before groundwater contamination resulted. Furthermore, the relative penetration of the 3H and 36Cl peaks show that under dry soil conditions even a "conservative" tracer such as chloride does not move with the soil water, but rather moves at one-quarter to one-third the water rate. Contaminants would presumable be retarded in a similar fashion.

The results of this study suggest that the 36Cl and 3H tracing techniques should be useful in evaluating vadose zone waste disposal sites. They could be applied at the time a specific site is suggested in order to test its suitability. The bomb-3H tracing would indicate the rate of soil water movement, which would be used to calculate the minimum possible time for contaminants to reach the groundwater. The bomb-36Cl tracing would give the actual solute transport velocity. The two techniques together would thus provide a conservative and a realistic estimate of the propensity for groundwater contamination.

The radioisotope tracing techniques could also be applied after the fact, to existing waste disposal sites, or even to accidental spills or illegal "dumps". In this case they could provide valuable information on the actual rate of contaminent progress through the vadose zone. Such information could be used to distinguish sites which are an immediate groundwater contamination hazard, and thus require rapid and expensive cleanup, from those where the contamination hazard is minimal (or in the distant future) and less expensive remediation measures are appropriate. In summary, we expect that the techniques described in this report will eventually find applications to a wide variety of contamination problems.

SUMMARY OF CONCLUSIONS

Knowledge of groundwater recharge rates and of the dispersive processes occurring during partially saturated flow are essential prior to identifying sites for waste disposal. Bomb-36Cl and -3H profiles provide thirty-year tracer tests and best identify long-term average moisture fluxes. In addition, the time required to make recharge estimates using these profiles is limited only to the time required to collect and analyze samples. Extensive field instrumentation and monitoring are not necessary.

Groundwater recharge rates determined from bomb-3H profiles at the SNWR and NMSUR are 3 and 4.7 percent of the average annual precipitation respectively. Recharge estimates are difficult to determine from bomb-36Cl profiles due to the multi-peaked nature of the profiles. It is possible, however, using the 36Cl profiles, to estimate the extent of the last thirty years of solute movement, and thus vertical infiltration rates.

Recharge estimates from soil-physics techniques at the SNWR were higher than those determined using soil-water chloride. For those sites at the base of steep slopes, this discrepancy is not surprising. On sloping locations, where unsaturated flow may have lateral components, the chloride method will yield recharge estimates lower than the actual local vertical flux because the method assumes one-dimensional vertical flow. On topographically flat locations, however, the chloride method should yield equivalent results. Comparison of 3H and 36Cl profiles indicates that vapor movement of tritiated water vapor allows the 3H to move more rapidly than chloride. Consequently, even on topographically flat locations, the chloride method may underestimate recharge, but will give accurate estimates of solute movement.

It is important to emphasize that local variability of recharge occurs as a result of topographic variation. Comparisons between physically and geochemically determined recharge rates should, therefore, only be made under equivalent conditions.

The most unexpected result of this study involves the relative positions of the bomb-3H and -36Cl peaks at both the SNWR and the NMSUR. Anion exclusion effects on chloride movement in soils are commonly observed, resulting in movement of chloride ahead of tritium. In our case, however, chemical interactions between the tracers and the porous medium appear to be relatively unimportant compared to the effects of vapor transport. Initially it was expected that vapor movement incorporating the 3H would merely disperse the 3H pulse relatively more than could be accounted for by liquid dispersion. Comparison of the 3H and 36Cl profiles, however, indicates that the chloride cannot move as readily through the soil as can the water in which it is dissolved. We hypothesize that this is due to vapor gaps which act as barriers to solute transports, but across which water can move in the vapor phase.

Soil-dispersive properties can be approximated using known input functions of 3H and 36Cl and the one-dimensional advective-dispersive equation. Numerical simulation of 3H transport through SNWR sands yields a hydrodynamic-dispersion coefficient equal to 70 cm^2/yr and a soil dispersivity equal to 5.3 cm. Numerical simulation of 36Cl transport through previously-studied (Phillips et al. 1984) sandy loams at the SNWR yields a hydrodynamic-dispersion coefficient equal to 47 cm^2/yr and a soil dispersivity equal to 8 cm.

ACKNOWLEDGEMENTS

We thank the staff of the Sevilleta National Wildlife Refuge and Dr. Peter Wierenga of New Mexico State University for their cooperationn and support of our research.

REFERENCES

Allison, G.B. 1981. The use of natural isotopes for measurment of groundwater recharge--a review. in: Proc. AWRC Groundwater Recharge Conference. Townsville, July, 1980. AWRC Conf. Series No. 3.

Allison, G.B., and M.W. Hughes. 1978. The use of environmental chloride and tritium to estimate total recharge to an unconfined aquifer. Aust. J. Soil Res. 16:181-195.

Allison, G.B., and M.W. Hughes. 1983. The use of natural tracers as indicators of soil-water movement in a temperate semi-arid region. Jour. of Hydrology 60:157-173.

Allison, G.B., W.J. Stone, and M.W. Hughes. 1985. Recharge in karst and dune elements of a semi-arid landscape as indicated by natural isotopes and chloride. Jour. of Hydrology 76:1-25.

Anderson, L.J., and T. Sevel. 1974. Six years' environmental tritium profiles in the unsaturated and saturated zones, Gronhoj, Denmark. in: Isotope Techniques in Groundwater Hydrology - Proceedings. IAEA-SM-182/1:3-20.

Bear, Jacob. 1979. Hydraulics of groundwater. New York: McGraw-Hill.

Bentley, H.W., F.M. Phillips, S.N. Davis, S. Gifford, D. Elmore, L.E. Tubbs, and H.E. Gove. 1982. Thermonuclear 36Cl pulse in natural water. Nature 300:737-740.

Bentley, H.W., F.M. Phillips, and S.N. Davis. 1986. Chlorine-36 in the terrestrial environment. in: Handbook of Environmental Isotope Geochemistry, Vol. 2B. J.C. Fontes, P. Fritz (eds.). Elsevier, Amsterdam, p.427-480.

Bentley, H.W., and S.N. Davis. 1982. Application of AMS to hydrology. in: 2nd Annual Symposium on Acceleration Mass Spectrometry. M. Kutchera (ed.). Argonne National Laboratories.

Biggar, J.W. and D.R. Nielsen. 1962. Miscible displacement: II. Behavior of tracers. Soil Sci. Soc. Am. Proc. 26:125-128.

Brady, N.C. 1974. The nature and properties of soils. Macmillan, New York, NY.

Byers, E. and D.B. Stephens. 1983. Statistical and stochastic analyses of hydraulic conductivity and particle size in a fluvial sand. Soil Sci. Soc. Am. J. 47:1072-1081.

Cass, A., G.S. Campbell, and T.L. Jones. 1984. Enhencement of thermal water vapor diffusion in soil. Soil Sci. Soc. Am. Proc. 48:25-32.

De Smedt, F. and P.J. Wierenga. 1978. Approximate analytical solution for solute flow during infiltration and redistribution. Soil Sci. Soc. Am. J. 42:407-412.

De Smedt, F. and P.J. Wierenga. 1984. Solute transfer through columns of glass beads. Water Resour. Res. 20(2):225-232.

Dincer, T., A. Al-Mugrin, and U. Zimmermann. 1974. Study of the infiltration and recharge through the sand dunes in arid zones with special reference to the stable isotopes and themonuclear tritium. Jour. of Hydrology 23:79-109.

Duval, T.A. 1986. Geochemical analysis of liquid and vapor transport of soil moisture in arid unsaturated soil. Master's study, Geoscience Dept., New Mexico Institute of Mining and Technology.

Ehhalt, D.H. 1973. On the uptake of tritium by soil water and groundwater. Water Resour. Res. 9(4):1073-1074.

Elmore, D., N. Conrad, and P.W. Kubik. 1984. Computer controlled isotope ratio measurements and data analysis. Nuclear Instruments and Methods in Physics Research B5:233-237.

Federal Radiation Council Report No 6. Washington D.C. 1964.

Feely, H.W. and H. Seitz. 1970. Use of lead 210 as a tracer of transport processes in the stratosphere. Journal of Geophysical Research. 75(15): 2885-2894.

Foster, S.S.D. and Amanda Smith-Carington. 1980. The interpretation of tritium in the chalk unsaturated zone. Jour of Hydrology. 46:343-364.

Freeze, R.A. and J.A. Cherry. 1979. Groundwater. New Jersey: Prentice-Hall, Inc.

Gupta, S.K. and S.R. Singh. 1980. Analytical solutions for predicting solute movement and their interpretation in reclamation. Jour. of Hydrology. 45:133-148.

Gurr, C.G., T.J. Marshall and J.T. Hutton. 1952. Movement of water in soil due to a temperature gradient. Soil Science. 74(5):335-345.

Hendry, M.J. 1983. Groundwater recharge through a heavy-textured soil. Jour. of Hydrology. 63:201-209.

Hillel, Daniel. 1980. Fundamentals of soil physics. New York: Academic Press, Inc.

IAEA Tech. Report Series, No. 228. Isotope techniques in the hydrogeological assessment of potential sites for the disposal of high-level radioactive wastes. IAEA, Vienna, 1983.

Jackson, R.D. 1964. Water vapor diffusion in relatively dry soil: 1. Theoretical considerations and sorption experiments. Soil Sci. Soc. Amer. Proc. 28:172-176.

Jackson, R.D., R.J. Reginato, B.A. Kimball, and F.S. Nakayama. 1974. Diurnal soil-water evaporation: Comparison of measured and calculated soil-water fluxes. Soil Sci. Soc. Amer. Proc. 38(6):861-866.

Kirda, C., D.R. Nielsen, and J.W. Biggar. 1973. Simultaneous transport of chloride and water during infiltration. Soil. Sci. Soc. Amer. Proc. 37:339-345.

Krupp, H.K., J.W. Biggar, and D.R. Nielsen. 1972. Relative flow rates of salt and water in soil. Soil Sci. Soc. Amer. Proc. 36:412-417.

McCord, J.T. 1986. Topographic controls on ground-water recharge at a sandy, arid site. Master's study, Geoscience Dept., New Mexico Institute of Mining and Technology.

McGurk, B.E. and W.J. Stone. 1985. Evaluation of laboratory procedures for determining soil-water chloride. New Mexico Bureau of Mines and Mineral Resources Open-File Report 215.

McWhorter, D.B., and D.K. Sunada. 1977. Ground-water hydrology and hydraulics. Water Resources Publications, Fort Collins, Colorado.

Milly, P.C.D. 1984. A simulation analysis of thermal effects on evaporation from soil. Water Resour. Res. 20(8):1087-1098.

Nielsen, D.R. and J.W. Biggar. 1962. Miscible displacement:III. Theoretical considerations. Soil Sci. Soc. Amer. Proc. 26:216-221.

Ogata, A. 1970. Theory of dispersion in a granular medium. U.S. Geological Survey Professional Paper 411-I.

Peterson, K.R. 1970. An empirical model for estimating world-wide deposition from atmospheric nuclear detonations. Health Physics. 18:357-378.

Philip, J. R., and D.A. de Vries. 1957. Moisture movement in porous materials under temperature gradients. Transactions, American Geophysical Union. 38(2):222-232.

Phillips, F.M., K.N. Trotman, H.W. Bentley, and S.N. Davis. 1984. The bomb-36Cl pulse as a tracer for soil-water movement near Socorro, New Mexico. in: Proc. Conf. on Water Quality and Pollution in New Mexico. W.J. Stone (ed.). New Mexico Bur. Mines Min. Resour. Special Publication.

Rabinowitz, D.D., C.R. Holmes, and G.W. Gross. 1971. Forced exchange of tritiated water with clays. In: A.A. Moghissi and M.W. Carter (eds.). Proc. Conf. Las Vegas, Nevada, 1971. 471-485.

Rabinowitz, D.D., G.W. Gross, and C.R. Holmes. 1977. Environmental tritium as a hydrometeorological tool in the Roswell basin, N.M. I. Tritium input function and precipitation-recharge relation. Jour. of Hydrology. 32:3-17.

Sammis, T.W., D.D. Evans, and A.W. Warrick. 1982. Comparison of methods to estimate deep percolation rates. Water Res. Bull. 18(3):465-470.

Schmalz, B.L., and W.L. Polzer. 1969. Tritiated water distribution in unsaturated soil. Soil Science. 108(1):43-47.

Scholl, D.G. 1976. Soil moisture flux and evapotranspiration determined from soil hydraulic properties in a chaparral stand. Soil Sci. Soc. Amer. J. 40:14-18.

Sharma, M.L., and M.W. Hughes. 1985. Groundwater recharge estimation using chloride, deuterium and oxygen-18 profiles in the deep coastal sands of Western Australia. Jour. of Hydrology. 81:93-109.

Stephens, D.B., S. Tyler, K. Lambert, R. Rabold, R. Knowlton, E. Byers, S. Yates, and S.P. Neuman. 1983. Insitu determination of hydraulic conductivity in the vadose zone using borehole infiltration tests. New Mexico Water Resource Res. Institute, Report No. 180, 140pp.

Stephens, D.B., R.G. Knowlton Jr., J. McCord, and W. Cox. 1985. Field study of natural ground-water recharge in a semi-arid lowland. New Mexico Water Resour. Res. Institute, Tech. Completion Report, Proj. No. 1345679.

Stone, W.J. 1984. Recharge in the Salt Lake coal field based on chloride in the unsaturated zone. New Mexico Bureau of Mines and Mineral Resources Open-File Report 214.

Thomas, G.W. and A.R. Swoboda. 1970. Anion exclusion effects on chloride movement in soils. Soil Science. 110(3):163-166.

Trotman, K.N. 1983. Thermonuclear chlorine-36 in arid soil. Master's thesis. Dept. of Hydrology and Water Resources. The University of Arizona.

van Genuchten, M. Th., and P.J. Wierenga. 1976. Mass transfer studies in sorbing porous media I. Analytical solutions. Soil Sci. Soc. Amer. J. 40(4):473-480.

van Genuchten, M. Th., and P.J. Wierenga. 1977. Mass transfer studies in sorbing porous media:II. Experimental evaluation with tritium (3H2O). Soil Sci. Soc. Amer. J. 41:272-278.

van Genuchten, M. Th., and W.J. Alves. 1982. Analytical solutions of the one-dimensional convective-dispersive solute transport equation. USDA Agricultural Research Service Technical Bulletin Number 1661.

Warrick, A.W., J.W. Biggar, and D.R. Nielsen. 1971. Simultaneous solute and water transfer for and unsaturated soil. Water Resour. Res. 7(5):1216-1225.

Wierenga, P.J., J.M.H. Hendrickx, M.H. Nash, J. Ludwig, and L.A. Daugherty. 1985. Variation of soil and vegetation with distance along a transect in the Chihuahuan Desert. Journal article number 1170, Agricultural Experiment Station, NMSU, Las Cruces, New Mexico.

Wilson, J.L. and L.W. Gelhar. 1974. Dispersive mixing in a partially saturated porous medium. Dept. of Civil Engineering, Mass. Inst. of Tech., Report No. 191.

APPENDIX A

CHLORIDE MERCURIC-NITRATE TITRATION

I. General Discussion

Chloride ion is one of the major anions in water. Chloride can be titrated with mercuric nitrate because of the formation of soluble, slightly dissociated mercuric chloride. In the pH range 2.3-2.8, diphenylcarbazone indicates the endpoint of this titration by formation of a purple complex with its excess mercuric ions.

Iodide and bromide will interfere since they are titrated with mercuric nitrate in the same manner as chloride. Sulfite, chromate, and ferric ions interfere when present in excess of 10 mg/liter.

II. Reagents

Standard Chloride Solution, 0.01411N: dissolve 0.8241 g pure dry sodium chloride in distilled water and dilute to 1 liter. 1ml = 0.50 mg Cl.

Standard Mercuric Nitrate Solution, 0.01411N: dissolve approximately 2.3 g anhydrous mercuric nitrate or 2.5 g of the monohydrate in water, and dilute to 1 liter. Standardize against 10 and 20 ml aliquots of standard 0.5 mg/ml Cl solution and 10 mg sodium bicarbonate diluted to about 100 ml.

Indicator: dissolve 0.5 g diphenylcarbazone and 50 mg. bromophenol blue indicator powder in alcohol reagent, and dilute to 100 ml with same. Store in glass bottle with dropper.

Nitric acid, 0.05N: dilute 33 ml of concentrated nitric acid to 100 ml. Dilute 10 ml of this solution to 100 ml.

III. Procedure

1. Measure 25 ml sample into a 250 ml flask and add 3 drops of indicator.
2. Neutralize the sample with 0.05N nitric acid until blue indicator goes to weak yellow. If the indicator color is not blue, add a drop of NaOH to obtain the blue color. Then add HNO3 until the weak yellow color is obtained.
3. Titrate slowly to the first permanent pink-violet color with the standardized mercuric nitrate solution.

IV. Calculations

$$\text{Chloride, ppm} = \frac{\text{ml of titrant} \times \text{N of titrant} \times 35.45 \times 1000}{\text{ml of aliquot}}$$

If N is exactly 0.01411 and 25 ml of sample is used:
Chloride, ppm = 20 x ml titrant

V. Bibliography

1. American Public Health Association, Standard Methods for the Examination of Water and Waste-water., 79-81 (1960).

APPENDIX B

AgCl PURIFICATION PROCEDURE

Equipment for AgCl Purification Procedure

fume hood

low temperature oven

hot plate

vacuum pump

1000 ml Erlenmeyer filtering flask

glass test tubes, 25x200mm

beakers, 200ml and 400ml

watch glasses

stirring rods

300ml millipore filter funnels

filter paper, 0.45 micron (to fit filter funnel, eg. 47 mm)

laboratory squeeze bottles containing: a)distilled deionized (DD) water, b)dilute HNO3, c)dilute NH4OH, and d)reagent grade NH4OH

amber glass sample bottles (30-60 ml) - or small glass vials, if wrapped to keep out light

parafilm

disposable polyethylene gloves

plastic forceps

distilled water

distilled-deionized water

chemicals:

- barium nitrate
- ammonium hydroxide (reagent grade)
- nitric acid (reagent grade)
- silver nitrate
- NaCl (table salt for blank or carrier)

AgCl Purification Procedure

Purification of chlorine-36 samples prior to analysis in the tandem-accelerator mass spectrometer is necessary to reduce the sulfur content of the samples. Sulfur-36 ions follow along a similar path as chlorine-36 ions in the accelerator, thus hindering chlorine-36 analysis.

Care must be taken during the purification process to avoid contamination. Samples should be covered whenever possible, even when in the filter funnels. The entire process is conducted in a laboratory fume hood. Disposable poly gloves should be worn during the entire process, and all equipment should be washed and treated each time it is used. Laboratory squeeze bottles of distilled deionized (DD) water, dilute HNO_3, and dilute NH_4OH are useful for treating equipment. Glass- and plasticware should first be washed with laboratory soap and water, and rinsed with distilled water. Next it should be rinsed with dilute HNO_3 followed by DD water, then rinsed with dilute NH_4OH followed by several rinses with DD water.

1 Add reagent grade $AgNO_3$ in an amount sufficient to precipitate at least 200mg AgCl. Let stand for 24 hours in the dark.

2 Decant and discard the supernatant. Filter the AgCl precipitate to near dryness in a filter funnel, with 0.45 micron filter paper, using a vacuum pump. Wash the precipitate thoroughly, in the filter funnel, with DD water and discard solution.

3 Transfer the filter funnel to an armed flask with a 25x200mm test tube inside (lower and raise test tube into and out of the flask with treated plastic forceps). Dissolve the precipitate by adding 25-50ml reagent grade NH_4OH to the filter funnel. Allow sufficient time for the precipitate to dissolve and gravity filter. Only if necessary, gently draw the solution into the test tube with the vacuum pump. Use a squeeze bottle of reagent grade NH_4OH to rinse and

dissolve any precipitate that may stick to the sides of the funnel. Remove filter funnel and discard used filter with any remaining precipitate.

4 Transfer solution from test tube to a treated 200ml beaker. Carefully add 1ml $Ba(NO3)2$ to solution in beaker, as sputtering may occur. Cover beaker with parafilm and allow to sit overnight. (To make the $Ba(NO3)2$ solution, place a good amount of solid $Ba(CO3)2$ in a flask. Add sufficient $HNO3$ to dissolve some of the $Ba(CO3)2$, but leave some in solid form in the bottom of the flask. When using the $Ba(NO3)2$ solution, draw off the liquid from the top.)

5 Filter solution into a test tube and transfer solution to a treated 400ml beaker (more efficient during evaporation process). Discard used filter paper.

6 Lay a glass stirring rod across the top of the beaker and cover with a chemical watch glass (concave side up). Evaporate the $NH4OH$ and reprecipitate the AgCl by heating the beaker at 50-65 'C for 1-1/2 to 3 hours. Add small amounts of DD water (from squeeze bottle) during the heating process to buoy up the precipitate and prevent it from sticking to the bottom of the beaker.

7 Using DD water, rinse the precipitate from the beaker into the filter apparatus. Wash the precipitate thoroughly with DD water and filter it to near dryness.

8 Transfer filter funnel to an armed flask with a test tube set up. Redissolve the AgCl precipitate by adding 25-50ml reagent grade $NH4OH$ to the filter funnel. Again allow sufficient time for the precipitate to dissolve and gravity filter. Only if necessary, draw solution into test tube with the vacuum pump. Use a squeeze bottle of reagent grade $NH4OH$ to rinse and dissolve any precipitate that may stick to the sides of the funnel. Remove the filter funnel and discard used filter paper.

9 Transfer solution to a 400ml beaker and repeat steps 6 and 7. If sulfur contamination is a concern (ie. solution has color) or a known problem, repeat step 9. During final filtering process, try to "gather" precipitate from filter funnel sides onto the micropore filter using DD water.

10 Crumple and then flatten a blue filter-cover paper (found between the individual 0.45 micron filters), and lay it on a treated watch glass (concave up). Using treated forceps, place the filter paper with the AgCl precipitate on top of the blue filter-cover paper. Place the watch glass in an oven allowing the precipitate to dry overnight at 45'C (if time is of the essence, a drying time of 1-2 hours at 65'C should be sufficient).

11 Weigh a treated and dried sample bottle. Transfer the dry powder sample to the dark-glass sample bottle, reweigh to obtain sample weight. Wrap parafilm around the bottle cap. Label, date, and store in a dark location.

APPENDIX C

MECHANICAL ANALYSIS OF SOIL

PROCEDURE

1. If no dispersing agent has already been prepared, prepare a dispersing agent from 66.5 grams sodium pyro phosphate per liter distilled water. Add 100 ml of dispersing agent to a 1000 ml hydrometer jar, and add distilled water to make 1000 ml. Mix thoroughly in blender 5 minutes. Record the temperature of the solution to cover a temperature range you will encounter in soil analysis. Lower the hydrometer into the jar and read the top of the miniscus surrounding the stem, RL. Record RL and temperature periodically during the following steps. Step 1 produces a "blank". The hydrometer reading, RL, will be a correction factor. Temperature must be known, especially if it cannot be held constant, because it effects viscosity.

2. With a mortar and pestle carefully disaggregate an oven-dried soil sample. Be careful not to crush individual grains.

3. Pass the sample through a No. 4 size sieve to remove pebbles and coarser. Weigh and save the retained fraction.

4. Split the fraction passing the No. 4 sieve into subsamples using a sample splitter and place a subsample into a metal milk shake mixing cup. (Weigh out 25-50 gram subsamples if the soil is mostly clay and 75-100 grams if it is sandy.)

5. If it appears that the sample does not have an appreciable amount of organic matter, it is unnecessary to oxidize the sample with hydrogen peroxide.

6. Add 100 ml of dispersing agent and enough distilled water to cover the soil sample, let stand for 5 minutes (due to the importance of dispersion, samples are often left standing for more than 18 hours). Fill the cup with distilled water to within about 2 inches of the top. Then stir with the mixer for 5 minutes if sandy, 10 minutes if clayey.

7. Transfer the suspension to a 1000 ml hydrometer jar. Remove any sediment from the mixing cup by rinsing with distilled water. Fill with distilled water to the 1000 ml mark.

8. Remove the hydrometer from the blank. Mix the suspension thoroughly for approximately 1 minute. As soon as mixing is complete, start a stop watch.

9. Carefully lower the hydrometer into the jar and read the top of the miniscus on the scale after about 15 seconds. Remove the hydrometer. Record temperature of the suspension. Record hydrometer reading, R.

10. Place the hydrometer in the jar about 10 seconds before subsequent readings at 1, 4, 20, 60, 120 minutes, 12 hours, and 24 hours. Record temperature and R for each reading. Rinse the hydrometer with distilled water and dry between readings.

11. After the final hydrometer reading, empty the hydrometer jar on a fine (200) mesh wet washing sieve (one with high sides). Thoroughly wash with tap water until wash water is clear. Transfer the retained material to a container and dry over night in the oven at 105 'C.

12. Prepare a nest of six sieves fining downward (eg. No. 20, 40, 60, 100, 140, 200) with a lid on top and a pan on the bottom. Place dried sample on top sieve and agitate in mechanical shaker for 15-20 minutes. Weigh the amount retained on each sieve. Be certain to remove as much of the granular material stuck on the screen as possible using a brush.

13. Calculate the concentration of the suspension in grams per liter from c=R-RL at the different times. This concentration times 1 liter gives the mass in suspension at each time. R is the hydrometer readingof the suspension, and RL is the hydrometer reading of the pure water and dispersant, taken at the same temperature.

14. Calculate the particle diameter d, in suspension at each time according to the procedure outlined in Methods of Soil Analysis by P.R. Day, 1965.

15. Prepare a table showing weight of sample retained for each particle size from both sieving and hydrometer analyses.

16. Compute Log (Mass percent per log size interval)

17. Classify the soil according to USDA textural triangle.

APPENDIX D

SNWR AND NMSUR GRAIN SIZE DISTRIBUTIONS

SNWR Grain Size

SAMPLE: S-1B 0-25 CM
MAXIMUM INTERMEDIATE DIAMETER: 1.00E+000mm

PARTICLE SIZE mm	WEIGHT gm	CUMULATIVE WEIGHT gm	WEIGHT PERCENT	CUMULATIVE WEIGHT PERCENT	LOG WEIGHT % PER LOG SIZE INTERVAL
8.50E-001	0.3000	0.3000	0.5561	0.5561	0.90
4.25E-001	8.4300	8.7300	15.6256	16.1816	1.72
2.50E-001	20.3800	29.1100	37.7757	53.9574	2.21
1.50E-001	16.7800	45.8900	31.1029	85.0602	2.15
1.06E-001	5.2200	51.1100	9.6756	94.7359	1.81
7.50E-002	1.8700	52.9800	3.4662	98.2020	1.36
6.00E-005	0.9700	53.9500	1.7980	100.0000	-0.24

SAMPLE: S-2B 25-50 CM
MAXIMUM INTERMEDIATE DIAMETER: 1.00E+000mm

PARTICLE SIZE mm	WEIGHT gm	CUMULATIVE WEIGHT gm	WEIGHT PERCENT	CUMULATIVE WEIGHT PERCENT	LOG WEIGHT % PER LOG SIZE INTERVAL
8.50E-001	0.3900	0.3900	0.7001	0.7001	1.00
4.25E-001	10.2700	10.6600	18.4348	19.1348	1.79
2.50E-001	25.8500	36.5100	46.4010	65.5358	2.30
1.50E-001	14.1900	50.7000	25.4712	91.0070	2.06
1.06E-001	3.3300	54.0300	5.9774	96.9844	1.60
7.50E-002	1.0300	55.0600	1.8489	98.8332	1.09
6.00E-005	0.6500	55.7100	1.1668	100.0000	-0.42

SAMPLE: S-3B 50-75 CM
MAXIMUM INTERMEDIATE DIAMETER: 1.00E+000mm

PARTICLE SIZE mm	WEIGHT gm	CUMULATIVE WEIGHT gm	WEIGHT PERCENT	CUMULATIVE WEIGHT PERCENT	LOG WEIGHT % PER LOG SIZE INTERVAL
8.50E-001	0.3300	0.3300	0.5969	0.5969	0.93
4.25E-001	8.0900	8.4200	14.6319	15.2288	1.69
2.50E-001	26.2200	34.6400	47.4227	62.6515	2.31
1.50E-001	14.9500	49.5900	27.0392	89.6907	2.09
1.06E-001	3.6000	53.1900	6.5111	96.2018	1.64
7.50E-002	1.2500	54.4400	2.2608	98.4627	1.18
6.00E-005	0.8500	55.2900	1.5373	100.0000	-0.30

SAMPLE: S-4B 75-100 CM
MAXIMUM INTERMEDIATE DIAMETER: 1.00E+000mm

PARTICLE SIZE mm	WEIGHT gm	CUMULATIVE WEIGHT gm	WEIGHT PERCENT	CUMULATIVE WEIGHT PERCENT	LOG WEIGHT % PER LOG SIZE INTERVAL
8.50E-001	0.7500	0.7500	1.3711	1.3711	1.29
4.25E-001	11.4900	12.2400	21.0055	22.3766	1.84
2.50E-001	24.9300	37.1700	45.5759	67.9525	2.30
1.50E-001	13.0900	50.2600	23.9305	91.8830	2.03
1.06E-001	2.9900	53.2500	5.4662	97.3492	1.56
7.50E-002	0.9500	54.2000	1.7367	99.0859	1.06
6.00E-005	0.5000	54.7000	0.9141	100.0000	-0.53

SAMPLE: S-5B 100-125 CM
MAXIMUM INTERMEDIATE DIAMETER: 1.00E+000mm

PARTICLE SIZE mm	WEIGHT gm	CUMULATIVE WEIGHT gm	WEIGHT PERCENT	CUMULATIVE WEIGHT PERCENT	LOG WEIGHT % PER LOG SIZE INTERVAL
8.50E-001	0.3100	0.3100	0.5319	0.5319	0.88
4.25E-001	5.5700	5.8800	9.5573	10.0892	1.50
2.50E-001	22.9000	28.7800	39.2931	49.3823	2.23
1.50E-001	17.0300	45.8100	29.2210	78.6033	2.12
1.06E-001	6.1800	51.9900	10.6040	89.2073	1.85
7.50E-002	3.2900	55.2800	5.6452	94.8524	1.57
6.00E-005	3.0000	58.2800	5.1476	100.0000	0.22

SAMPLE: S-6B 125-150 CM
MAXIMUM INTERMEDIATE DIAMETER: 1.00E+000mm

PARTICLE SIZE mm	WEIGHT gm	CUMULATIVE WEIGHT gm	WEIGHT PERCENT	CUMULATIVE WEIGHT PERCENT	LOG WEIGHT % PER LOG SIZE INTERVAL
8.50E-001	1.1900	1.1900	2.1167	2.1167	1.48
4.25E-001	7.6000	8.7900	13.5183	15.6350	1.65
2.50E-001	22.9400	31.7300	40.8040	56.4390	2.25
1.50E-001	16.3100	48.0400	29.0110	85.4500	2.12
1.06E-001	5.0500	53.0900	8.9826	94.4326	1.78
7.50E-002	1.9300	55.0200	3.4329	97.8655	1.36
6.00E-005	1.2000	56.2200	2.1345	100.0000	-0.16

SAMPLE: S-7B 150-175 CM
MAXIMUM INTERMEDIATE DIAMETER: 1.00E+000mm

PARTICLE SIZE mm	WEIGHT gm	CUMULATIVE WEIGHT gm	WEIGHT PERCENT	CUMULATIVE WEIGHT PERCENT	LOG WEIGHT % PER LOG SIZE INTERVAL
8.50E-001	1.5500	1.5500	2.8254	2.8254	1.60
4.25E-001	10.7500	12.3000	19.5953	22.4207	1.81
2.50E-001	27.2900	39.5900	49.7448	72.1655	2.33
1.50E-001	11.5500	51.1400	21.0536	93.2191	1.98
1.06E-001	2.5000	53.6400	4.5571	97.7762	1.48
7.50E-002	0.7900	54.4300	1.4400	99.2162	0.98
6.00E-005	0.4300	54.8600	0.7838	100.0000	-0.60

SAMPLE: S-8B 175-200 CM
MAXIMUM INTERMEDIATE DIAMETER: 1.00E+000mm

PARTICLE SIZE mm	WEIGHT gm	CUMULATIVE WEIGHT gm	WEIGHT PERCENT	CUMULATIVE WEIGHT PERCENT	LOG WEIGHT % PER LOG SIZE INTERVAL
8.50E-001	1.2100	1.2100	2.1150	2.1150	1.48
4.25E-001	5.7600	6.9700	10.0682	12.1832	1.52
2.50E-001	20.0000	26.9700	34.9589	47.1421	2.18
1.50E-001	20.2500	47.2200	35.3959	82.5380	2.20
1.06E-001	6.4900	53.7100	11.3442	93.8822	1.88
7.50E-002	2.3200	56.0300	4.0552	97.9374	1.43
6.00E-005	1.1800	57.2100	2.0626	100.0000	-0.18

SAMPLE: S-9 213-262 CM
MAXIMUM INTERMEDIATE DIAMETER: 1.00E+000mm

PARTICLE SIZE mm	WEIGHT gm	CUMULATIVE WEIGHT gm	WEIGHT PERCENT	CUMULATIVE WEIGHT PERCENT	LOG WEIGHT % PER LOG SIZE INTERVAL
8.50E-001	0.6300	0.6300	1.1236	1.1236	1.20
4.25E-001	5.9000	6.5300	10.5226	11.6462	1.54
2.50E-001	19.9500	26.4800	35.5805	47.2267	2.19
1.50E-001	18.9200	45.4000	33.7435	80.9702	2.18
1.06E-001	6.3300	51.7300	11.2895	92.2597	1.87
7.50E-002	2.5000	54.2300	4.4587	96.7184	1.47
6.00E-005	1.8400	56.0700	3.2816	100.0000	0.03

SAMPLE: S-10 262-310 CM
MAXIMUM INTERMEDIATE DIAMETER: 1.00E+000mm

PARTICLE SIZE mm	WEIGHT gm	CUMULATIVE WEIGHT gm	WEIGHT PERCENT	CUMULATIVE WEIGHT PERCENT	LOG WEIGHT % PER LOG SIZE INTERVAL
8.50E-001	1.0700	1.0700	1.9680	1.9680	1.45
4.25E-001	5.7000	6.7700	10.4837	12.4517	1.54
2.50E-001	19.0600	25.8300	35.0561	47.5078	2.18
1.50E-001	18.1600	43.9900	33.4008	80.9086	2.18
1.06E-001	6.2300	50.2200	11.4585	92.3671	1.88
7.50E-002	2.4800	52.7000	4.5613	96.9285	1.48
6.00E-005	1.6700	54.3700	3.0715	100.0000	0.00

SAMPLE: S-11 310-358 CM
MAXIMUM INTERMEDIATE DIAMETER: 1.00E+000mm

PARTICLE SIZE mm	WEIGHT gm	CUMULATIVE WEIGHT gm	WEIGHT PERCENT	CUMULATIVE WEIGHT PERCENT	LOG WEIGHT % PER LOG SIZE INTERVAL
8.50E-001	0.9800	0.9800	1.7805	1.7805	1.40
4.25E-001	6.7600	7.7400	12.2820	14.0625	1.61
2.50E-001	21.4900	29.2300	39.0443	53.1068	2.23
1.50E-001	18.2500	47.4800	33.1577	86.2645	2.17
1.06E-001	4.9500	52.4300	8.9935	95.2580	1.78
7.50E-002	1.6400	54.0700	2.9797	98.2376	1.30
6.00E-005	0.9700	55.0400	1.7624	100.0000	-0.24

SAMPLE: S-12 358-404 CM
MAXIMUM INTERMEDIATE DIAMETER: 1.00E+000mm

PARTICLE SIZE mm	WEIGHT gm	CUMULATIVE WEIGHT gm	WEIGHT PERCENT	CUMULATIVE WEIGHT PERCENT	LOG WEIGHT % PER LOG SIZE INTERVAL
8.50E-001	1.0200	1.0200	1.8462	1.8462	1.42
4.25E-001	7.1700	8.1900	12.9774	14.8235	1.63
2.50E-001	20.3600	28.5500	36.8507	51.6742	2.20
1.50E-001	18.1800	46.7300	32.9050	84.5792	2.17
1.06E-001	5.3900	52.1200	9.7557	94.3348	1.81
7.50E-002	1.9200	54.0400	3.4751	97.8100	1.36
6.00E-005	1.2100	55.2500	2.1900	100.0000	-0.15

SAMPLE: S-13 404-432 CM
MAXIMUM INTERMEDIATE DIAMETER: 1.00E+000mm

PARTICLE SIZE mm	WEIGHT gm	CUMULATIVE WEIGHT gm	WEIGHT PERCENT	CUMULATIVE WEIGHT PERCENT	LOG WEIGHT % PER LOG SIZE INTERVAL
8.50E-001	1.9900	1.9900	3.6025	3.6025	1.71
4.25E-001	5.1500	7.1400	9.3230	12.9254	1.49
2.50E-001	12.3400	19.4800	22.3389	35.2643	1.99
1.50E-001	16.2600	35.7400	29.4352	64.6995	2.12
1.06E-001	8.3700	44.1100	15.1521	79.8516	2.00
7.50E-002	4.4900	48.6000	8.1282	87.9797	1.73
6.00E-005	6.6400	55.2400	12.0203	100.0000	0.59

SAMPLE: S-14 432-457 CM
MAXIMUM INTERMEDIATE DIAMETER: 1.00E+000mm

PARTICLE SIZE mm	WEIGHT gm	CUMULATIVE WEIGHT gm	WEIGHT PERCENT	CUMULATIVE WEIGHT PERCENT	LOG WEIGHT % PER LOG SIZE INTERVAL
8.50E-001	7.7200	7.7200	14.0287	14.0287	2.30
4.25E-001	7.0600	14.7800	12.8294	26.8581	1.63
2.50E-001	16.0500	30.8300	29.1659	56.0240	2.10
1.50E-001	14.2200	45.0500	25.8405	81.8644	2.07
1.06E-001	5.5700	50.6200	10.1218	91.9862	1.83
7.50E-002	2.3500	52.9700	4.2704	96.2566	1.45
6.00E-005	2.0600	55.0300	3.7434	100.0000	0.08

SAMPLE: S-15 485-503 CM
MAXIMUM INTERMEDIATE DIAMETER: 1.00E+000mm

PARTICLE SIZE mm	WEIGHT gm	CUMULATIVE WEIGHT gm	WEIGHT PERCENT	CUMULATIVE WEIGHT PERCENT	LOG WEIGHT % PER LOG SIZE INTERVAL
8.50E-001	6.3300	6.3300	12.2201	12.2201	2.24
4.25E-001	5.6500	11.9800	10.9073	23.1274	1.56
2.50E-001	17.2100	29.1900	33.2239	56.3514	2.16
1.50E-001	16.9800	46.1700	32.7799	89.1313	2.17
1.06E-001	3.8300	50.0000	7.3938	96.5251	1.69
7.50E-002	1.1000	51.1000	2.1236	98.6486	1.15
6.00E-005	0.7000	51.8000	1.3514	100.0000	-0.36

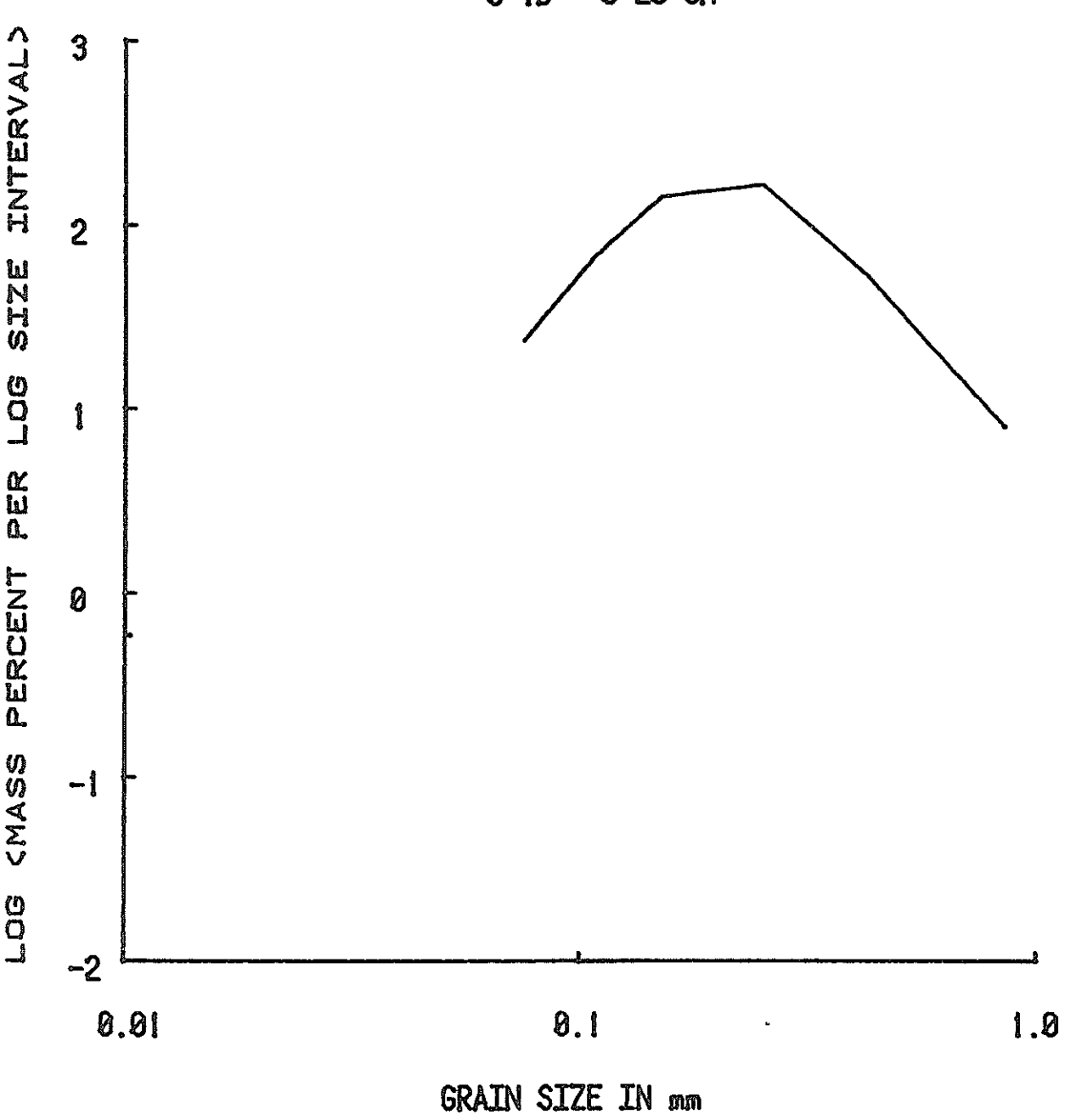
S-1B 0-25 CM
LOG <MASS PERCENT PER LOG SIZE INTERVAL>
3
2
1
0
-1
-2
0.01
0.1
1.0
GRAIN SIZE IN mm

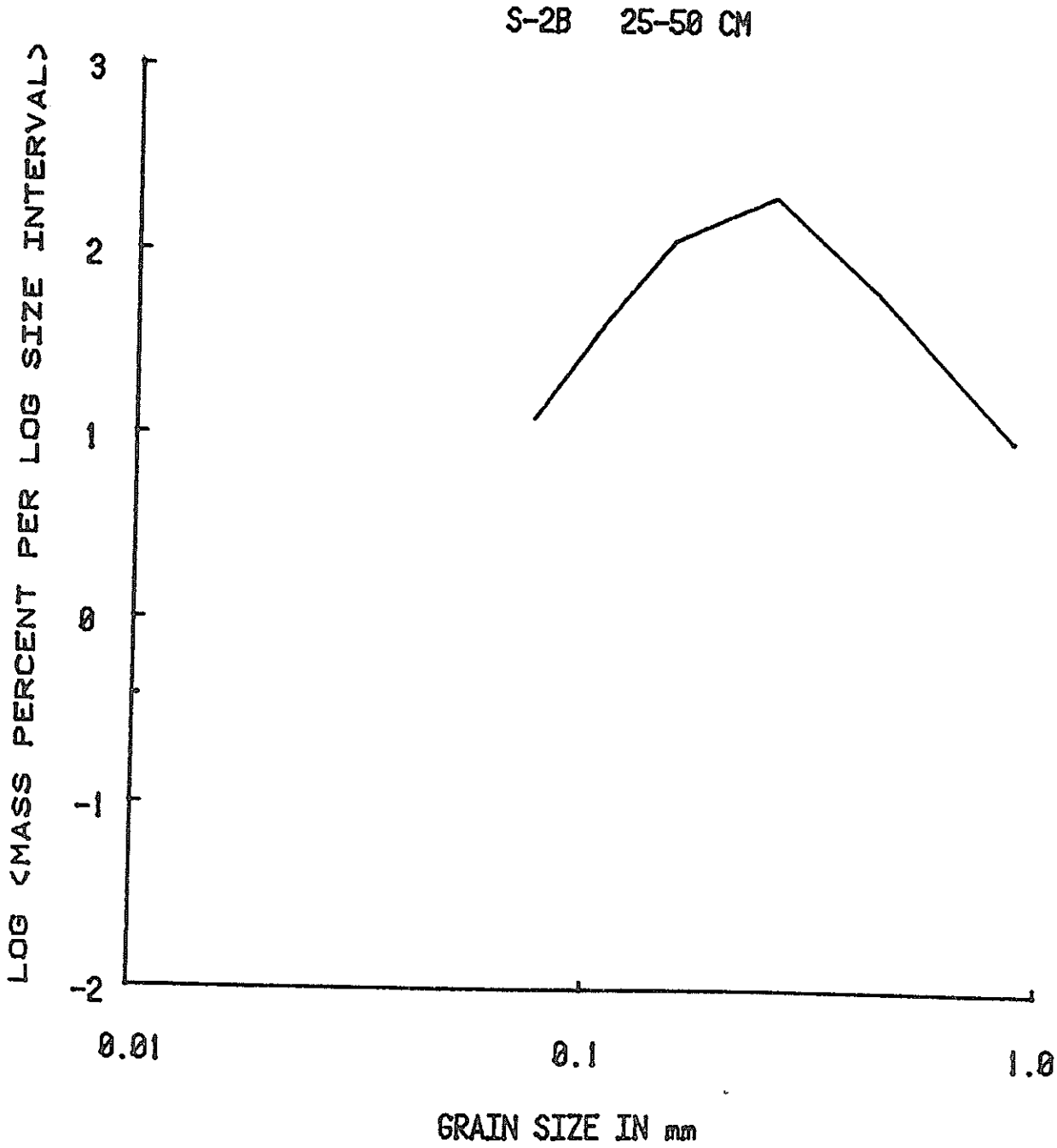
S-2B 25-50 CM
LOG <MASS PERCENT PER LOG SIZE INTERVAL>
3
2
1
0
-1
-2
0.01
0.1
1.0
GRAIN SIZE IN mm

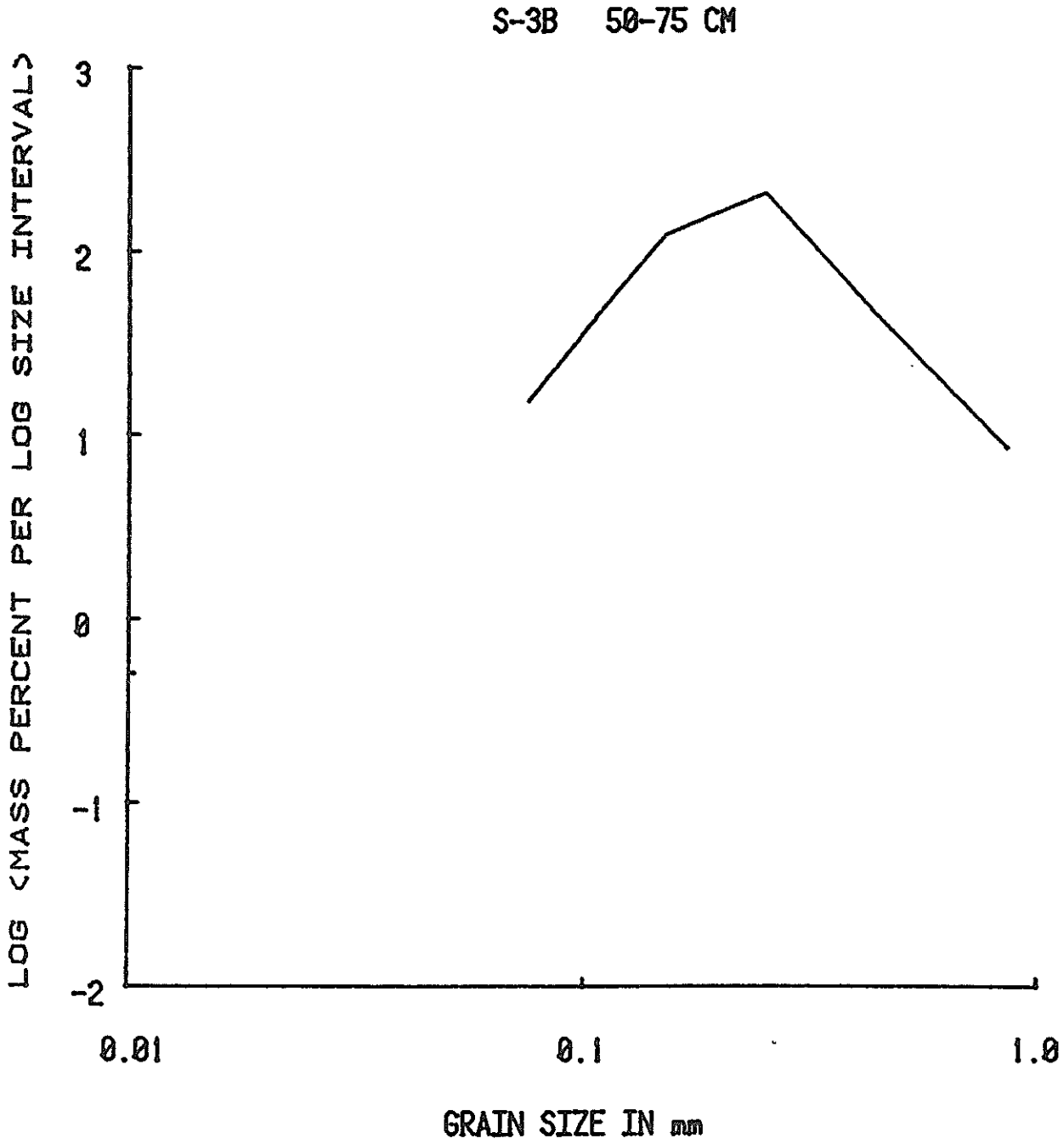
S-3B 50-75 CM
LOG <MASS PERCENT PER LOG SIZE INTERVAL>
3
2
1
0
-1
-2
0.01
0.1
1.0
GRAIN SIZE IN mm

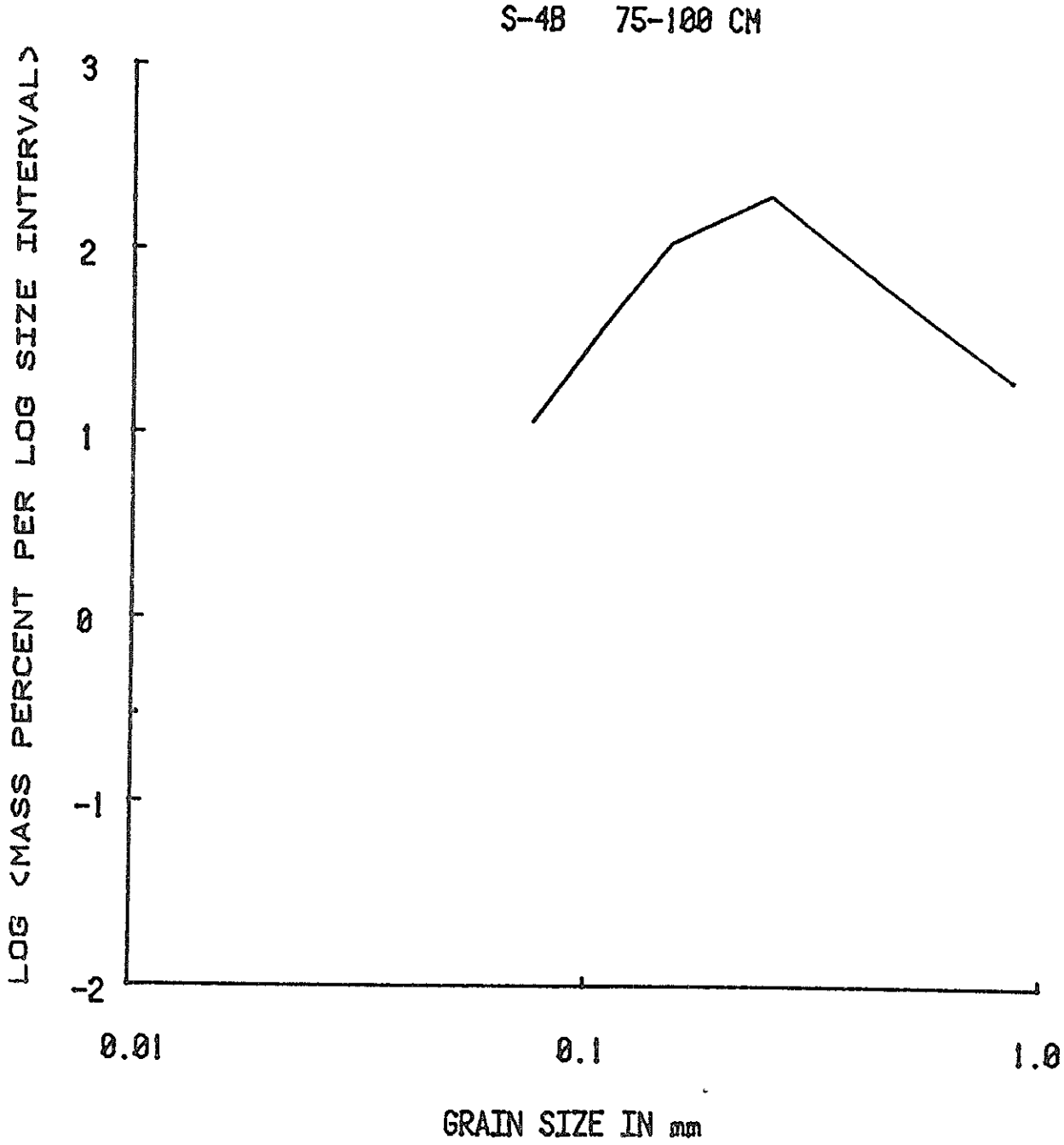
S-4B 75-100 CM
LOG <MASS PERCENT PER LOG SIZE INTERVAL>
3
2
1
0
-1
-2
0.01
0.1
1.0
GRAIN SIZE IN mm

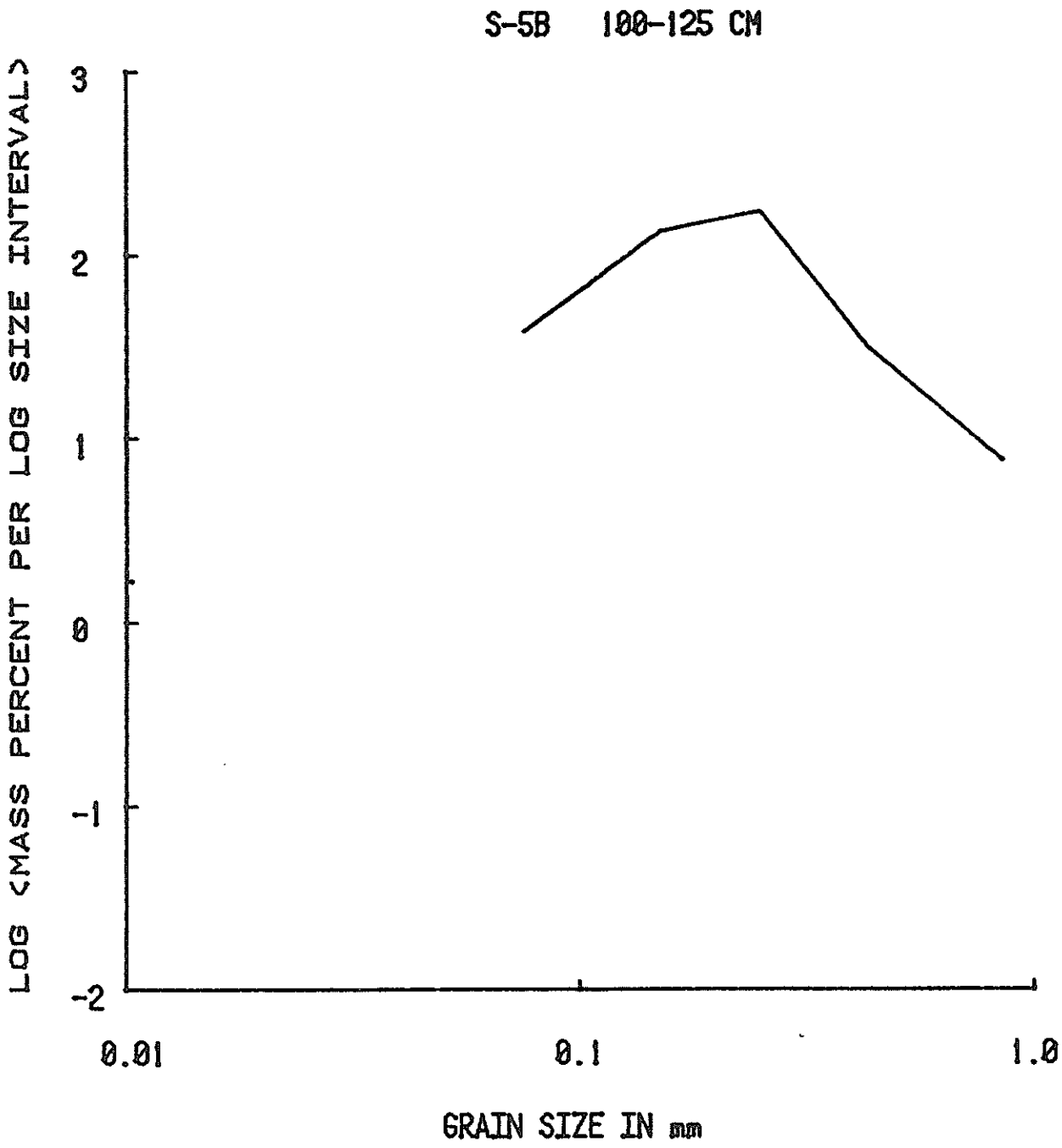
S-5B 100-125 CM
LOG <MASS PERCENT PER LOG SIZE INTERVAL>
3
2
1
0
-1
-2
0.01
0.1
1.0
GRAIN SIZE IN mm

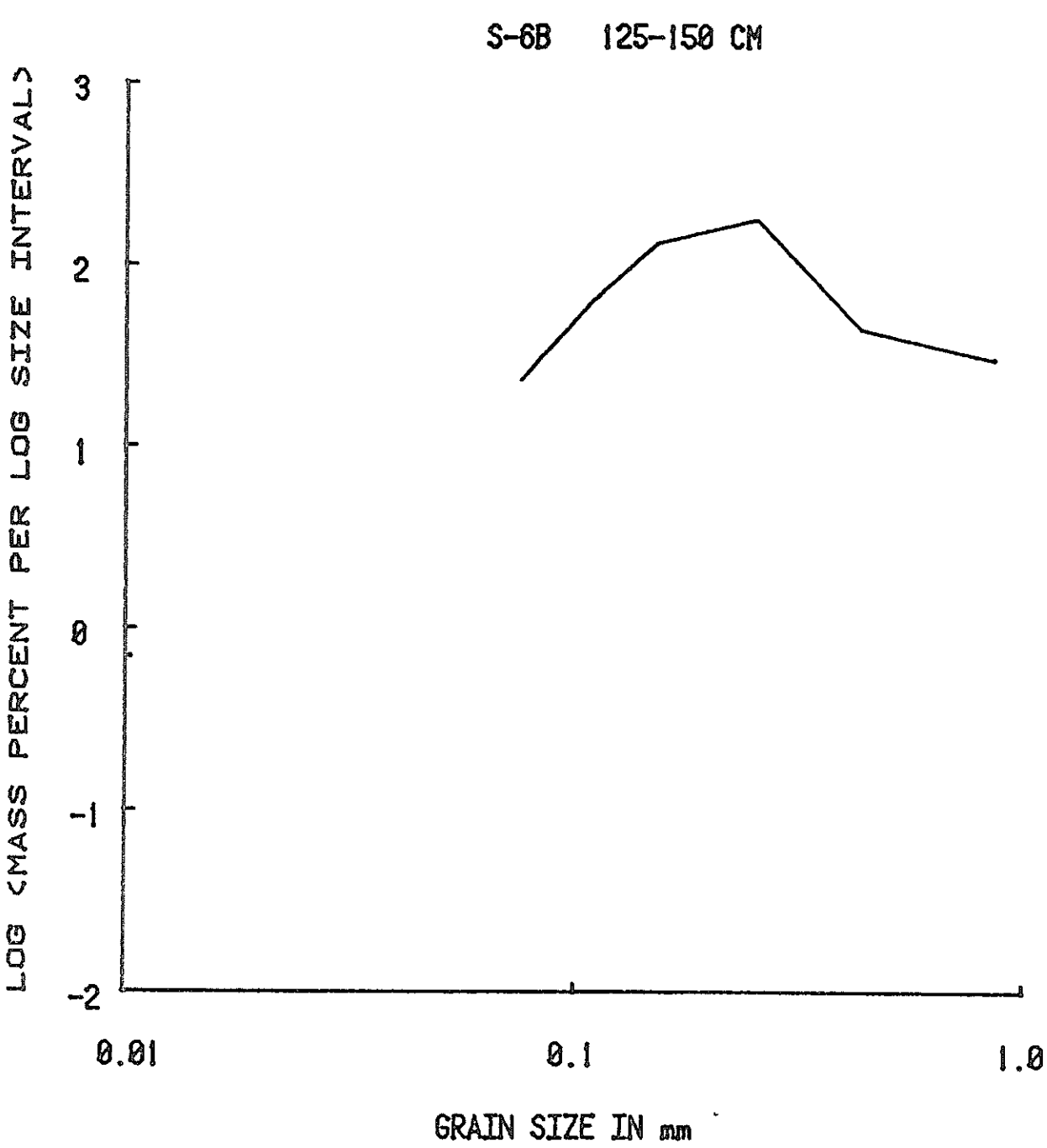
S-6B 125-150 CM
LOG <MASS PERCENT PER LOG SIZE INTERVAL>
3
2
1
0
-1
-2
0.01
0.1
1.0
GRAIN SIZE IN mm

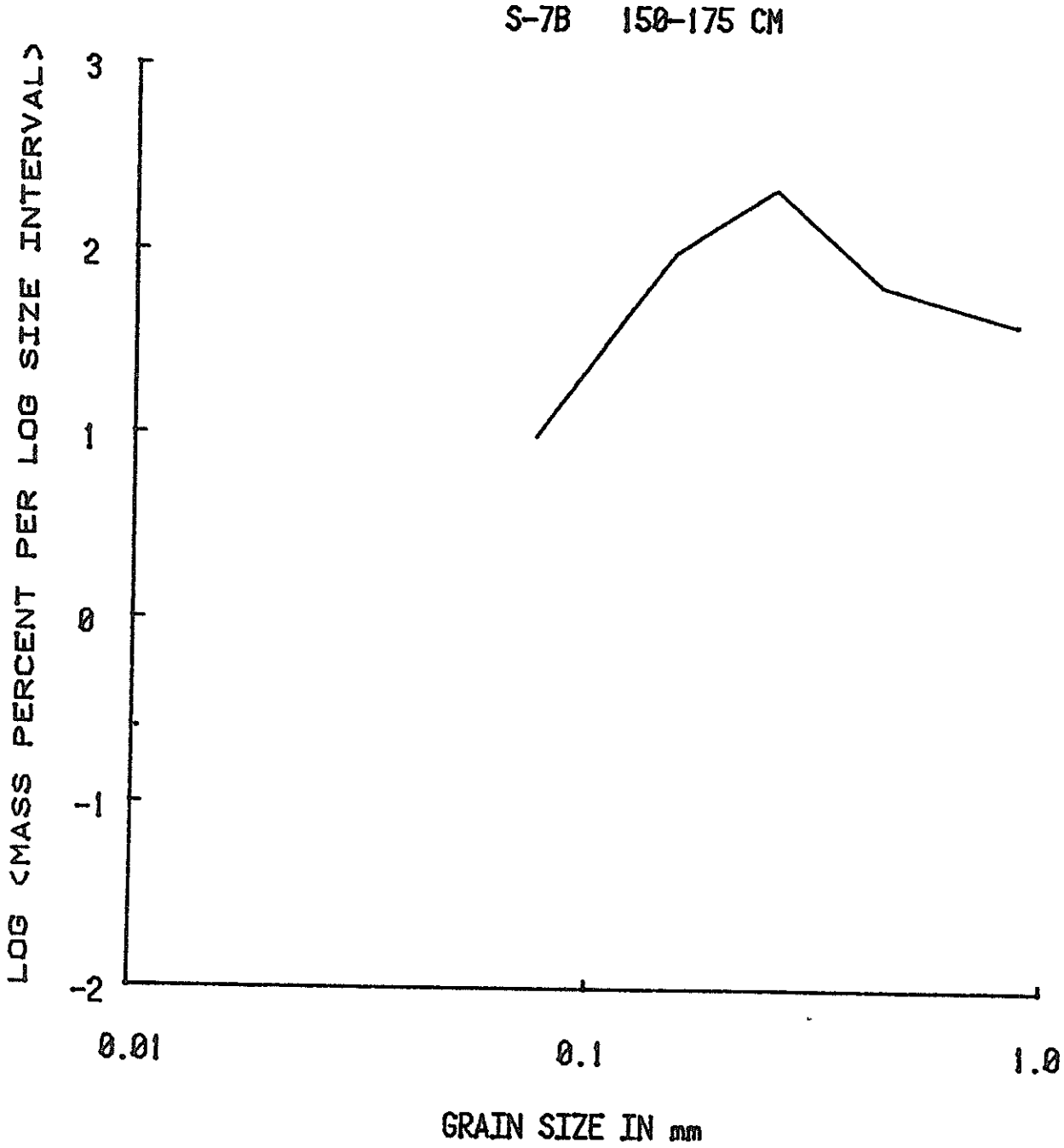
S-7B 150-175 CM
LOG <MASS PERCENT PER LOG SIZE INTERVAL>
3
2
1
0
-1
-2
0.01
0.1
1.0
GRAIN SIZE IN mm

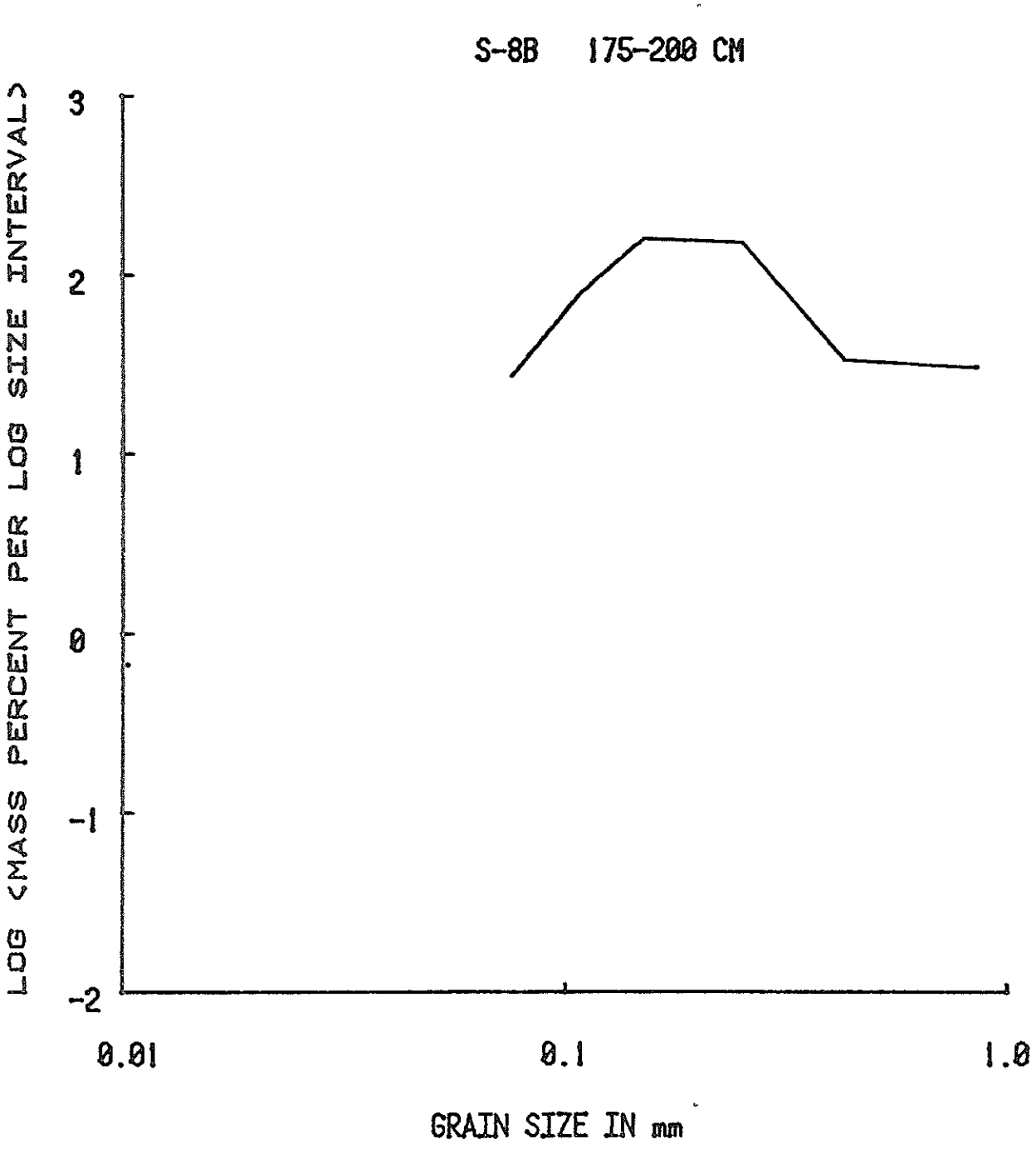
S-8B 175-200 CM
LOG <MASS PERCENT PER LOG SIZE INTERVAL>
3
2
1
0
-1
-2
0.01
0.1
1.0
GRAIN SIZE IN mm

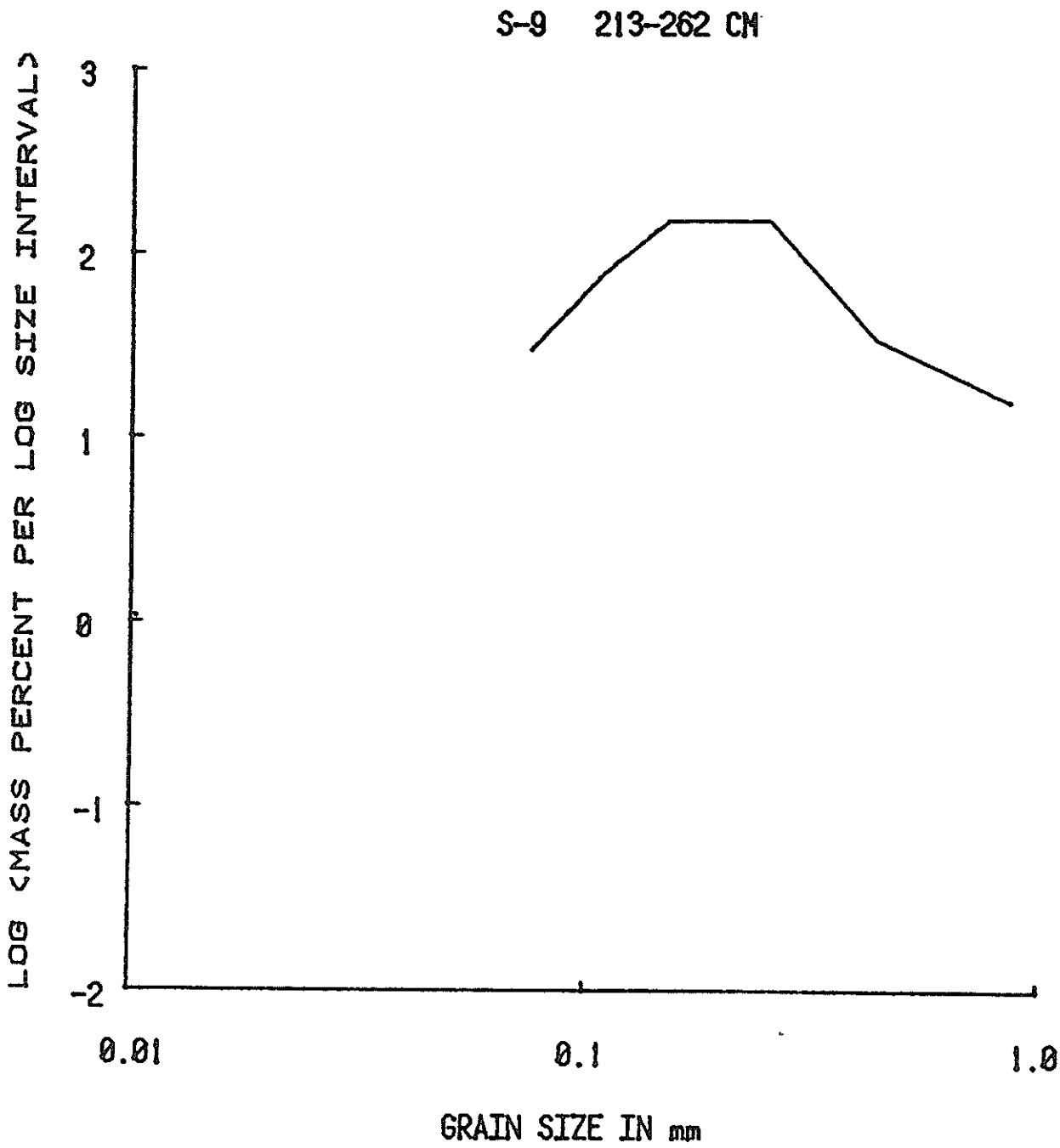
S-9 213-262 CM
LOG <MASS PERCENT PER LOG SIZE INTERVAL>
3
2
1
0
-1
-2
0.01
0.1
1.0
GRAIN SIZE IN mm

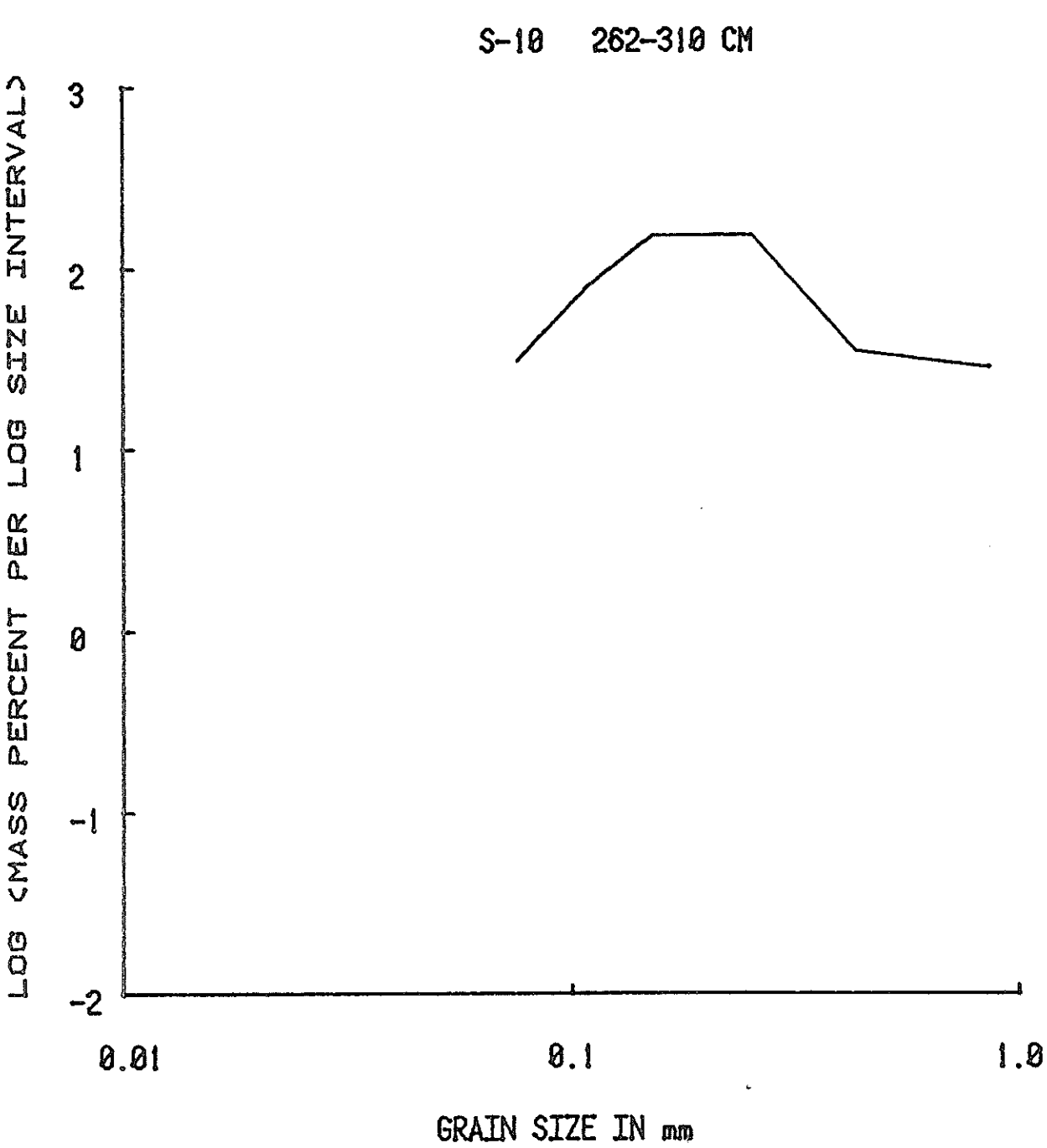
S-10 262-310 CM
LOG <MASS PERCENT PER LOG SIZE INTERVAL>
3
2
1
0
-1
-2
0.01
0.1
1.0
GRAIN SIZE IN mm

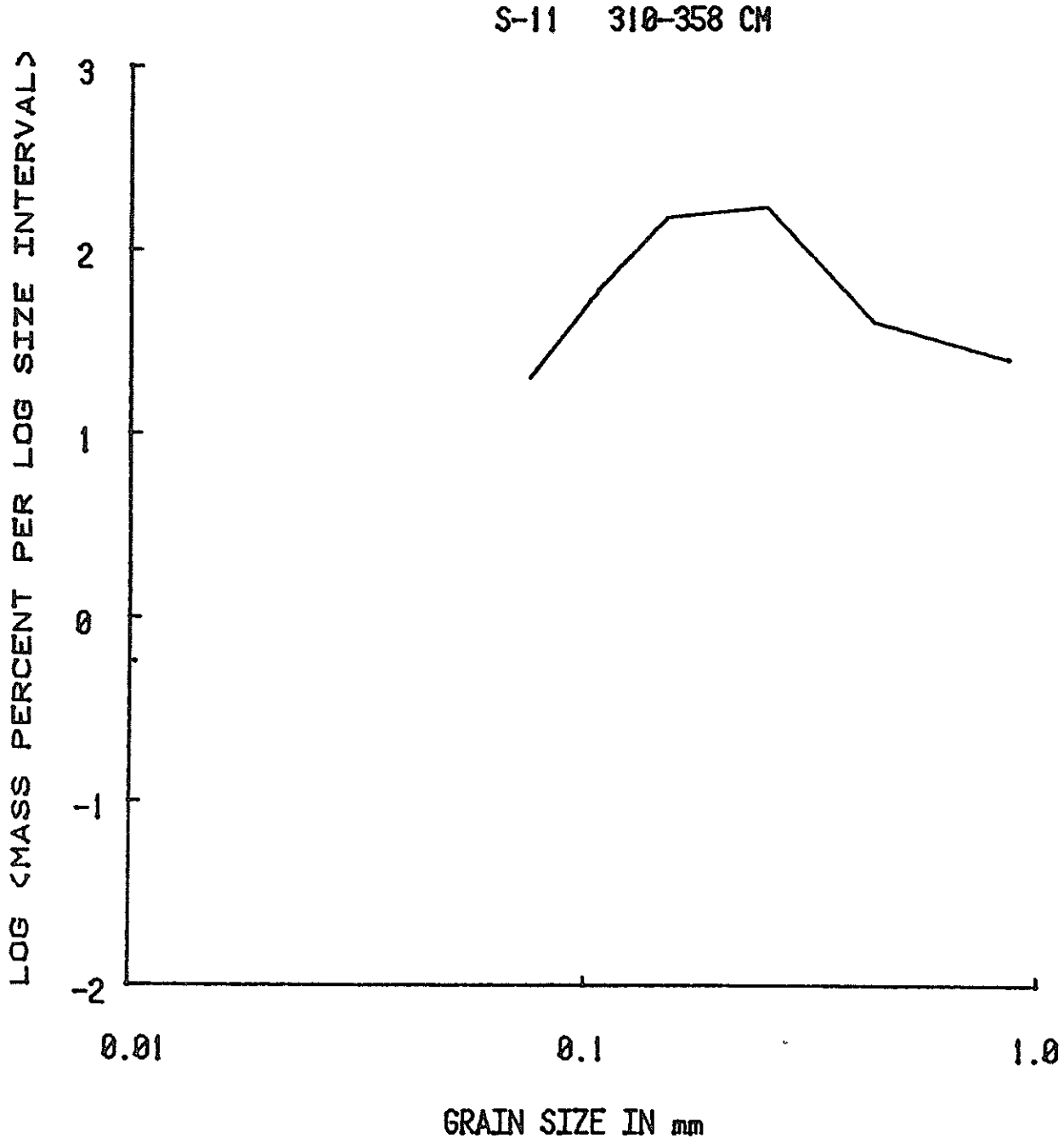
S-11 310-358 CM
LOG <MASS PERCENT PER LOG SIZE INTERVAL>
3
2
1
0
-1
-2
0.01
0.1
1.0
GRAIN SIZE IN mm

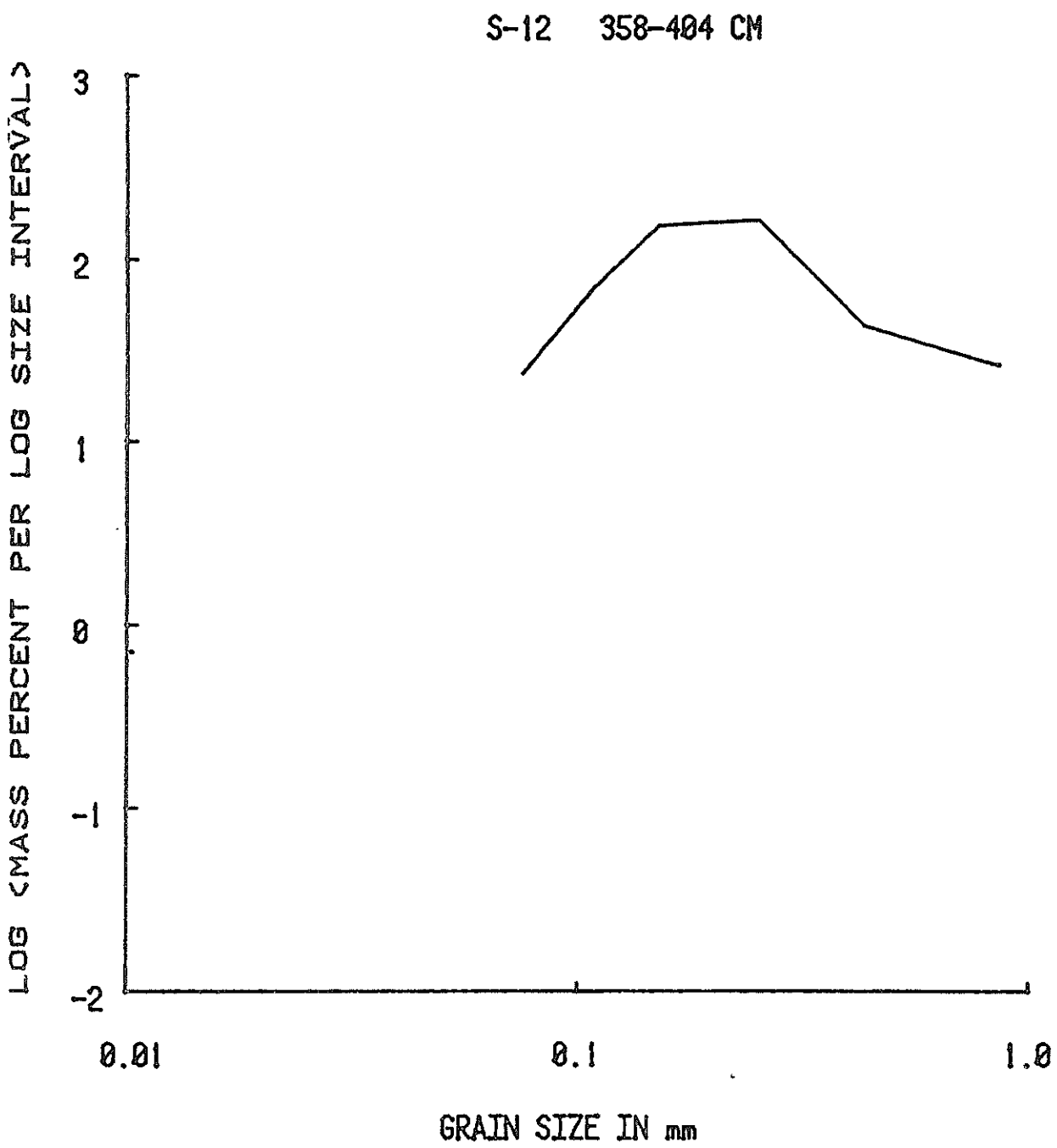
S-12 358-404 CM
LOG <MASS PERCENT PER LOG SIZE INTERVAL>
3
2
1
0
-1
-2
0.01
0.1
1.0
GRAIN SIZE IN mm

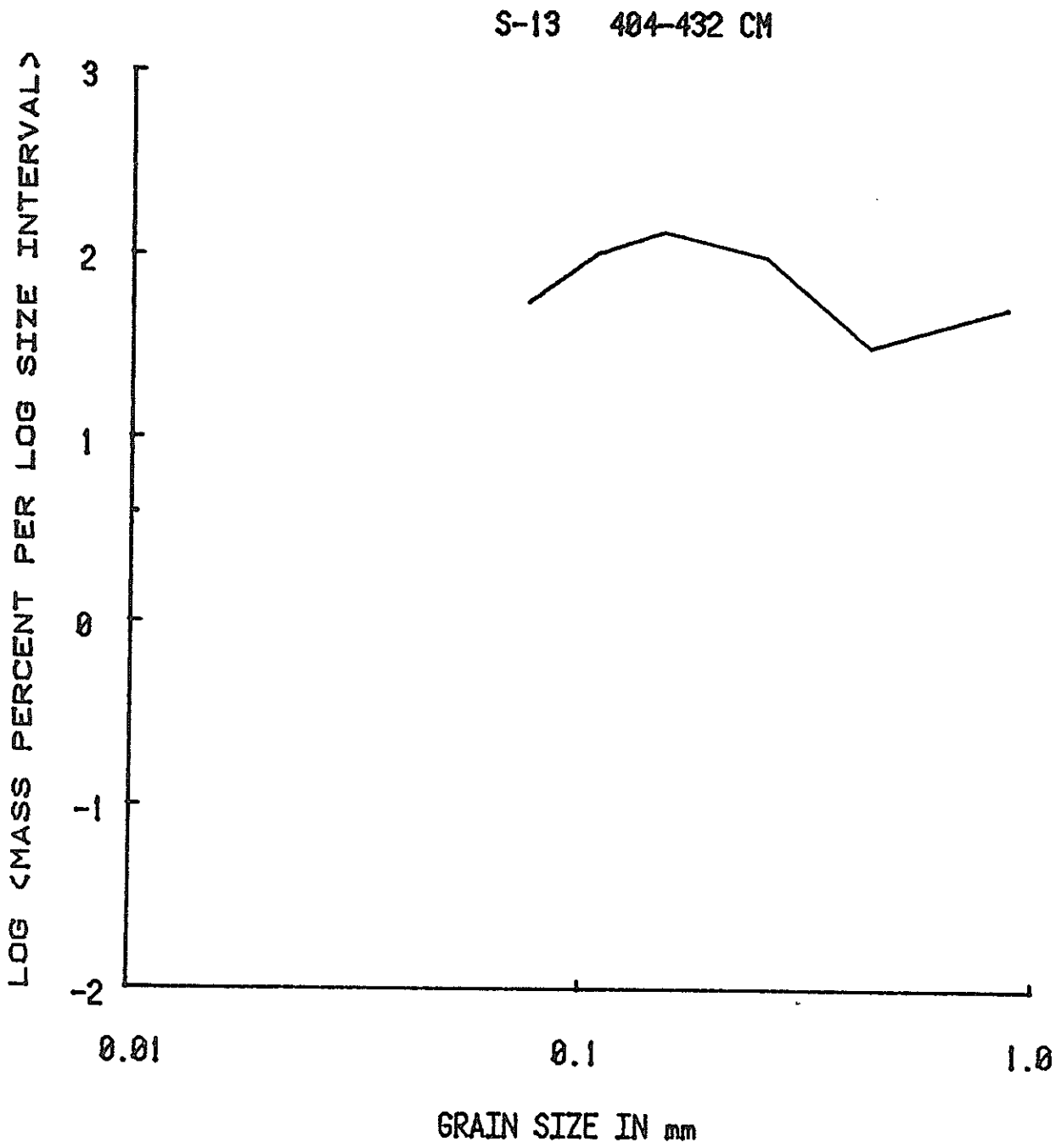
S-13 404-432 CM
LOG <MASS PERCENT PER LOG SIZE INTERVAL>
3
2
1
0
-1
-2
0.01
0.1
1.0
GRAIN SIZE IN mm

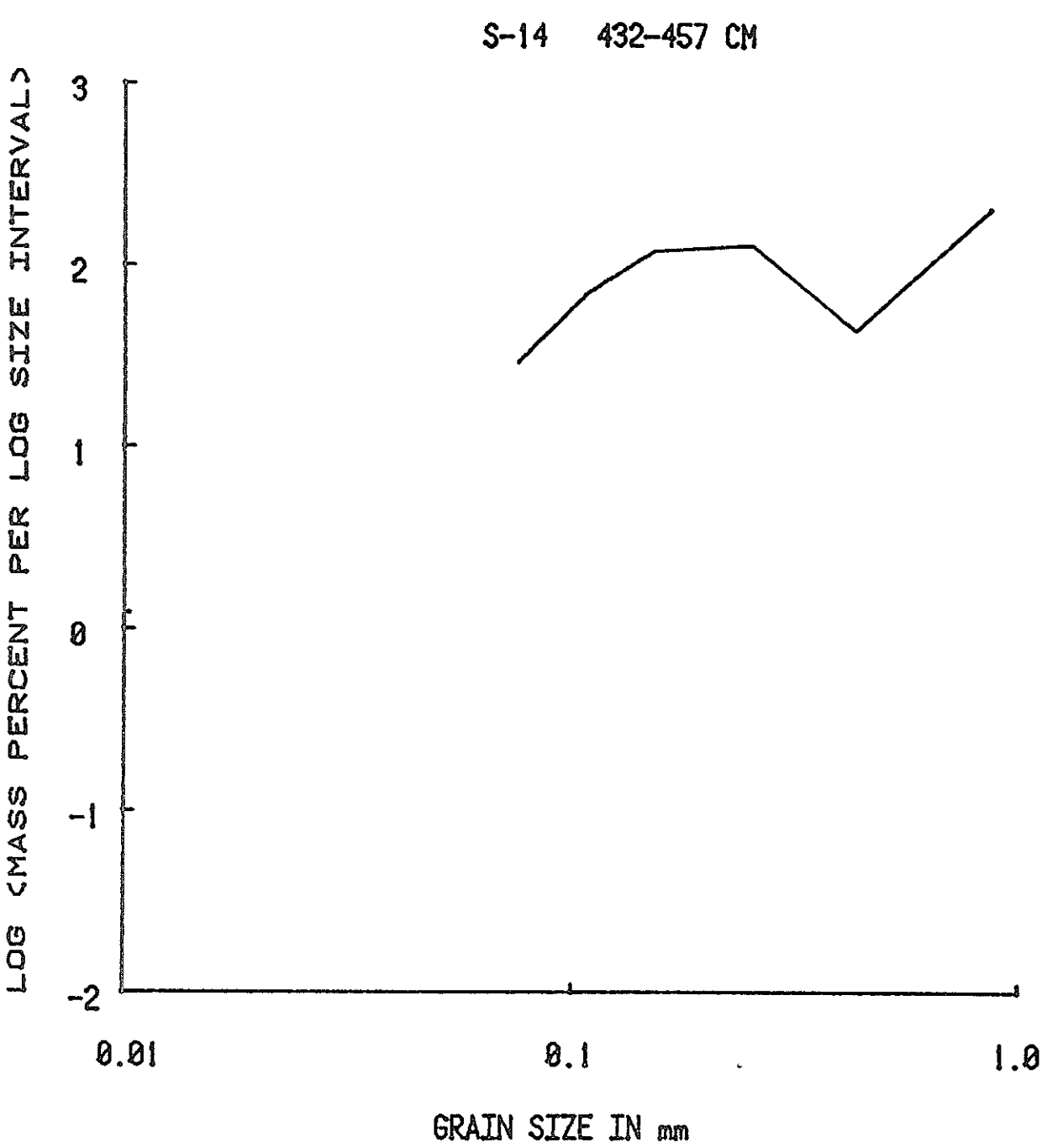
S-14 432-457 CM
LOG <MASS PERCENT PER LOG SIZE INTERVAL>
3
2
1
0
-1
-2
0.01
0.1
1.0
GRAIN SIZE IN mm

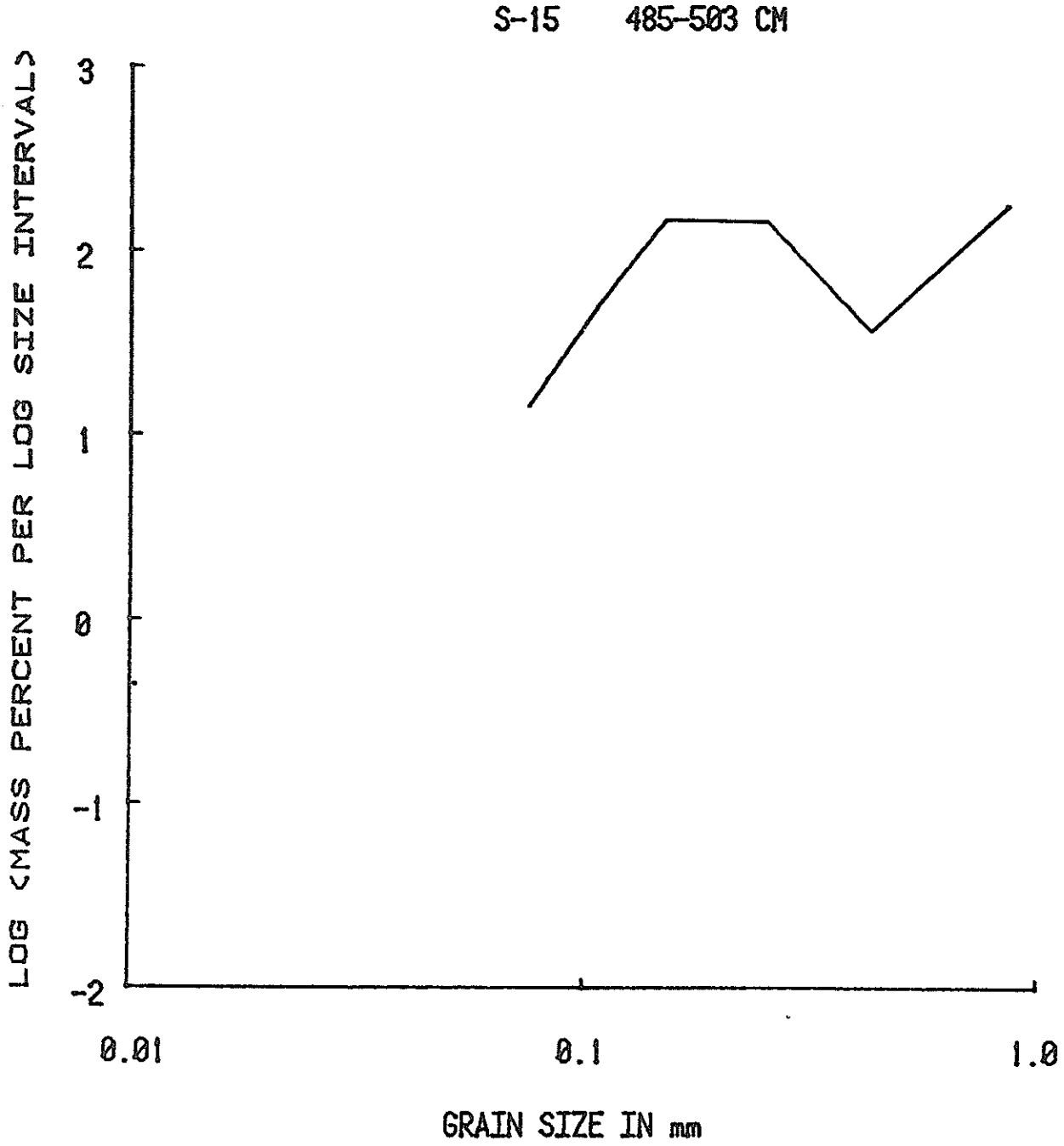
S-15 485-503 CM
LOG <MASS PERCENT PER LOG SIZE INTERVAL>
3
2
1
0
-1
-2
0.01
0.1
1.0
GRAIN SIZE IN mm

SAMPLE: LCP-1 0-25cm
MAXIMUM INTERMEDIATE DIAMETER: 1.00E+000mm

PARTICLE SIZE mm	WEIGHT gm	CUMULATIVE WEIGHT gm	WEIGHT PERCENT	CUMULATIVE WEIGHT PERCENT	LOG WEIGHT % PER LOG SIZE INTERVAL
8.50E-001	9.6900	9.6900	16.3406	16.3406	2.36
4.25E-001	10.8700	20.5600	18.3305	34.6712	1.78
2.50E-001	8.4200	28.9800	14.1990	48.8702	1.79
1.50E-001	6.7900	35.7700	11.4503	60.3204	1.71
1.06E-001	4.3300	40.1000	7.3019	67.6223	1.69
7.50E-002	3.2000	43.3000	5.3963	73.0185	1.56
4.98E-002	4.0000	47.3000	6.7454	79.7639	1.58
2.52E-002	2.0000	49.3000	3.3727	83.1366	1.06
1.14E-002	1.5000	50.8000	2.5295	85.6661	0.87
6.60E-003	0.5000	51.3000	0.8432	86.5093	0.55
4.70E-003	0.2500	51.5500	0.4216	86.9309	0.46
1.90E-003	2.2500	53.8000	3.7943	90.7251	0.98
1.40E-003	1.0000	54.8000	1.6863	92.4115	1.10
9.70E-004	0.5000	55.3000	0.8432	93.2546	0.72
6.00E-005	4.0000	59.3000	6.7454	100.0000	0.75

SAMPLE: LCP-2 25-50cm
MAXIMUM INTERMEDIATE DIAMETER: 1.00E+000mm

PARTICLE SIZE mm	WEIGHT gm	CUMULATIVE WEIGHT gm	WEIGHT PERCENT	CUMULATIVE WEIGHT PERCENT	LOG WEIGHT % PER LOG SIZE INTERVAL
8.50E-001	10.2200	10.2200	19.0850	19.0850	2.43
4.25E-001	9.0300	19.2500	16.8627	35.9477	1.75
2.50E-001	6.1200	25.3700	11.4286	47.3763	1.70
1.50E-001	5.4000	30.7700	10.0840	57.4603	1.66
1.06E-001	3.8100	34.5800	7.1148	64.5752	1.67
7.50E-002	2.9700	37.5500	5.5462	70.1214	1.57
4.98E-002	3.0000	40.5500	5.6022	75.7236	1.50
2.52E-002	3.0000	43.5500	5.6022	81.3259	1.28
1.14E-002	0.5000	44.0500	0.9337	82.2596	0.43
6.60E-003	1.0000	45.0500	1.8674	84.1270	0.90
4.70E-003	0.7500	45.8000	1.4006	85.5275	0.98
1.90E-003	1.2500	47.0500	2.3343	87.8618	0.77
1.40E-003	1.0000	48.0500	1.8674	89.7292	1.15
9.70E-004	0.5000	48.5500	0.9337	90.6629	0.77
6.00E-005	5.0000	53.5500	9.3371	100.0000	0.89

SAMPLE: LCP-3 55-77cm
MAXIMUM INTERMEDIATE DIAMETER: 1.00E+000mm

PARTICLE SIZE mm	WEIGHT gm	CUMULATIVE WEIGHT gm	WEIGHT PERCENT	CUMULATIVE WEIGHT PERCENT	LOG WEIGHT % PER LOG SIZE INTERVAL
8.50E-001	11.8700	11.8700	22.0878	22.0878	2.50
4.25E-001	7.8800	19.7500	14.6632	36.7510	1.69
2.50E-001	5.3600	25.1100	9.9739	46.7250	1.64
1.50E-001	4.8100	29.9200	8.9505	55.6755	1.61
1.06E-001	3.8100	33.7300	7.0897	62.7652	1.67
7.50E-002	3.5100	37.2400	6.5314	69.2966	1.64
4.98E-002	5.5000	42.7400	10.2345	79.5311	1.76
2.52E-002	2.5000	45.2400	4.6520	84.1831	1.20
1.14E-002	2.5000	47.7400	4.6520	88.8351	1.13
6.60E-003	1.0000	48.7400	1.8608	90.6959	0.89
4.70E-003	0.5000	49.2400	0.9304	91.6263	0.80
1.90E-003	1.5000	50.7400	2.7912	94.4176	0.85
9.70E-004	0.5000	51.2400	0.9304	95.3480	0.50
6.00E-005	2.5000	53.7400	4.6520	100.0000	0.59

SAMPLE: LCP-4 75-100cm
MAXIMUM INTERMEDIATE DIAMETER: 1.00E+000mm

PARTICLE SIZE mm	WEIGHT gm	CUMULATIVE WEIGHT gm	WEIGHT PERCENT	CUMULATIVE WEIGHT PERCENT	LOG WEIGHT % PER LOG SIZE INTERVAL
8.50E-001	12.5200	12.5200	23.4941	23.4941	2.52
4.25E-001	8.6200	21.1400	16.1756	39.6697	1.73
2.50E-001	4.9700	26.1100	9.3263	48.9961	1.61
1.50E-001	3.9200	30.0300	7.3560	56.3520	1.52
1.06E-001	2.7700	32.8000	5.1980	61.5500	1.54
7.50E-002	2.4900	35.2900	4.6725	66.2226	1.49
4.98E-002	4.0000	39.2900	7.5061	73.7287	1.63
2.52E-002	3.0000	42.2900	5.6296	79.3582	1.28
1.14E-002	1.5000	43.7900	2.8148	82.1730	0.91
6.60E-003	1.0000	44.7900	1.8765	84.0495	0.90
4.70E-003	0.7500	45.5400	1.4074	85.4569	0.98
1.90E-003	1.2500	46.7900	2.3457	87.8026	0.78
1.40E-003	1.0000	47.7900	1.8765	89.6791	1.15
9.70E-004	0.5000	48.2900	0.9383	90.6174	0.77
6.00E-005	5.0000	53.2900	9.3826	100.0000	0.89

SAMPLE: LCP-5 100-125cm
MAXIMUM INTERMEDIATE DIAMETER: 1.00E+000mm

PARTICLE SIZE mm	WEIGHT gm	CUMULATIVE WEIGHT gm	WEIGHT PERCENT	CUMULATIVE WEIGHT PERCENT	LOG WEIGHT % PER LOG SIZE INTERVAL
8.50E-001	13.9600	13.9600	25.7422	25.7422	2.56
4.25E-001	8.5100	22.4700	15.6924	41.4346	1.72
2.50E-001	5.4900	27.9600	10.1235	51.5582	1.64
1.50E-001	4.3000	32.2600	7.9292	59.4874	1.55
1.06E-001	2.9300	35.1900	5.4029	64.8903	1.55
7.50E-002	2.5400	37.7300	4.6838	69.5740	1.49
4.98E-002	5.0000	42.7300	9.2200	78.7940	1.71
2.52E-002	1.5000	44.2300	2.7660	81.5600	0.97
1.14E-002	1.5000	45.7300	2.7660	84.3260	0.90
6.60E-003	1.5000	47.2300	2.7660	87.0920	1.07
4.70E-003	0.2500	47.4800	0.4610	87.5530	0.50
1.90E-003	0.7500	48.2300	1.3830	88.9360	0.55
1.40E-003	1.5000	49.7300	2.7660	91.7020	1.32
6.00E-005	4.5000	54.2300	8.2980	100.0000	0.78

SAMPLE: LCP-6 120-150cm
MAXIMUM INTERMEDIATE DIAMETER: 1.00E+000mm

PARTICLE SIZE mm	WEIGHT gm	CUMULATIVE WEIGHT gm	WEIGHT PERCENT	CUMULATIVE WEIGHT PERCENT	LOG WEIGHT % PER LOG SIZE INTERVAL
8.50E-001	9.4900	9.4900	17.5871	17.5871	2.40
4.25E-001	8.0300	17.5200	14.8814	32.4685	1.69
2.50E-001	5.3700	22.8900	9.9518	42.4203	1.64
1.50E-001	4.2600	27.1500	7.8947	50.3150	1.55
1.06E-001	2.8900	30.0400	5.3558	55.6709	1.55
7.50E-002	2.4200	32.4600	4.4848	60.1557	1.47
4.69E-002	3.0000	35.4600	5.5597	65.7153	1.44
2.38E-002	2.5000	37.9600	4.6331	70.3484	1.20
1.07E-002	1.5000	39.4600	2.7798	73.1282	0.90
6.20E-003	1.0000	40.4600	1.8532	74.9815	0.89
4.70E-003	1.0000	41.4600	1.8532	76.8347	1.19
1.90E-003	2.0000	43.4600	3.7064	80.5411	0.97
9.70E-004	1.0000	44.4600	1.8532	82.3944	0.80
6.00E-005	9.5000	53.9600	17.6056	100.0000	1.16

SAMPLE: LCP-7 150-175cm
MAXIMUM INTERMEDIATE DIAMETER: 1.00E+000mm

PARTICLE SIZE mm	WEIGHT gm	CUMULATIVE WEIGHT gm	WEIGHT PERCENT	CUMULATIVE WEIGHT PERCENT	LOG WEIGHT % PER LOG SIZE INTERVAL
8.50E-001	12.6600	12.6600	23.4618	23.4618	2.52
4.25E-001	8.6500	21.3100	16.0304	39.4922	1.73
2.50E-001	5.0400	26.3500	9.3403	48.8325	1.61
1.50E-001	3.5500	29.9000	6.5789	55.4114	1.47
1.06E-001	2.4200	32.3200	4.4848	59.8962	1.47
7.50E-002	2.1400	34.4600	3.9659	63.8621	1.42
4.73E-002	3.5000	37.9600	6.4863	70.3484	1.51
2.42E-002	3.5000	41.4600	6.4863	76.8347	1.35
1.09E-002	1.5000	42.9600	2.7798	79.6145	0.90
6.30E-003	0.5000	43.4600	0.9266	80.5411	0.59
4.70E-003	1.0000	44.4600	1.8532	82.3944	1.16
1.90E-003	0.5000	44.9600	0.9266	83.3210	0.37
6.00E-005	9.0000	53.9600	16.6790	100.0000	1.05

SAMPLE: LCP-8 175-200cm
MAXIMUM INTERMEDIATE DIAMETER: 1.00E+000mm

PARTICLE SIZE mm	WEIGHT gm	CUMULATIVE WEIGHT gm	WEIGHT PERCENT	CUMULATIVE WEIGHT PERCENT	LOG WEIGHT % PER LOG SIZE INTERVAL
8.50E-001	15.8200	15.8200	28.3614	28.3614	2.60
4.25E-001	7.7700	23.5900	13.9297	42.2911	1.67
2.50E-001	4.4600	28.0500	7.9957	50.2868	1.54
1.50E-001	3.5000	31.5500	6.2747	56.5615	1.45
1.06E-001	2.5300	34.0800	4.5357	61.0972	1.48
7.50E-002	2.2000	36.2800	3.9441	65.0412	1.42
4.81E-002	4.0000	40.2800	7.1710	72.2123	1.57
2.43E-002	2.0000	42.2800	3.5855	75.7978	1.08
1.10E-002	2.0000	44.2800	3.5855	79.3833	1.02
6.40E-003	1.0000	45.2800	1.7928	81.1760	0.88
4.50E-003	0.5000	45.7800	0.8964	82.0724	0.77
1.90E-003	2.5000	48.2800	4.4819	86.5543	1.08
6.00E-005	7.5000	55.7800	13.4457	100.0000	0.95

SAMPLE: LCP-9 200-220cm
MAXIMUM INTERMEDIATE DIAMETER: 1.00E+000mm

PARTICLE SIZE mm	WEIGHT gm	CUMULATIVE WEIGHT gm	WEIGHT PERCENT	CUMULATIVE WEIGHT PERCENT	LOG WEIGHT % PER LOG SIZE INTERVAL
8.50E-001	11.1200	11.1200	19.8962	19.8962	2.45
4.25E-001	7.8200	18.9400	13.9918	33.8880	1.67
2.50E-001	5.7000	24.6400	10.1986	44.0866	1.65
1.50E-001	5.3000	29.9400	9.4829	53.5695	1.63
1.06E-001	3.4400	33.3800	6.1549	59.7245	1.61
7.50E-002	2.5100	35.8900	4.4910	64.2154	1.48
4.73E-002	3.5000	39.3900	6.2623	70.4777	1.50
2.40E-002	2.5000	41.8900	4.4731	74.9508	1.18
1.09E-002	2.0000	43.8900	3.5785	78.5293	1.02
6.30E-003	1.0000	44.8900	1.7892	80.3185	0.88
4.50E-003	0.5000	45.3900	0.8946	81.2131	0.79
1.90E-003	2.0000	47.3900	3.5785	84.7916	0.98
1.30E-003	0.5000	47.8900	0.8946	85.6862	0.73
9.40E-004	0.5000	48.3900	0.8946	86.5808	0.80
6.00E-005	7.5000	55.8900	13.4192	100.0000	1.05

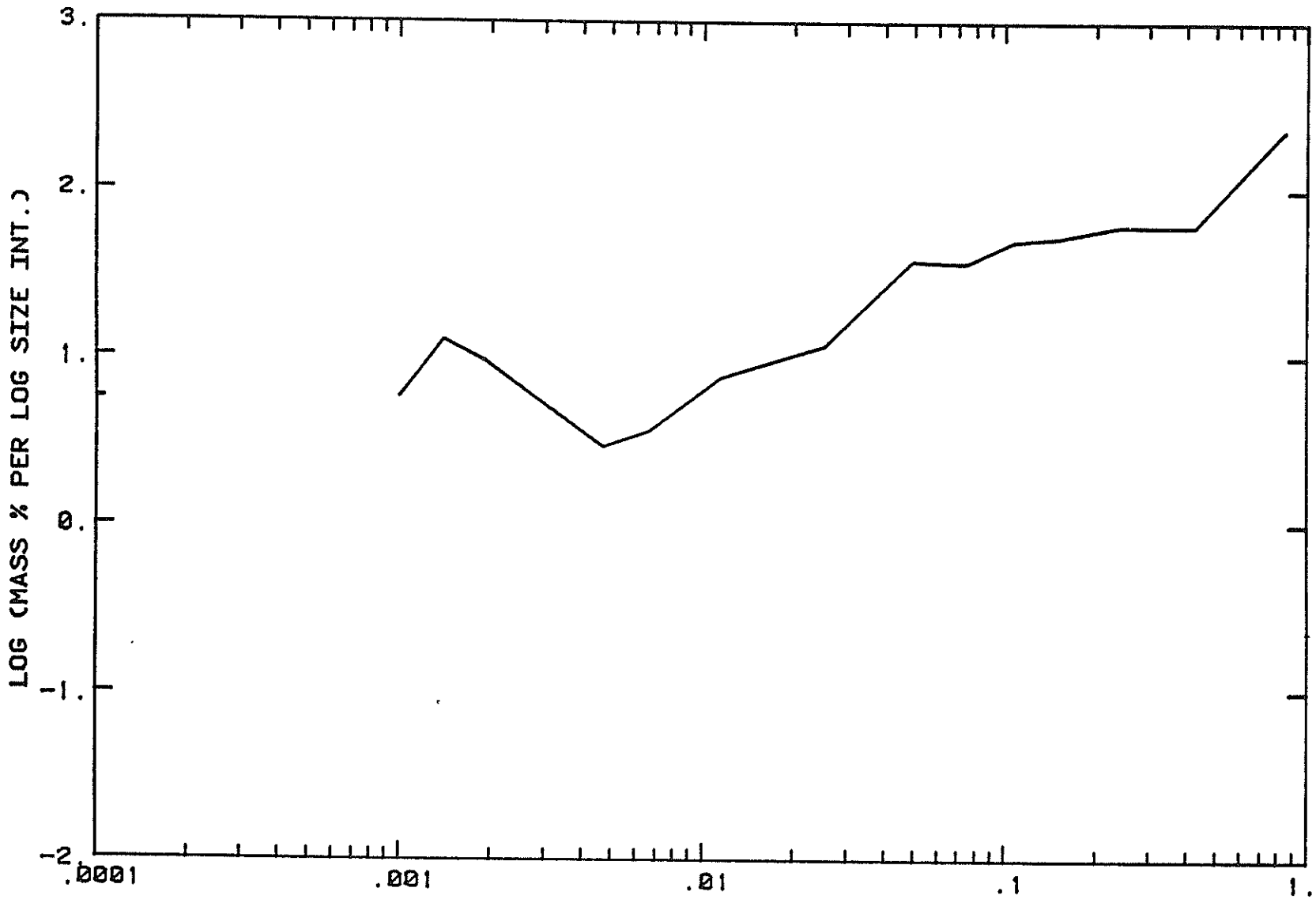
3.
2.
1.
0.
-1.
-2
.0001
.001
.01
.1
1.
LOG (MASS % PER LOG SIZE INT.)
GRAIN SIZE IN MM

LCP-1 0-25 CM

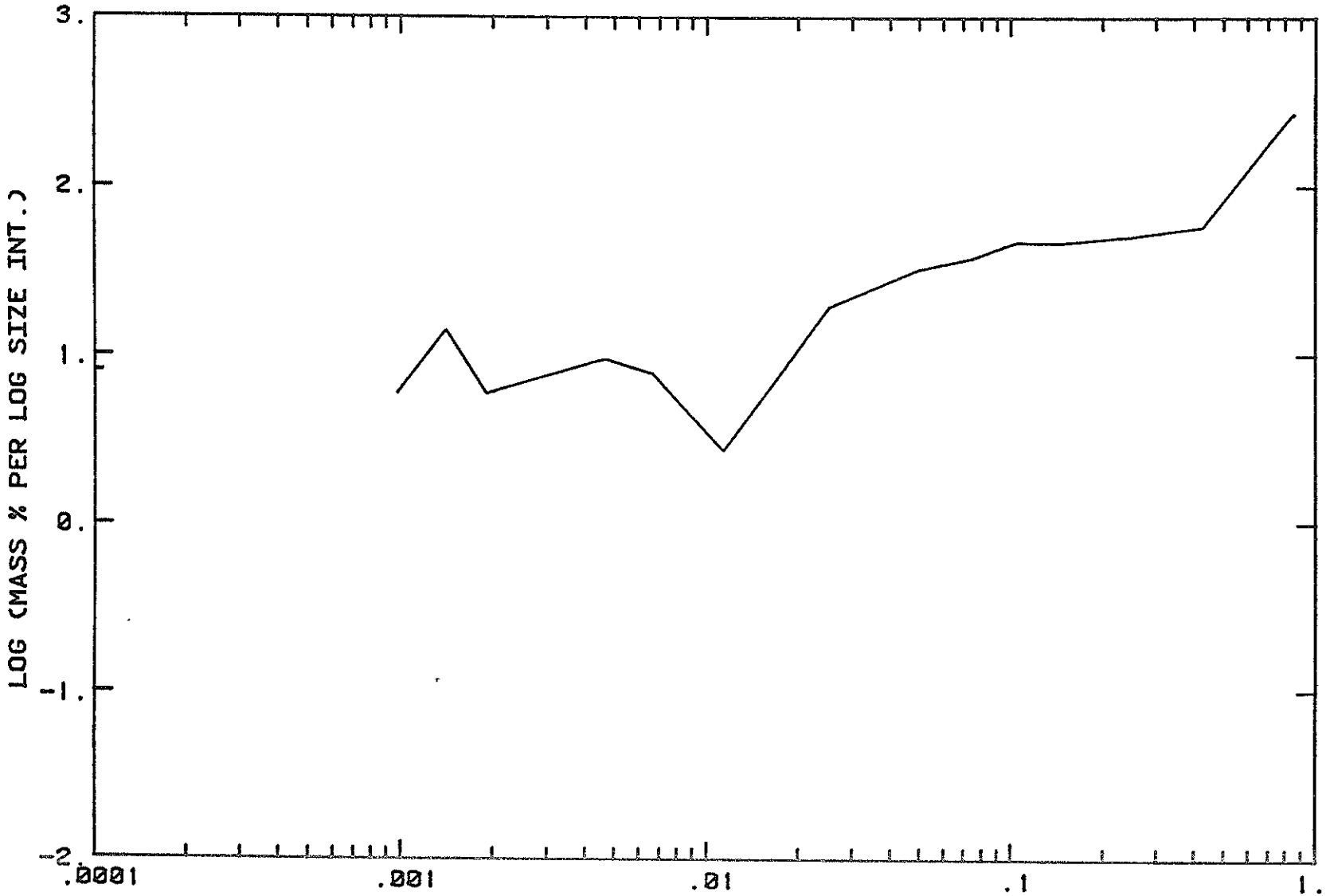
3.
2.
1.
0.
-1.
-2
LOG (MASS % PER LOG SIZE INT.)
.0001
.001
.01
.1
1.
GRAIN SIZE IN MM

LCP-2 25-50 CM

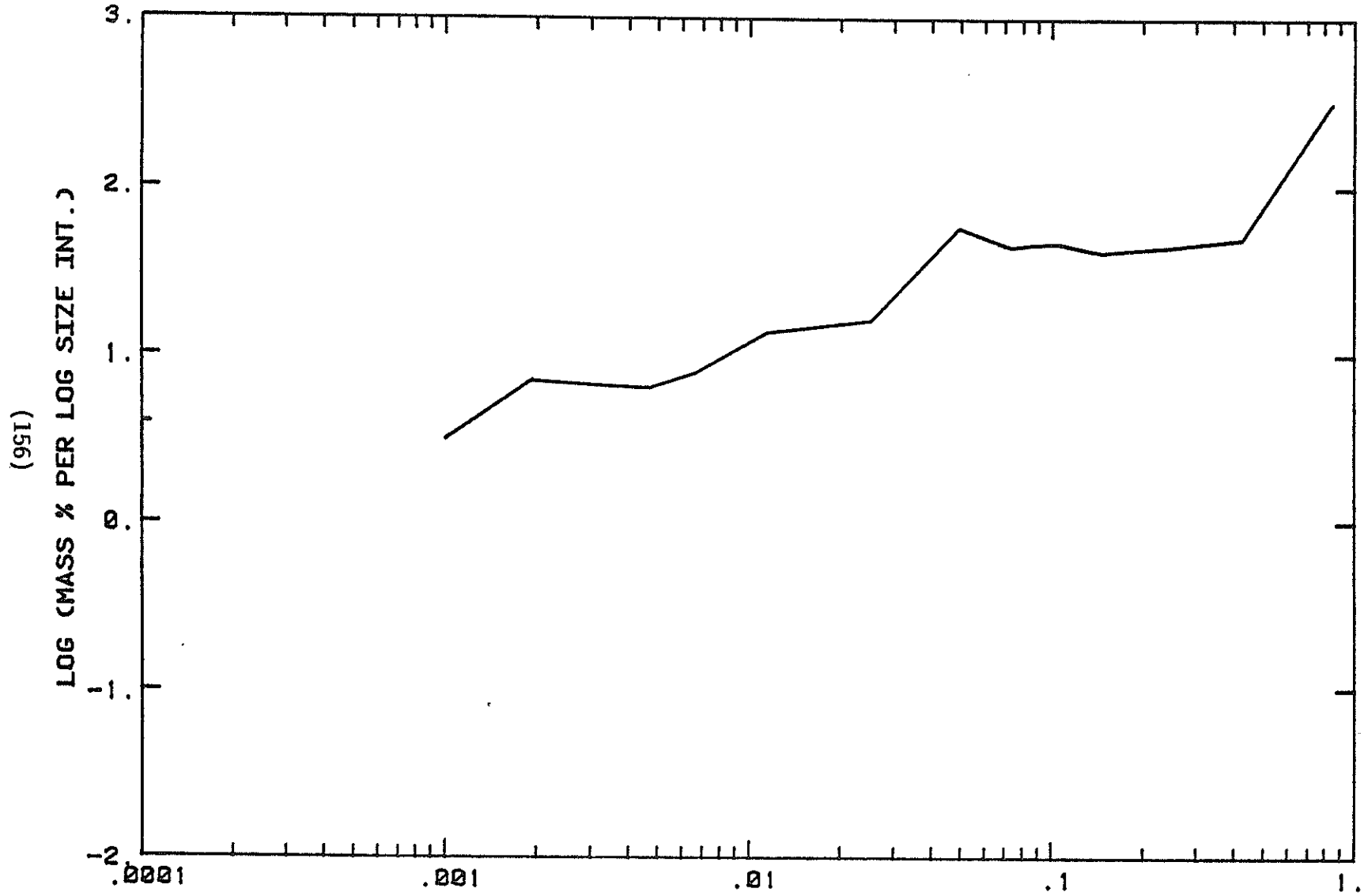
3.
2.
1.
0.
-1.
-2
.0001
.001
.01
.1
1.
LOG (MASS % PER LOG SIZE INT.)
GRAIN SIZE IN MM

LCP-3 55-77 CM

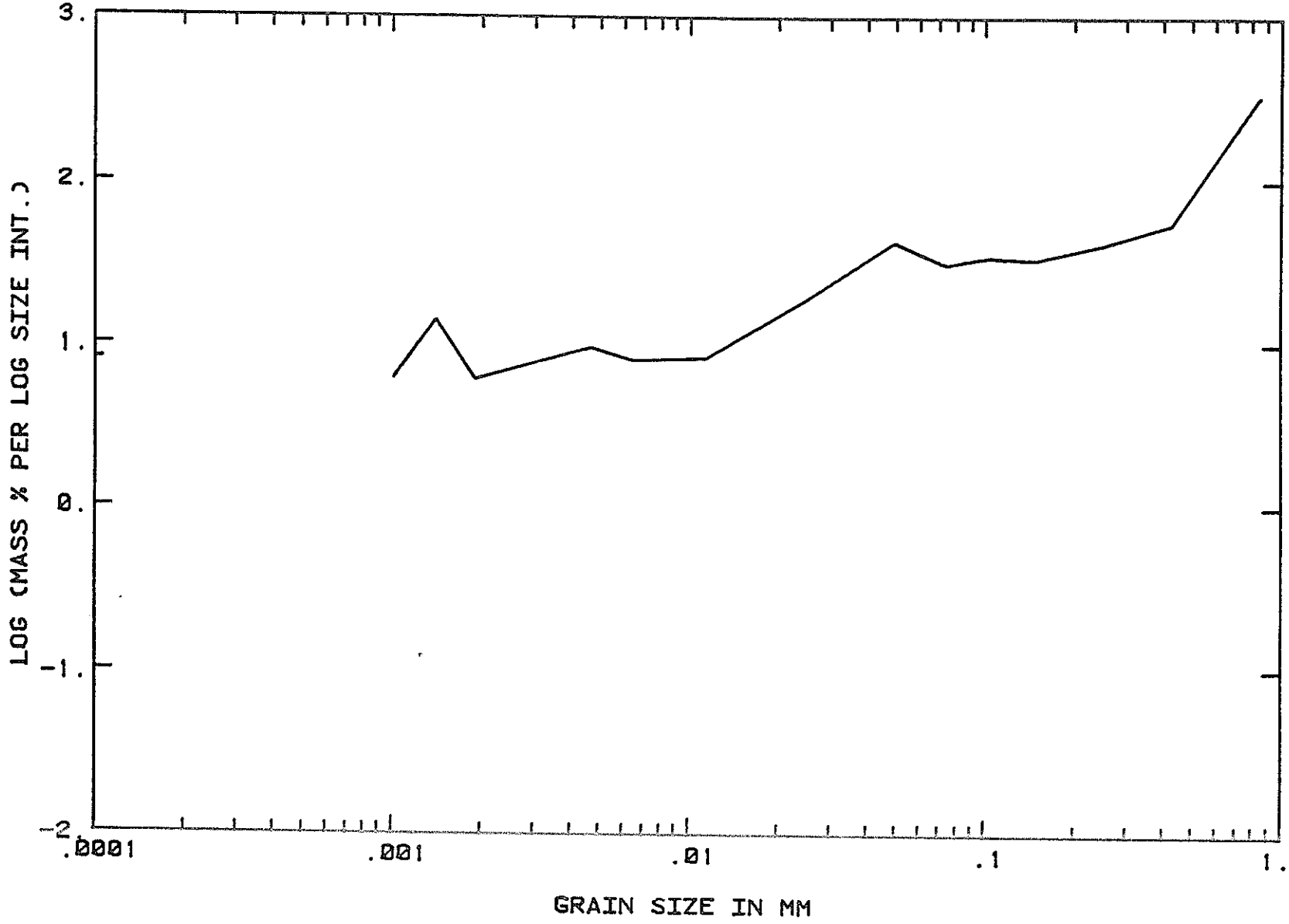

LCP-4 75-100 CM

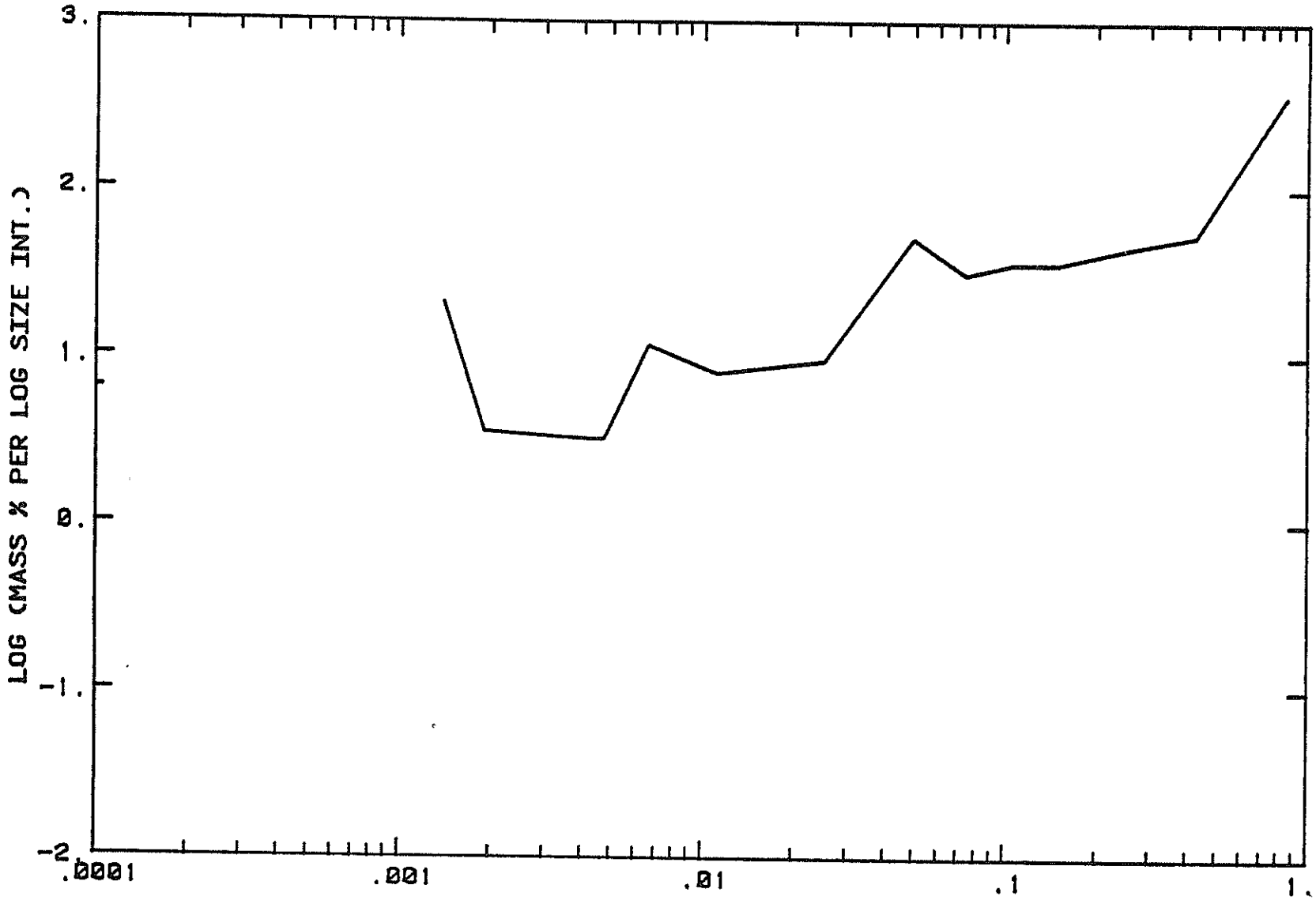

LCP-5 100-125 CM

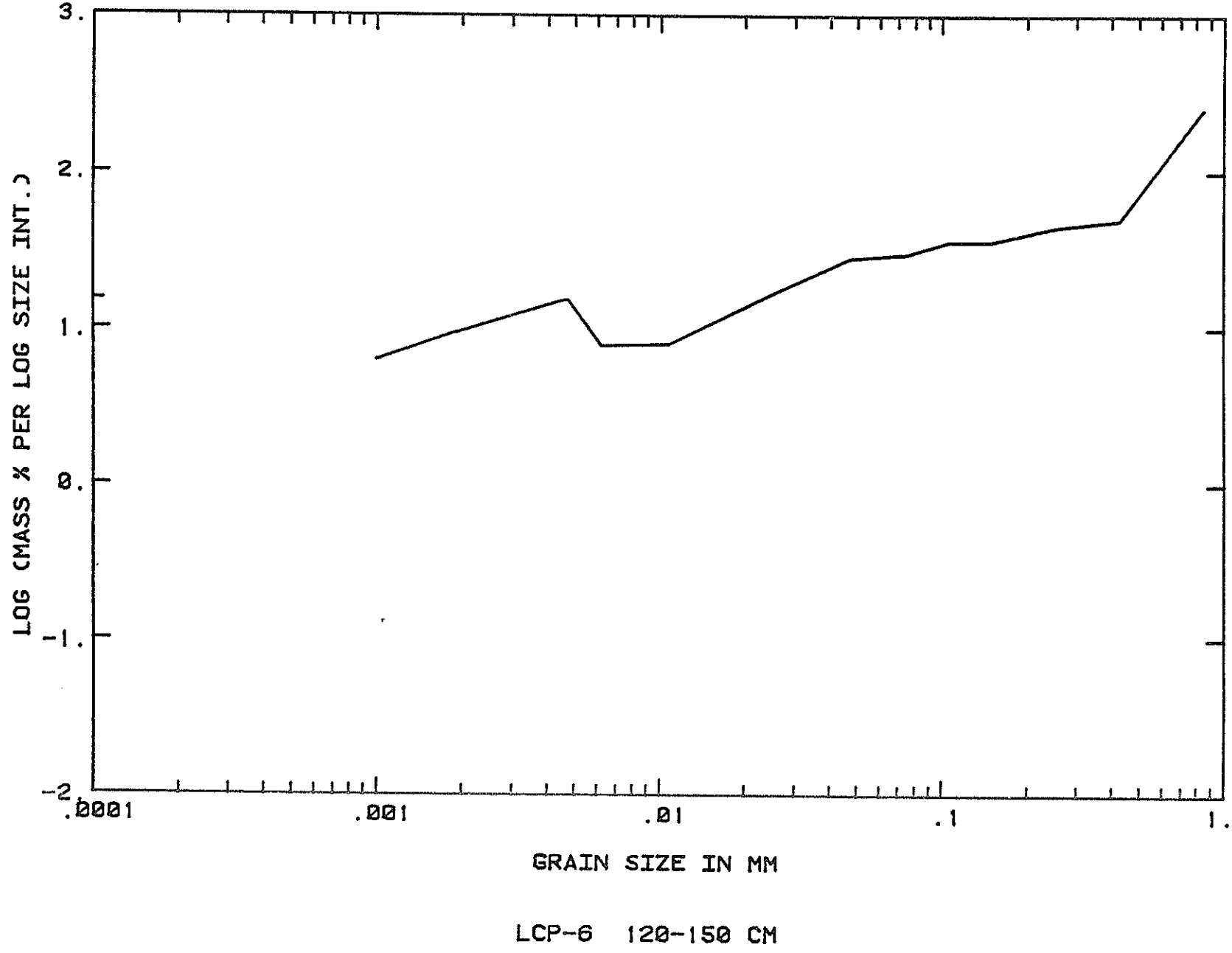

LCP-6 120-150 CM

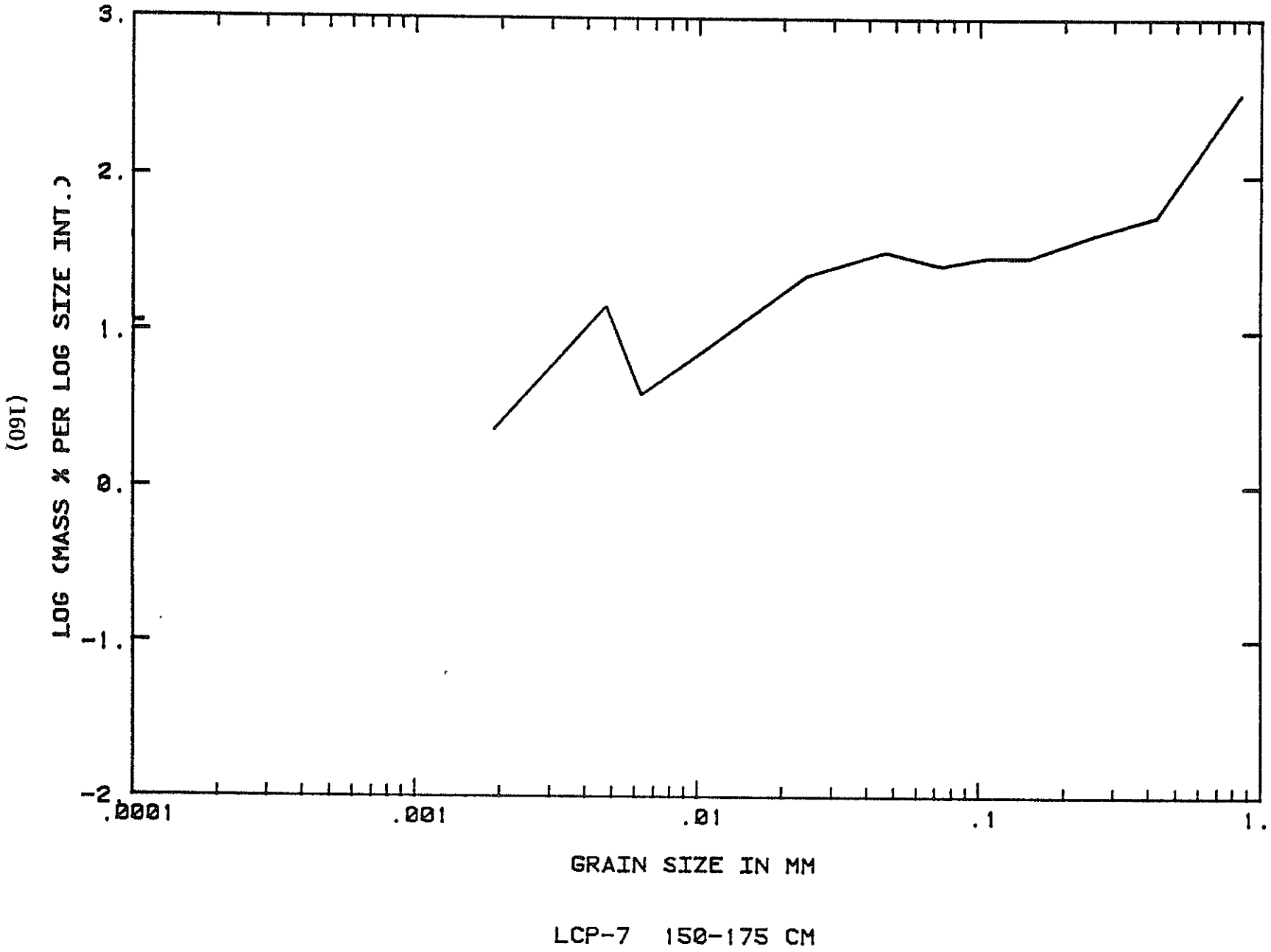

LCP-7 150-175 CM

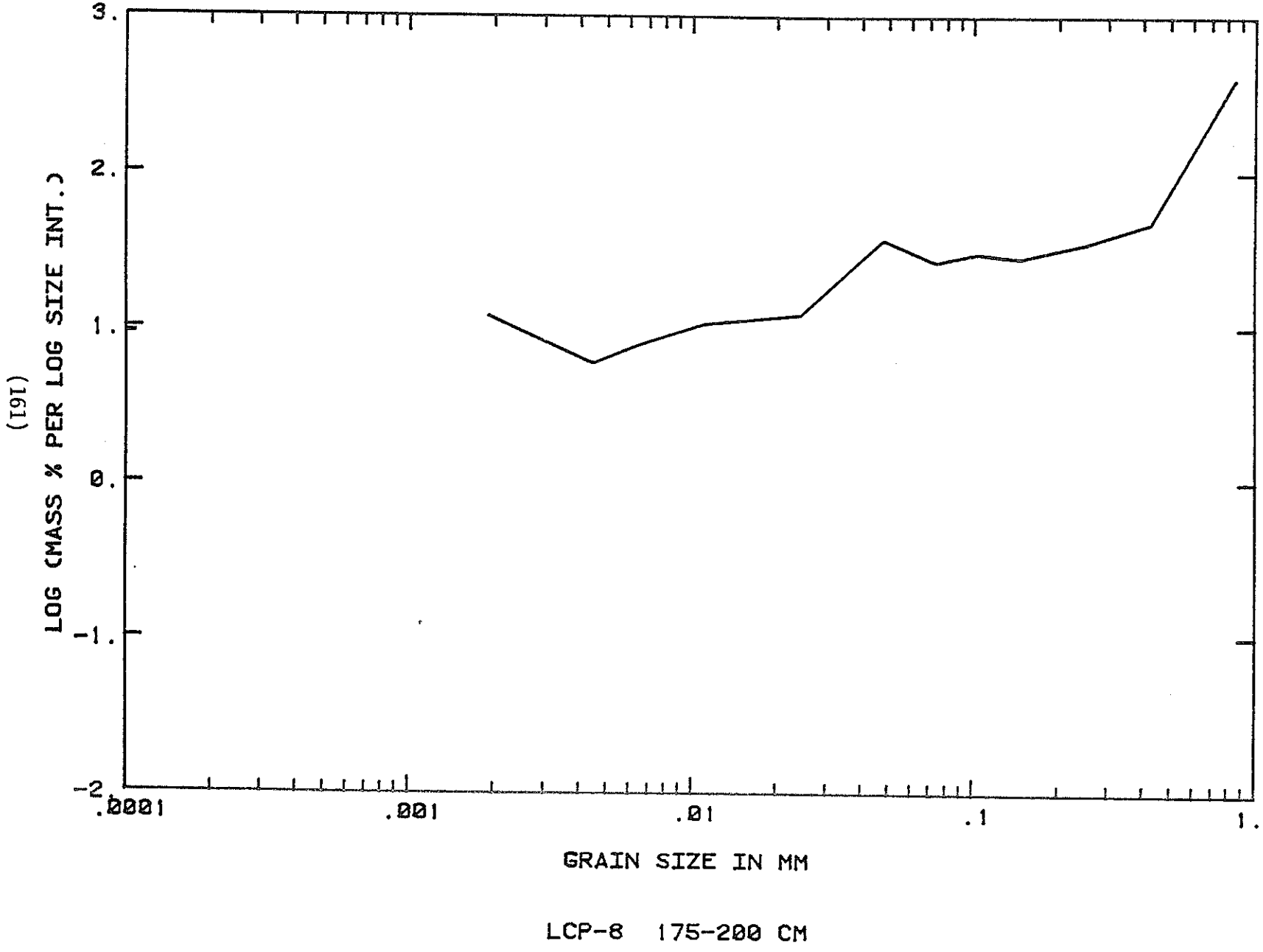

LCP-8 175-200 CM

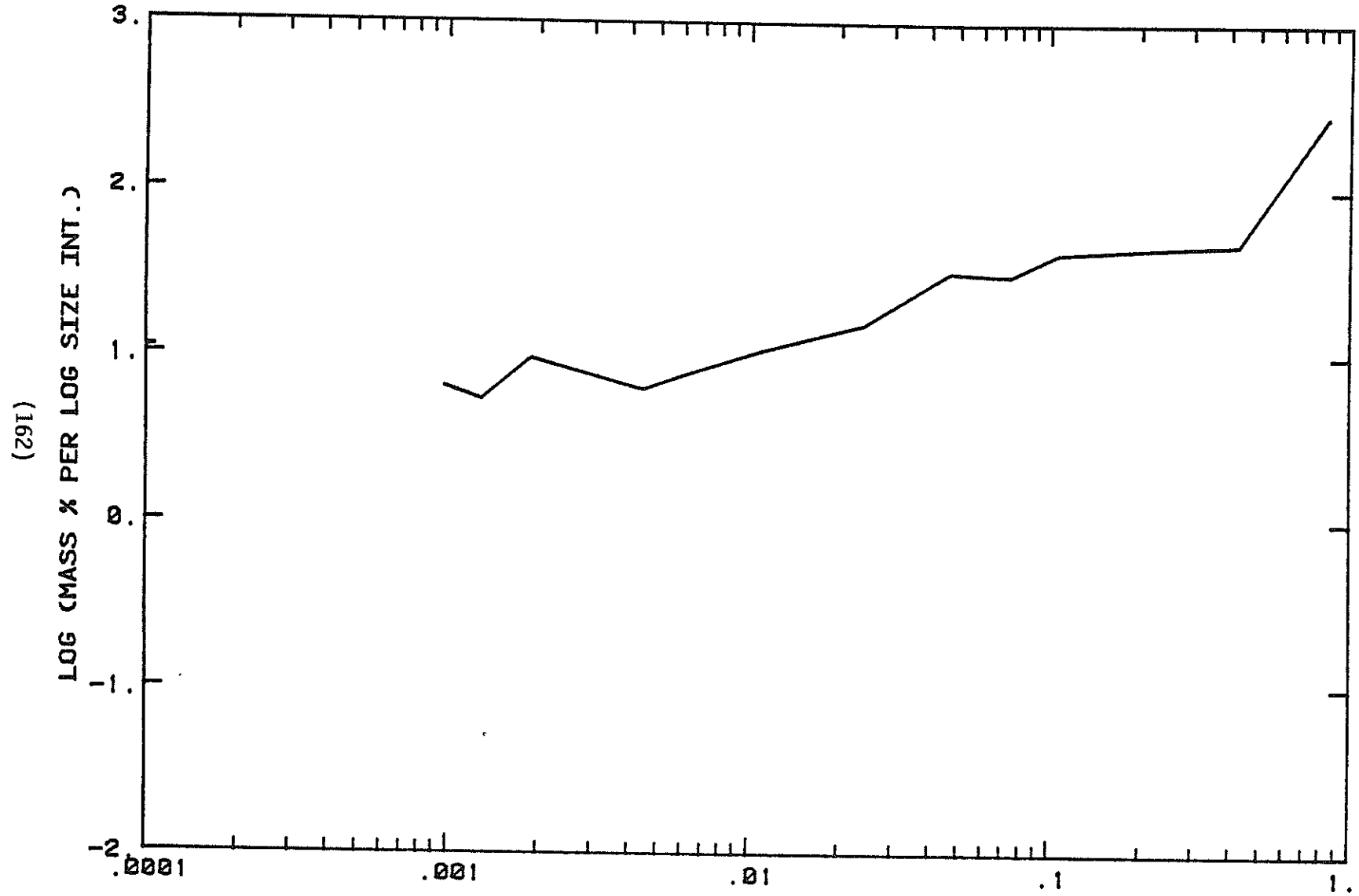

LCP-9 200-220 CM

APPENDIX E

FORTRAN PROGRAM USED TO CALCULATE VALUES IN TABLES 1 THROUGH 5

```
C**********************************************************************
C MASBAL.FOR SOLVES FOR THE TRAVEL TIME TO THE BOTTOM OF THE
C I'TH SOIL DEPTH INTERVAL. IT IS BASED ON THE MASS-BALANCE
C ARGUMENT WHICH STATES THAT THE DIFFERENCE BETWEEN THE CHLORIDE
C CONCENTRATION MEASURED AT ANY DEPTH IN THE SOIL AND THE
C ORIGINAL ATMOSPHERIC INPUT CONCENTRATION MAY BE ATTRIBUTED
C TO EVAPOTRANSPIRATIVE ENRICHMENT.
C**********************************************************************

C INPUT VARIABLES:

C NS    =NUMBER OF SAMPLES
C W     =GRAVIMETRIC MOISTURE CONTENT (GM H2O/GM DRY SOIL)
C CO    =ATMOSPHERIC INPUT CHLORIDE CONCENTRATION IN MG/L
C P     =ANNUAL PRECIPITATION IN CMS
C BD    =DRY BULK DENSITY IN GMS PER CC
C PPM   =CHLORIDE CONCENTRATION OF EXTRACT IN PPM
C ADH2O=WEIGHT OF H2O ADDED TO DRY SOIL SAMPLE
C DRYWT=DRY WEIGHT OF SOIL SAMPLE
C INTF  =TOP OF INTERVAL (CM)
C INTL  =BOTTOM OF INTERVAL (CM)

C PROGRAM VARIABLES:

C AVD    =AVERAGE SAMPLE DEPTH IN CM
C d      =SAMPLE INTERVAL THICKNESS IN CM
C AGE    =TIME, IN YEARS, TO THE BOTTOM OF THE I'TH SOIL DEPTH
C          INTERVAL
C THETA  =VOLUMETRIC MOISTURE CONTENT (CC H2O / CC DRY SOIL)
C Q      =PORE VELOCITY (CM/YEAR)
C R      =RECHARGE RATE IN CM/YEAR
C M      =MG CL/KG SOIL
C C      =MG CL/L H2O
C CUMCL  =CUMULATIVE CHLORIDE (G/M**2)
C CUMH2O=CUMULATIVE WATER (M)

C**********************************************************************

      INTEGER NS, AGE(0:22), INTF(22), INTL(22)
      REAL W(22),THETA(22), Q(22), CO, P, R(22), d(22), AVD(0:22)
      REAL M(22), C(22), PPM(22), ADH2O(22), DRYWT(22), CUMCL(0:22)
      REAL CUMH2O(0:22)

C CREATE INPUT, OUTPUT AND PLOT FILES

      NREAD=33
      NWRITE=34
      NPLOT=35
      NPLOT2=36
      NPLOT3=37
      NPLOT4=32
      OPEN(UNIT=33, FILE='CLIN.DAT', ACCESS= 'SEQIN')
      OPEN(UNIT=34, FILE='CLOUT.DAT')
      OPEN(UNIT=35, FILE='WDPLT.DAT')
      OPEN(UNIT=36, FILE='CDPLT.DAT')
      OPEN(UNIT=37, FILE='CMPLT.DAT')
      OPEN(UNIT=32, FILE='AGPLT.DAT')

C READ IN DATA
```

```
      READ(NREAD,*)NS, RO, CO, P
      DO 10 I=1,NS
      READ(NREAD,*)INTF(I), INTL(I), DRYWT(I), ADH2O(I), PPM(I), W(I)
10    CONTINUE
C
C     MASS BALANCE
C
      AVD(0)=0
      AGE(0)=0
      CUMCL(0)=0
      CUMH2O(0)=0
C
      DO 20 I=1,NS
      AVD(I)=(FLOAT(INTL(I))-FLOAT(INTF(I)))/2.0 + FLOAT(INTF(I))
      d(I)=AVD(I)-AVD(I-1)
      M(I)=(PPM(I)*ADH2O(I))/DRYWT(I)
      C(I)=M(I)/W(I)
      R(I)=(CO*P)/C(I)
      THETA(I)=W(I)*RO
      q(I)=R(I)/THETA(I)
      AGE(I)=((RO*M(I)*d(I))/(CO*P))+AGE(I-1)
      CUMCL(I)=(THETA(I)*C(I)*d(I)/100)+CUMCL(I-1)
      CUMH2O(I)=(THETA(I)*d(I)/100)+CUMH2O(I-1)
20    CONTINUE
C
C     PRINT RESULTS
C
      WRITE(NWRITE,1002)
1002  FORMAT(3X,'SAMPLE',4X,'AVG.',4X,'d',4X,'THETA',7X,'M',8X,'C',
     *8X,'R',7X,'q',5X,'AGE',3X,'CUMCL',3X,'CUMH2O')
      WRITE(NWRITE,1003)
1003  FORMAT(2X,'INTERVAL',1X,'SAMPLE',3X,'INT.',2X,'CC H2O',
     *4X,'MG CL',5X,'MG CL',5X,'CM',6X,'CM',4X,'YEARS',2X,'G/M**2',
     *5X,'M')
      WRITE(NWRITE,1004)
1004  FORMAT(5X,'CM',5X,'DEPTH',2X,'THICK',2X,'CC SOIL',2X,'KG SOIL',
     *4X,'H2O',5X,'YEAR',4X,'YEAR')
      WRITE(NWRITE,1005)
1005  FORMAT(13X,'CM')
      WRITE(5,*)
      WRITE(5,*)
      DO 30 I=1,NS
      WRITE(NWRITE,1006)INTF(I), INTL(I), AVD(I), d(I), THETA(I), M(I),
     *C(I), R(I), q(I), AGE(I), CUMCL(I), CUMH2O(I)
1006  FORMAT(2X,I3,'-',I3,3X,F5.1,3X,F4.1,1X,F7.4,2X,F6.1,2X,F8.1,
     *4X,F5.2,3X,F5.2,2X,I5,4X,F6.2,3X,F5.2)
30    CONTINUE
C
C     WRITE DATA FOR PLOTTING
C
      DO 40 I=1,NS
      WRITE(NPLOT,1007)I, W(I), - AVD(I)
      WRITE(NPLOT2,1007)I, C(I), - AVD(I)
      WRITE(NPLOT3,1007)I, CUMCL(I),- CUMH2O(I)
      WRITE(NPLOT4,1008)I, AGE(I), - AVD(I)
1007  FORMAT(I6,2F20.10)
1008  FORMAT(I6,I10,F20.10)
40    CONTINUE
C
      STOP
```

APPENDIX F

LAS CRUCES AREA ATMOSPHERIC INPUT CHLORIDE CONCENTRATION CALCULATIONS

According to figure 1, natural fallout at the latitude of Las Cruces, New Mexico (32^{0} 30′) is approximately 25 atoms $^{36}Cl\ m^{-2}yr^{-1}$. From figure 2, natural background 36Cl/Cl equals 640×10^{-15}. Stable chloride fallout, therefore, equals:

$$\frac{25 \text{ atoms } ^{36}Cl\ m^{-2}s^{-1}}{} = 3.9 \times 10^{13} \text{ atoms Cl } m^{-2}s^{-1}$$
$$= 73 \text{ mg Cl } m^{-2}yr^{-1}$$

Using 22 cm/yr average annual precipitation,

$$73 \text{ mg Cl } m^{-2}yr^{-1}/22 \text{ cm } yr^{-1}$$

$$= \frac{3.3 \text{mg Cl}}{10{,}000 \text{ cm}^3} \times \frac{1 \text{ cm}^3}{.001 \text{ L}} \simeq 0.35 \text{ mg/L}$$

APPENDIX G

DATA FOR SOIL-WATER CHLORIDE CALCULATIONS

SNWR UNVEGETATED SITE

depth interval cm	dry wght of soil g	wght added DD water g	chloride in extract ppm	W moisture g H2O/g dry soil
0-13	70.84	93.23	3.8	0.012
25-36	60.81	89.03	2.4	0.021
36-43	63.50	88.33	1.4	0.022
51-58	60.61	88.58	1.0	0.021
76-86	61.52	93.04	1.0	0.022
103-112	54.06	90.30	1.0	0.034
129-138	52.27	85.77	1.0	0.034
146-156	50.93	91.24	1.0	0.040
166-175	59.19	88.59	1.0	0.042
186-195	49.06	87.94	1.5	0.050
204-212	52.43	93.15	1.0	0.036
220-230	65.20	88.67	1.5	0.041
240-249	48.36	91.09	2.8	0.018
258-269	62.14	92.39	1.9	0.033
279-289	57.86	90.57	1.0	0.032
299-309	51.81	92.82	1.9	0.055
317-325	66.71	88.85	2.4	0.027
334-344	72.63	92.73	2.3	0.020
353-364	72.68	90.76	5.3	0.023
371-381	74.55	92.07	12.3	0.016
381-389	57.81	93.56	15.1	0.018
389-400	63.24	90.43	142.7	0.075

SNWR SOIL-WATER STATION 15

depth interval cm	dry wght of soil g	wght added DD water g	chloride in extract ppm	W moisture g H2O/g dry soil
0-6	76.60	94.00	0.626	0.0129
24-33	63.45	91.17	0.642	0.0301
44-55	62.46	89.83	0.738	0.0306
67-79	65.57	87.10	0.958	0.0473
95-106	67.46	91.38	0.693	0.0314
117-127	65.70	92.92	0.626	0.0365
138-149	64.53	88.00	0.939	0.0335
158-167	60.57	91.80	0.626	0.0343
178-188	68.20	93.82	0.939	0.0299
198-208	66.23	93.97	0.626	0.0412
218-228	60.06	93.06	0.626	0.0485
237-246	64.93	87.60	0.947	0.0413
254-264	55.85	91.63	0.939	0.0428
274-284	62.89	90.24	0.939	0.0404
293-303	59.41	87.73	1.118	0.0411
313-325	72.33	89.92	0.955	0.0384
334-343	63.99	89.91	0.732	0.0378
353-362	66.69	82.42	0.955	0.0382
373-383	62.14	87.65	0.939	0.0389
383-393	61.83	85.18	0.725	0.0438
393-402	64.99	89.29	0.962	0.0455

SNWR SOIL-WATER STATION 1

depth interval cm	dry wght of soil g	wght added DD water g	chloride in extract ppm	W moisture g H2O/g dry soil
0-5	57.83	92.7	2.08	0.060
15-20	57.71	90.1	2.08	0.021
40-45	69.41	90.2	3.17	0.024
60-65	65.05	90.0	2.08	0.028
80-85	63.21	92.1	2.08	0.033
100-105	65.82	90.1	1.56	0.029
120-125	64.72	91.0	1.56	0.079
140-145	63.52	90.2	1.56	0.043
165-170	61.82	90.0	3.64	0.045
190-195	57.38	90.0	2.08	0.054
215-220	70.70	91.0	2.60	0.039
235-240	63.15	90.1	2.08	0.051
255-260	65.17	90.1	3.64	0.057
275-280	62.66	90.0	2.08	0.074
295-300	60.48	90.0	3.12	0.056

SNWR ISOTOPE SAMPLING SITE

depth interval cm	dry wght of soil g	wght added DD water g	chloride in extract ppm	W moisture g H2O/g dry soil
0-25	69.63	100.0	1.74	0.054
25-50	57.46	100.0	1.16	0.059
50-75	58.23	100.0	1.16	0.060
75-100	53.35	100.0	1.16	0.068
100-125	55.52	100.0	1.16	0.078
125-150	57.62	100.0	1.16	0.077
150-175	55.59	100.0	2.33	0.058
175-200	60.43	101.0	2.33	0.032
213-262	62.43	100.0	2.40	0.027
262-310	62.28	100.0	1.19	0.030
310-358	67.09	101.0	3.60	0.032
358-404	62.52	100.0	4.65	0.021
404-432	50.57	100.0	116.04	0.120
432-457	62.89	100.0	18.96	0.030
485-503	58.94	100.0	18.91	0.073

NMSUR ISOTOPE SAMPLING SITE

depth interval cm	dry wght of soil g	wght added DD water g	chloride in extract ppm	W moisture g H2O/g dry soil
0-5	72.28	98.36	3.918	0.0809
5-20	72.09	97.21	2.798	0.0444
20-30	58.22	97.42	3.358	0.0646
30-40	71.48	95.62	2.518	0.0718
40-55	71.11	96.76	2.239	0.0790
60-73	67.21	96.50	2.239	0.0853
73-77	66.69	95.06	1.959	0.0873
75-100	60.72	95.42	1.399	0.0982
100-125	60.92	96.87	2.275	0.1139
120-150	66.24	96.49	7.060	0.1229
150-175	55.70	100.00	26.30	0.0937
175-200	82.47	87.00	35.35	0.0547
200-220	66.16	100.00	23.32	0.0521

APPENDIX H

COMPUTATION OF 36CL CONCENTRATIONS

Depth Interval (cm)	C136/Cl	C136/Cl - 700 bckgrnd	Atoms C136/m^2	C136/cm^3	C136 Atoms/cm^3 soil
0-25	1509×10^{-15}	809×10^{-15}	3.22×10^{9}	1.74×10^{5}	1.29×10^{4}
25-50	4682×10^{-15}	3982×10^{-15}	3.52×10^{10}	2.52×10^{6}	1.41×10^{5}
50-75	4928×10^{-15}	4228×10^{-15}	5.84×10^{10}	3.91×10^{6}	2.34×10^{5}
75-100	5886×10^{-15}	5186×10^{-15}	1.18×10^{11}	7.23×10^{6}	4.7×10^{5}
100-125	5420×10^{-15}	4720×10^{-15}	2.19×10^{11}	1.4×10^{7}	8.7×10^{5}
125-150	2403×10^{-15}	1703×10^{-15}	1.5×10^{11}	1.4×10^{7}	6.0×10^{5}
150-175	1633×10^{-15}	933×10^{-15}	3.0×10^{11}	2.4×10^{7}	1.2×10^{6}
175-225	789×10^{-15}	89×10^{-15}	9.8×10^{10}	3.3×10^{6}	2.0×10^{5}
225-275	717×10^{-15}	17×10^{-15}	1.6×10^{10}	5.6×10^{5}	3.3×10^{4}
275-300	717×10^{-15}	17×10^{-15}	7.1×10^{9}	4.8×10^{5}	2.8×10^{4}
300-350	718×10^{-15}	18×10^{-15}	2.2×10^{10}	7.9×10^{5}	4.3×10^{4}
350-400	717×10^{-15}	17×10^{-15}	3.4×10^{10}	1.2×10^{6}	6.5×10^{4}
		total	1.06×10^{12}		1.06×10^{8}

Volume/m^2 x bulk density x mg chloride/kg soil x Atoms chloride/mg x 36Cl/Cl = Atoms 36Cl/m^2

eg. sample 1: (0.25 m^3/m^2) x (1300 Kg/m^3) x (0.72 mg/Kg) x(6.02×10^{23} Atoms Cl/35400 mg) x (809×10^{-15} atoms 36Cl/atoms Cl)

36Cl Atoms/Cl Atoms x mg Cl/L water x .001 L/cm^3 x 6.02×10^{23} Atoms Cl/35400 mg Cl = 36Cl/cm^3 soil

or 36Cl Atoms/cm^3 soil = 36Cl/cm^3 x(cm^3 water/cm^3 soil)

Total 36Cl fallout between 30°N and 50°N = 7.13×10^{12} atoms 36Cl m^{-2}

1.06×10^{12} 36Cl m^{-2}/7.13×10^{12} 36Cl m^{-2} = 0.14 Total bomb 36Cl fallout at this location is 14% of that predicted by model. It is assumed that this implies the fallout rate was also 14% of that predicted.

Sample Interval (cm)	Mg Cl/Kg soil	Gravimetric moisture (%)
0-25	0.72	5.7
25-50	1.6	4.3
50-75	2.5	4.6
75-100	4.1	5.0
100-125	8.4	4.8
125-150	15.9	3.3
150-175	58.0	3.8
175-225	100.1	4.6
225-275	87.8	4.5
275-300	75.5	4.5
300-350	108.7	4.2
350-400	182.1	4.2

From: Trotman (1983)

APPENDIX I

NUMERICAL MODEL AND INPUT PARAMETERS

```
C-----------------------------------------------------------------------
C     GALERKIN FINITE-ELEMENT PROGRAM TO SOLVE 1-D CONVECTIVE-
C     DISPERSION EQUATION FOR PARTIALLY SATURATED FLOW.
C-----------------------------------------------------------------------
C
C     INPUT VARIABLES:
C
C     TL     =TOTAL LENGTH OF MODEL (CM)
C     NE     =NO. ELEMENTS
C     NNE    =NO. NODES/ELEMENT
C     D      =HYDRODYNAMIC DISPERSION COEFFICIENT (CM**2/DAY)
C     V      =VELOCITY (CM/DAY)
C     DELT   =TIME INCREMENT (DAYS)
C     E      =WEIGHTING FACTOR
C     FINTIM=TOTAL SIMULATION TIME
C     THETA  =VOL. MOISTURE CONTENT
C     N      =POROSITY
C     OBSCO  =OBSERVED 36CL CONCENTRATION
C
C     PROGRAM VARIABLES:
C
C     LE     =ELEMENT LENGTH (CM)
C     NN     =NO. NODES
C     CCO    =NUMERICALLY CALCULATED CONCENTRATION
C-----------------------------------------------------------------------
C
      DIMENSION A(405), B(405), C(405), RHS(405), CCO(405), Z(405),
     *          V(405), THETA(405), D(405),  OBSCO(405),
     *          A211(405), A212(405), A221(405), A222(405),
     *          A111(405), A112(405), A121(405), A122(405)
C
      REAL LE, N, INPUT
C
C     CREATE INPUT, OUTPUT, AND PLOT FILES
C
      NREAD=30
      NWRITE=31
      NPLOT=32
      OPEN (UNIT=30, FILE='C36IN.DAT')
      OPEN (UNIT=31, FILE='C36OUT.DAT')
      OPEN (UNIT=32, FILE='C36PLT.DAT')
C
C     READ IN DATA
C
      READ(NREAD,*) TL, NE, NNE, DELT, E, TPRINT, FINTIM, N,
     *              DELC, CL
      LE=TL/FLOAT(NE)
      NN=NE*(NNE-1)+1
C
C     SET NODE DEPTHS, THETAS, VELS., & HYD. DISPS.
C
      DO 10 I=1,NN
      Z(I)=FLOAT(I-1)*LE
      IF(Z(I).LT.25.0)THEN
       obsco(I)=1.29E+4
      END IF
      IF(Z(I).GE.25.0)THEN
       obsco(I)=1.41E+5
```

```
      END IF
      IF(Z(I).GE.50.0)THEN
       obsco(I)=2.34E+5
      END IF
      IF(Z(I).GE.75.0)THEN
       obsco(I)=4.7E+5
      END IF
      IF(Z(I).GE.100.0)THEN
       oosco(I)=8.7E+5
      END IF
      IF(Z(I).GE.125.0)THEN
       obsco(I)=6.E+5
      END IF
      IF(Z(I).GE.150.0)THEN
       obsco(I)=1.2E+6
      END IF
      IF(Z(I).GE.175.0)THEN
       obsco(I)=1.97E+5
      END IF
      IF(Z(I).GE.225.0)THEN
       OBSCO(I)=3.3E+4
      END IF
      IF(Z(I).GE.275.0)THEN
       OBSCO(I)=2.8E+4
      END IF
      IF(Z(I).GE.300.0)THEN
       OBSCO(I)=4.3E+4
      END IF
      DISP=8.
      V(I)=0.01*2
      THETA(I)=0.06344
      D(I)=DISP*V(I)+(((THETA(I)/N)**2)*1.04/3)
10    CONTINUE

      WRITE(NWRITE,1000) TL, NE, NNE, DELT, E, FINTIM, LE, NN
1000  FORMAT('TOTAL LENGTH=',F8.2,3X,'NO. ELEMENTS=',I6,3X,
     * 'NODES/ELEMENT=',I2,/'DELT=',F8.2,3X,'E=',F6.2,3X,
     * 'FINTIM=',F10.2,3X,/'ELEMENT LENGTH=',F6.4,3X,
     * 'NO.NODES=',I6/)

C     SET INITIAL CONDITIONS

      DO 20 I=1,NN
20     CCO(I)=0.0

C     FORM ELEMENT MATRICES A1 & A2

      DO 30 I=1,NN
      A111(I)=(D(I)/LE)*1.0
      A112(I)=(D(I)/LE)*-1.0
      A121(I)=(D(I)/LE)*-1.0
      A122(I)=(D(I)/LE)*1.0
30    CONTINUE

      DO 40 I=1,NN
      A211(I)=(V(I)/2-(D(I)*DELC/CL))
      A212(I)=(V(I)/2-(D(I)*DELC/CL))
      A221(I)=(V(I)/2-(D(I)*DELC/CL))*-1.0
      A222(I)=(V(I)/2-(D(I)*DELC/CL))*-1.0
40    CONTINUE
```

```
C
C       FORM B ELEMENT MATRIX
C
        B11=(LE/DELT)/3.0
        B12=(LE/DELT)/6.0
        B21=(LE/DELT)/6.0
        B22=(LE/DELT)/3.0
C
C       FORM A, B, & C DIAGONALS OF GLOBAL MATRIX
C
        DO 50 I=2,NN
          A(I)=E*(A121(I)+A221(I))+B21
50      CONTINUE
        DO 60 I=2,NN-1
          B(I)=E*(A111(I)+A122(I)+A211(I)+A222(I))+B11+B22
60      CONTINUE
        B(1)=E*(A111(1)+A211(1))+B11
        B1=B(1)
        B(NN)=E*(A122(NN)+A222(NN))+B22
        DO 70 I=1,NN-1
          C(I)=E*(A112(I)+A212(I))+B12
70      CONTINUE
C
C       BEGIN TIME
C
        TIME=0
C0      TIME=TIME+DELT
C
C       FORM RIGHT-HAND-SIDE MATRIX
C
        RHS(1)=(E-1)*(A111(1)*CCO(1)+A112(1)*CCO(2))+
     * (E-1)*(A211(1)*CCO(1)+A212(1)*CCO(2))+
     * (B11*CCO(1)+B12*CCO(2))
        DO 90 I=2,NN-1
        RHS(I)=(E-1)*(A121(I)*CCO(I-1)+(A111(I)+A122(I))*
     * CCO(I)+A112(I)*CCO(I+1))+(E-1)*(A221(I)*CCO(I-1)+
     * (A211(I)+A222(I))*CCO(I)+A212(I)*CCO(I+1))+
     * (B21*CCO(I-1)+(B11+B22)*CCO(I)+B12*CCO(I+1))
90      CONTINUE
        RHS(NN)=(E-1)*(A121(NN)*CCO(NN-1)+A122(NN)*CCO(NN))+
     * (E-1)*(A221(NN)*CCO(NN-1)+A222(NN)*CCO(NN))+
     * (B21*CCO(NN-1)+B22*CCO(NN))
C
C       INCORPORATE BOUNDARY CONDITIONS
C
        IF(TIME.LE.250)THEN
        RHS(1)=RHS(1)+(0.0241)*4.5E+5
        END IF
        IF(TIME.GT.250.AND.TIME.LE.750)THEN
        RHS(1)=RHS(1)+(0.0241)*1.1E+6
        END IF
        IF(TIME.GT.750.AND.TIME.LE.1250)THEN
        RHS(1)=RHS(1)+(0.0241)*2.1E+6
        END IF
        IF(TIME.GT.1250.AND.TIME.LE.1500)THEN
        RHS(1)=RHS(1)+(0.0241)*1.2E+6
        END IF
        IF(TIME.GT.1500.AND.TIME.LE.2000)THEN
        RHS(1)=RHS(1)+(0.0241)*1.6E+6
        END IF
```

```
      IF(TIME.GT.2000.AND.TIME.LE.2250)THEN
      RHS(1)=RHS(1)+(0.0241)*8.6E+5
      END IF
      IF(TIME.GT.2250.AND.TIME.LE.2750)THEN
      RHS(1)=RHS(1)+(0.0241)*1.4E+6
      END IF
      IF(TIME.GT.2750.AND.TIME.LE.3000)THEN
      RHS(1)=RHS(1)+(0.0241)*8.1E+5
      END IF
      IF(TIME.GT.3000.AND.TIME.LE.3500)THEN
      RHS(1)=RHS(1)+(0.0241)*4.3E+5
      END IF
      IF(TIME.GT.3500.AND.TIME.LE.4000)THEN
      RHS(1)=RHS(1)+(0.0241)*1.1E+5
      END IF
      IF(TIME.GT.4000)THEN
      RHS(1)=RHS(1)+(0.0241)*0.0
      END IF
C
C     CALL SUBROUTINE TRIDAG TO SOLVE FOR CCO AT NEXT TIME STEP
C
      CALL TRIDAG (1,NN,A,B,C,RHS,CCO)
      IF(TIME.EQ.TPRINT.OR.TIME.EQ.FINTIM)GO TO 3
      GO TO 80
C
C     CALCULATE AREAS UNDER CURVES
C
3     CSUMO=0.0
      CSUM=0.0
      DO 102 K=1,NE
      CSUMO=(OBSCO(K)+OBSCO(K+1))/2+CSUMO
102   CSUM=(CCO(K)+CCO(K+1))/2+CSUM
      WRITE(5,*)'CSUMO=',CSUMO
      WRITE(5,*)'CSUM=',CSUM
C
C     PRINT RESULTS
C
      WRITE(NWRITE,1001)
1001  FORMAT('  I',3X,'     Z     ',3X,'    CCO(I)   ',
     *       2X,'   OBSCO(I)   ',2X,'     D(I)     ')
      DO 110 I=1,NN
      WRITE(NWRITE,1002) I, Z(I), CCO(I), OBSCO(I), D(I)
1002  FORMAT(1X,I3,3X,E12.4,3X,E12.6,3X,E12.6,3X,E12.6)
110   CONTINUE
C
C     WRITE DATA FOR PLOTTING
C
      DO 120 I=1,NN
120   WRITE(NPLOT,1003) I, CCO(I)*1E-3,-Z(I)
      DO 140 I=1,NN
140   WRITE(NPLOT,1003) I, OBSCO(I)*1E-3,-Z(I)
1003  FORMAT(I6,5X,E12.6,5X,E12.6)
C
      STOP
C
      END
C-----------------------------------------------------------------------
      SUBROUTINE TRIDAG (IF,L,A,B,C,D,V)
```

```
      DIMENSION A(405), B(405), C(405), D(405), V(405), BETA(405),
     *          GAMMA(405)
C
      BETA(IF)=B(IF)
      GAMMA(IF)=D(IF)/BETA(IF)
      IFP1=IF+1
      DO 1 I=IFP1,L
      BETA(I)=B(I) - A(I)*C(I-1)/BETA(I-1)
1     GAMMA(I)=(D(I) - A(I)*GAMMA(I-1))/BETA(I)
C
      V(L)=GAMMA(L)
      LAST=L-IF
      DO 2 K=1,LAST
      I=L-K
2     V(I)=GAMMA(I) - C(I)*V(I+1)/BETA(I)
      RETURN
      END
C-----------------------------------------------------------------------
```

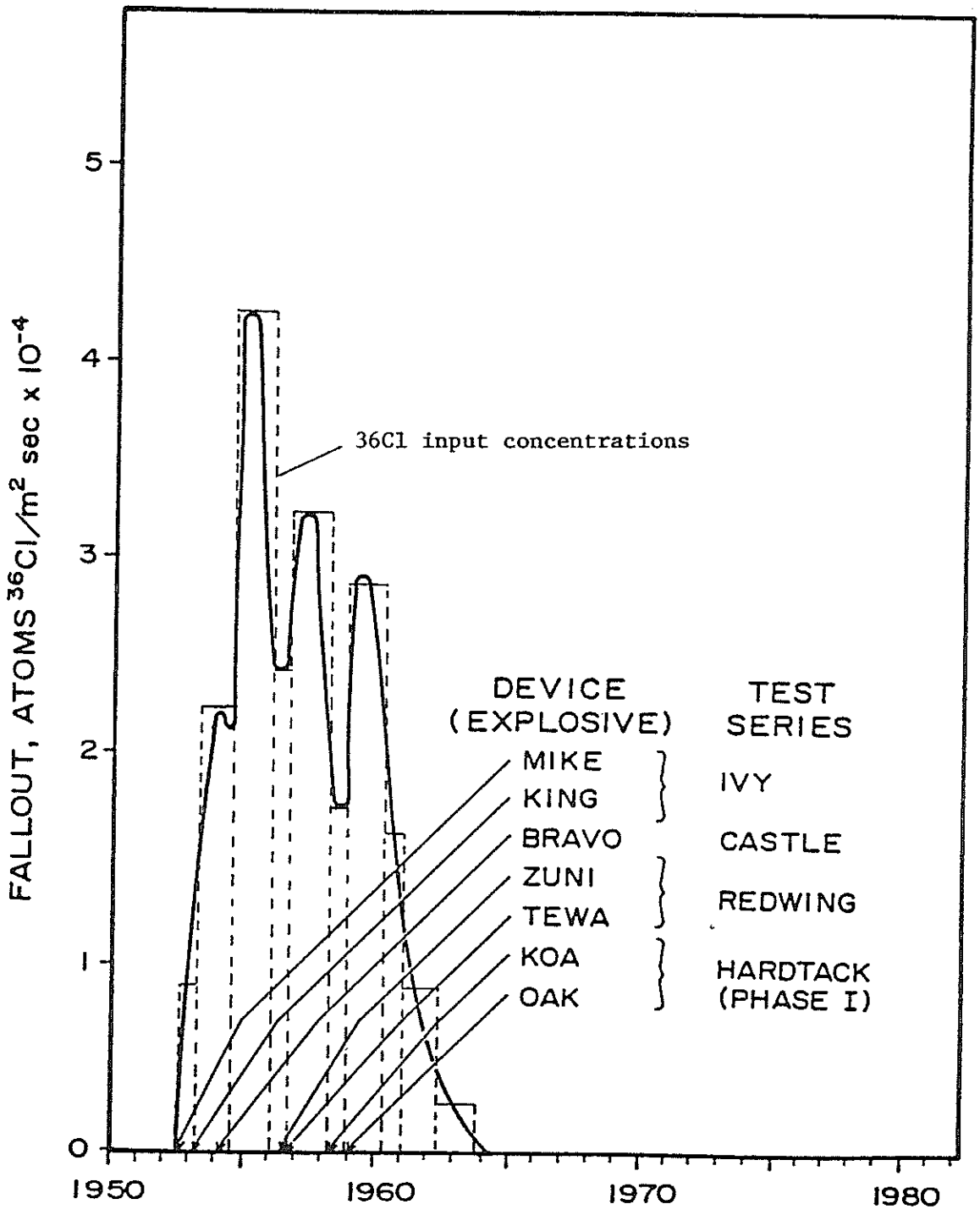
FALLOUT, ATOMS $^{36}Cl/m^2$ sec x 10^{-4}
5
4
3
2
1
0
1950
1960
1970
1980
36Cl input concentrations
DEVICE (EXPLOSIVE)
TEST SERIES
MIKE
KING
IVY
BRAVO
CASTLE
ZUNI
TEWA
REDWING
KOA
OAK
HARDTACK (PHASE I)

Input Calculations

$$\frac{(36Cl/m^2 sec)(sec/yr)}{\text{Recharge (cm/yr)}} \times \frac{m^2}{10{,}000\ cm^2} \times \text{vol. moisture} = \frac{36Cl}{cm^3\ soil}$$

Step	($^{36}Cl/cm^3$ soil)	No. of days
1	4.5×10^5	0–250
2	1.1×10^6	250–750
3	2.1×10^6	750–1250
4	1.2×10^6	1250–1500
5	1.6×10^6	1500–2000
6	8.6×10^5	2000–2250
7	1.4×10^6	2250–2750
8	8.1×10^5	2750–3000
9	4.3×10^5	3000–3500
10	1.1×10^5	3500–4000